

The Photoelectric Effect, Wave-Particle Duality,

and

Atomic Structure

A Thesis

by

David Johnson



December 2018

Table of Contents (Active hyperlinks by Chapter heading)

Figures.....	2
Abstract.....	3
Electrons, Positrons and Concentrated Energy Sources (CESs)	3
Quarks.....	5
The Nucleons	6
Electron-Positron Annihilation	6
Beta Decay and Electron Capture	7
Electron and Positron Generation	10
Atomic Structure of the Elements of the Periodic Table	11
Bonding and Free Electrons.....	22
Complex Chemical Compounds	24
Photons, Energy Transfer and Spectral Lines	29
The Photoelectric Effect	34
Plasma and Cosmic Radiation	35
Spin and the Orbital Nuclear Model.....	36
Conclusions	38
Acknowledgements and References	39
Appendix A: Electromagnetic Radiation	40
Micro and Radio Waves	40
Constructive and Destructive Interference	41
Appendix B: Electricity	45
Dielectrics and Electrical Capacitors	46
Chemical DC Electricity Generation and Recharge	47
Van de Graaff Generators.....	48
Electromagnetic Induction.....	49
Appendix C: The Pull of Gravity	51

Figures

<i>Figure 1: Examples of Electron/Positron Torus Models</i>	3
<i>Figure 2: Electron and Positron Electromagnetic Field Patterns</i>	Error! Bookmark not defined.
<i>Figure 3: CES</i>	5
<i>Figure 4: Up and Down Quark Structure and Electromagnetic Pole Patterns</i>	5
<i>Figure 5: 'L' Form Proton and Neutron Structure</i>	6
<i>Figure 6: Electron-Positron Annihilation</i>	7
<i>Figure 7: Plot of Beta Decay by Atomic Mass</i>	8
<i>Figure 8: Beta Minus Decay and Examples of Electron Capture</i>	9
<i>Figure 9: Laser Generated Electron and Positron Generation Setup</i>	10
<i>Figure 10: 'L' Form Proton and Neutron Structure</i>	11
<i>Figure 11: Models of Diatomic Hydrogen Molecule</i>	11
<i>Figure 12: 'L' form Protons and Neutrons Interlock to create 'I' form Proton and Neutron Layers Structure</i>	12
<i>Figure 13: Bar Model of He-3 and He-4</i>	13
<i>Figure 14: Bar Model of Beryllium-9 and Beryllium-10</i>	14
<i>Figure 15: Bar Model of C-12 Graphite: Side and Plan Orthographic Views</i>	14
<i>Figure 16: C-12 Allotropic Forms and Bar Models of Graphite Sheets</i>	15
<i>Figure 17: Bar Model of C-12 Diamond</i>	16
<i>Figure 18: Bar Model of Dioxygen (O_2)</i>	17
<i>Figure 19: Nuclei Polygonal Forms for Periods 1 to 3 of the Periodic Table</i>	18
<i>Figure 20: 4-8-16 Polygonal Embedding of Nuclei (Period 3 and Onwards)</i>	18
<i>Figure 21: Bar Model of Copper-63</i>	19
<i>Figure 22: Bar Model of Silver-107</i>	20
<i>Figure 23: Bar Model of Gold-197</i>	21
<i>Figure 24: Inter-Quark and Bitron Bonding</i>	23
<i>Figure 25: Free Electron Attachment to an 'I' form Neutron</i>	23
<i>Figure 26: Electromagnetic Adsorption between Copper and Gold Atoms</i>	24
<i>Figure 27: Models for Gold Nanoparticles in Water</i>	25
<i>Figure 28: Valency Groupings and Diagrams</i>	26
<i>Figure 29: Bar Model for Methane (CH_4)</i>	27
<i>Figure 30: Bar Model for Water (H_2O)</i>	27
<i>Figure 31: Bond Variation of Gaseous Water (steam)</i>	28
<i>Figure 32: Atomic Geometry of Chemical Compounds</i>	28
<i>Figure 33: A Photon as a Helical Solenoid</i>	29
<i>Figure 34: Photon Creation/Emission and Capture/Re-Emission</i>	30
<i>Figure 35: Emission Spectra for Common Element Groupings</i>	31
<i>Figure 36: Absorption and Re-Emission Spectra</i>	31
<i>Figure 37: Electromagnetic Fields of an Unpolarised Photon</i>	32
<i>Figure 38: Optic Vortex and Linear, Circular and Polarised Light Forms</i>	33
<i>Figure 39: Reflection of Circular Polarised Light</i>	34
<i>Figure 40: Plasma Temperature/Density Distribution</i>	36
<i>Figure 41: The Stern-Gerlach Experiment Setup</i>	37
<i>Figure 42: The Stern-Gerlach Experiment - Silver Atom Structure and Deflection Pattern</i>	37
<i>Figure 43: Electron and Positron Electromagnetic Field Patterns</i>	40
<i>Figure 44: Man-Made Micro and Radio Waves</i>	40
<i>Figure 45: Electromagnetic Field Patterns for a Dipolar Antenna</i>	41
<i>Figure 46: Michelson Interferometer setup: parallel merged beams</i>	42
<i>Figure 47: Michelson Interferometer Interference Patterns</i>	42
<i>Figure 48: Surface Plasmons</i>	42
<i>Figure 49: Light Wavefront Created by Progressive Photon Deflection</i>	43
<i>Figure 50: 2-Slit Electron Electromagnetic Deflection and Distribution Pattern</i>	44
<i>Figure 51: Electric Current: Electron and Positron Movement</i>	45
<i>Figure 52: Electric Capacitor Charge and Discharge Phases</i>	46
<i>Figure 53: Galvanic and Electrolytic Cells</i>	47
<i>Figure 54: Van de Graaff Generators</i>	48
<i>Figure 55: Magnetic Field Induced Current</i>	49
<i>Figure 56: Magnet-Motion Induced Current within a Loop</i>	49
<i>Figure 57: Electromagnetic fields around a Loop Current</i>	50
<i>Figure 58: Model for Earth's Gravity</i>	51

Abstract

In 1905 Albert Einstein provided an explanation of the [photoelectric effect](#) by postulating the existence of "light quanta" (later called photons) to explain the photoelectric effect which the wave theory of light of that time was incapable of explaining: this sparked the particle versus wave debate because the particle approach cannot adequately explain interference, diffraction and polarisation and the wave approach cannot explain the photoelectric effect. The De Broglie hypothesis, which attributed wave-like nature to matter, was confirmed experimentally for the electron, and **wave-particle duality** was formalised by Schrödinger's equation, and extended by Dirac's equations, to form a theoretical foundation for Quantum Mechanics. Although the use of the wave-particle duality has been widely accepted, the meaning or physical interpretation has not been satisfactorily resolved.

In this thesis paper, electrons, positrons and preons are postulated to have a **toroidal solenoid** structure, whereas photons are postulated to have a **helical solenoid** structure (these solenoidal models are similar to those proposed by Oliver Consa in 2018 for non-static electrons and preons). The proposed helical solenoidal structure of photons provides them with wave-like and particle characteristics supportive of a **wave-particle duality**.

Quarks are postulated to be built from preons, and nucleons from up- and down-quarks. The model for atomic structure developed using these fundamental and derived sub-atomic particles is considerably different to the orbital nuclear model based upon the monopole electrons and protons. The model developed provides a feasible explanation of different allotropic forms of elements and their various bonding geometries, beta decay, electron capture, electron-positron annihilation, electric current (a 'hole' free explanation), the ionization process during plasma formation, Gravity and Gravity waves. It also provides good correlation between the atomic structure of the elements within the Periodic Table and their physical and chemical characteristics, which is something the orbital nuclear model fails to do.

Electrons, Positrons and Concentrated Energy Sources (CESs)

A **toroidal ring** model for electrons was first proposed by Alfred Lauck Parson in 1915. Originally known as the Parson magneton or magnetic electron, similar models have since been referred to as a plasmoid ring, vortex ring, and helicon ring. Since 1997 there have been numerous papers, articles and videos related to torus models of electrons and photons: a representative sample of these models is shown in figure 1.

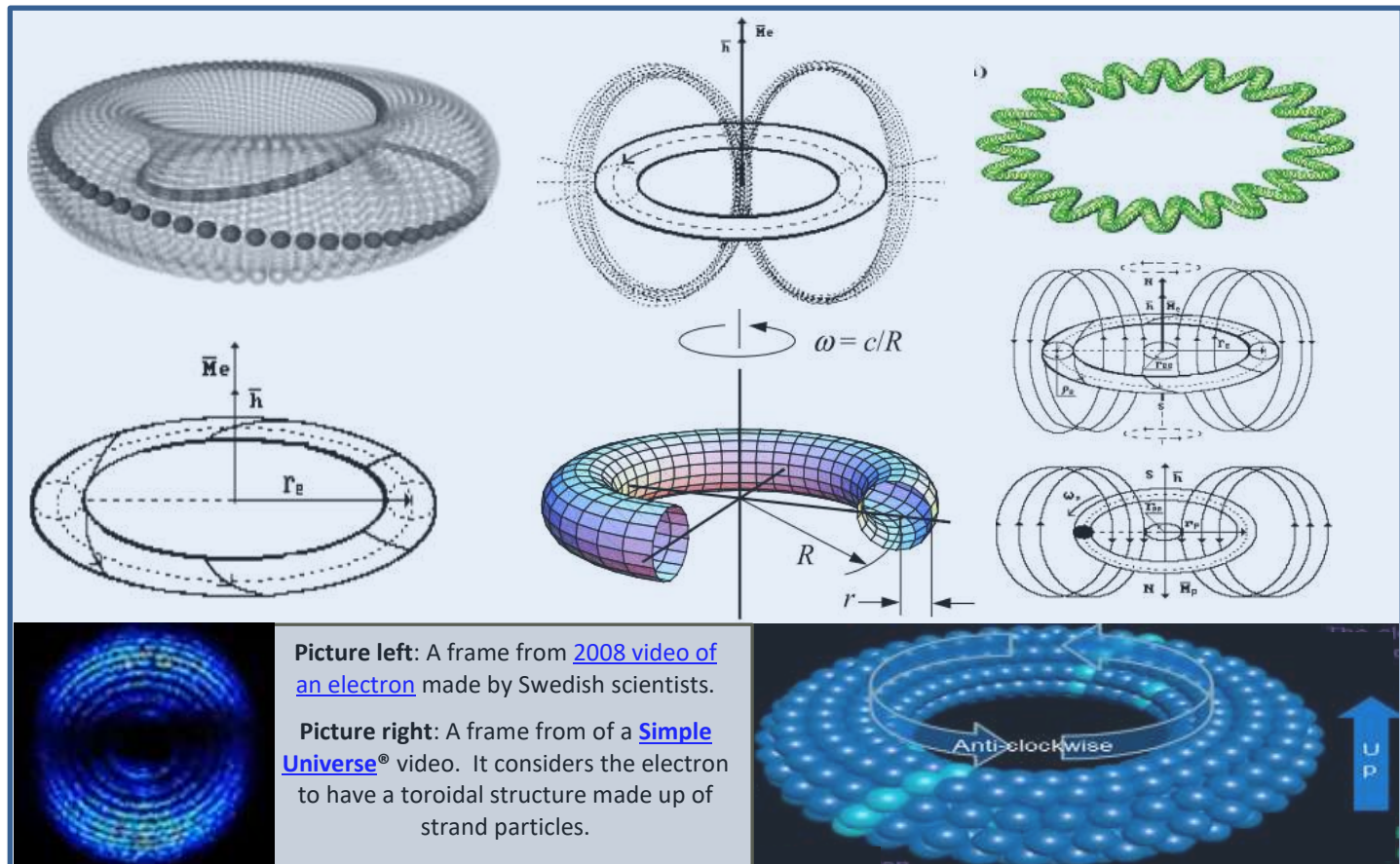


Figure 1: Examples of Electron/Positron Torus Models

W.H Bostick proposed a **toroidal solenoid** structure for the electron in 1956, with electric charge circulating internally at the speed of light. Along similar lines, this thesis considers that the electron's torus consists of a fast moving **concentrated energy** continuum flowing in a swirling solenoid pattern but presenting as a toroidal structure. The flow pattern forming the electron's torus is considered to be accompanied by a swirling cloud-like atmosphere of less concentrated energy moving in unison with the concentrated energy to present as external **electromagnetic field of** the electron.

The later **helical toroidal** model for an electron, as defined by [Oliver Consa in 2018](#), has been used in this thesis to define the [structure of a photon](#). It consists of an electric charge moving around the major radius (R or r_e in figure 1) of the torus and rotating around the inner circular section (minor radius r): at rest it is equivalent to a toroidal solenoid.

Considering the toroidal solenoidal model for an electron, the up/down component of the external electromagnetic field provides the field's North/South magnetic orientation, with the North Pole defined by the **divergent** energy flow and the South by the **convergent** flow. The circular flow component of the electromagnetic field around the North/South axis provides its electrical characteristics: the convention assumed is **clockwise** for the **positive** pole and **anti-clockwise** for the **negative** when looking from outside towards the torus along its North-South axis (see figure 2).

The electromagnetic field orientation of the electromagnetic energy defines the chirality (or helicity) of the tori. The convention adopted is that a N- (North-Negative) pole or a corresponding S+ (South-Positive) pole defines an **electron**, and that a N+ or S- pole an **positron**, as shown by a green torus in figure 2, with the electromagnetic field encompassing the torus with its positive electric field side indicated by **blue** highlighting and the negative side by **red**.

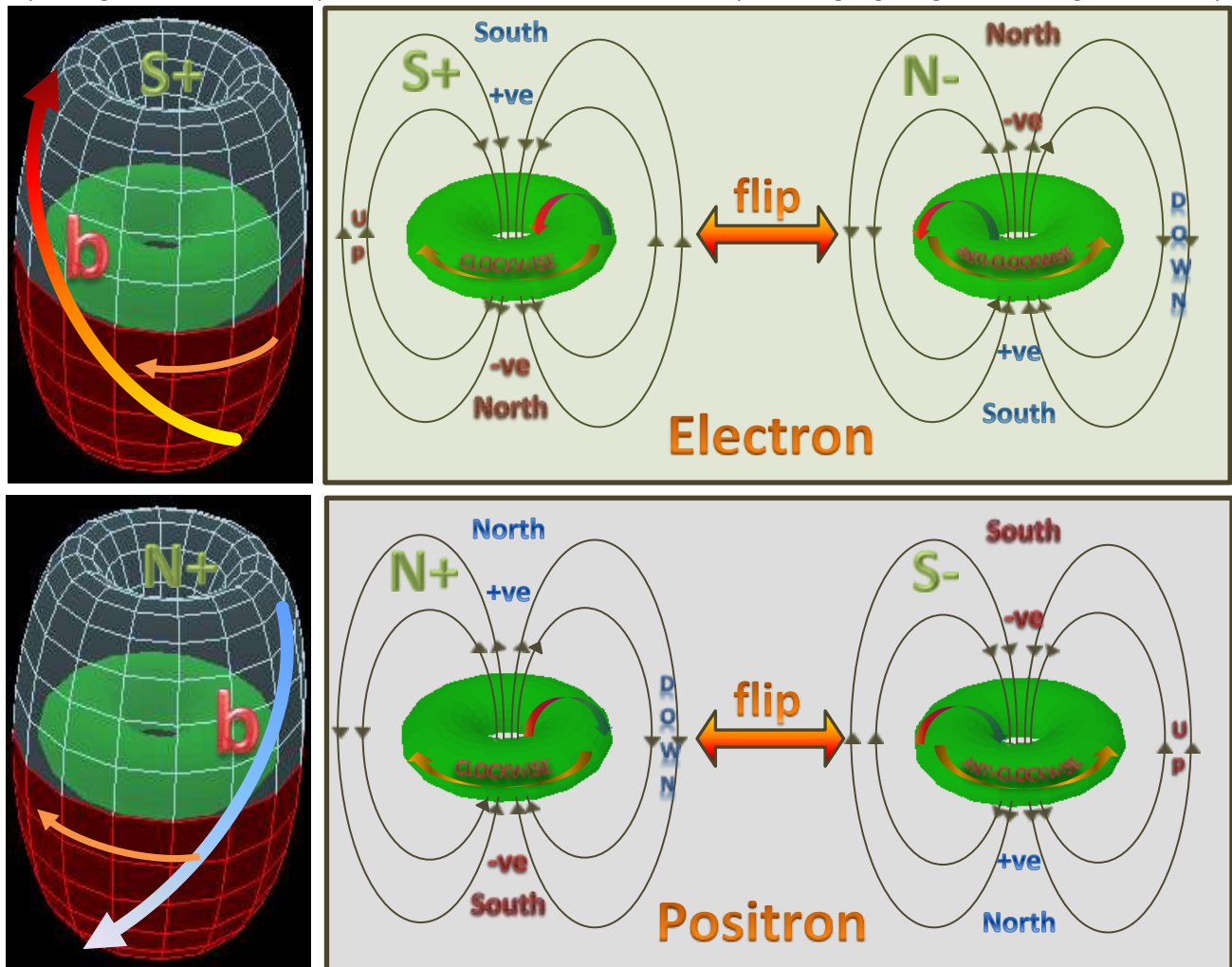


Figure 2: Electron and Positron Electromagnetic Field Patterns

The same toroidal solenoidal model proposed for electrons and positrons has been extended to the **Preon**, the primary fundamental particle that builds into quarks and thus into the nucleons. The result is an energy-centric approach to atomic structure called the '**Energy to Matter**' (or E2M) model. This thesis relates to version 13 of E2M.

In order to avoid problems associated with other definitions of preons, E2M uses the term **Concentrated Energy Source** (or CES) to refer to a preon. The CES is represented diagrammatically by a yellow torus (figure 3) to distinguish them from electrons and positrons (shown with a green torus). As for electrons and positrons, CESs can have different chirality and, importantly, are considered to be the primary energy source for ordinary matter.

The rest mass of a CES is in the order of $52 \text{ MeV}/c^2$, which in energy terms means that it contains about 100 times more energy than an electron (or positron), which has a rest mass of $0.511 \text{ MeV}/c^2$.

CESs have the additional ability of being able to capture, absorb and store extra electromagnetic energy from other electromagnetic sources, thus increasing their net energy, or to lose some energy to their environment. Both processes are ongoing and in parallel, providing CESs with dynamic, responsive energy transfer and balancing capabilities.

Unlike CESs, the electromagnetic energy level of electrons and photons remains relatively constant until it is absorbed (fully or partially) by another structure or field. E2M also addresses the possibility that electrons and positrons are derived or secondary energy sources that are created by or derived from CESs.

Another important feature of CESs is their ability to group together to form **up** and **down quarks**, which in turn form into the **nucleons** (i.e. protons and neutrons), which build into normal matter. These capabilities are discussed next.

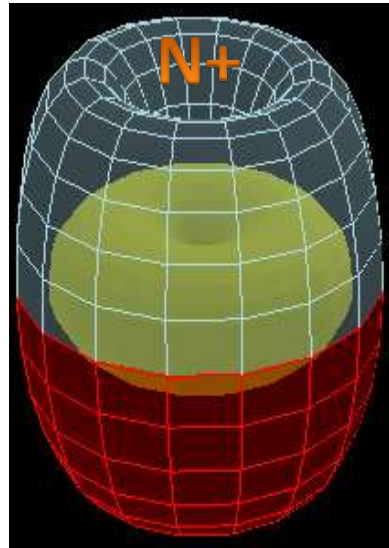


Figure 3: CES

Quarks

E2M considers that each up and down quark consists of a three-dimensional array of 6 CESs, held in place by their respective electromagnetic fields, as shown in the figure 4. Note that...

- The green cube is purely to highlight the spatial position of the CESs forming the quark structure.
- For a given electromagnetic polarity the rotational direction around the longitudinal axis can be clockwise or anti-clockwise. Where possible, it would be reasonable to assume that most pairs of CESs sharing the same longitudinal axis within a quark would both have the same rotational direction (e.g. a N- CES would most likely match with a S+ or a N+ CES).

An **up quark** consists of five outwardly pointing positive polarity CESs and one negative polarity CES. The electric charge corresponding to each pole can be considered to equate to a point charge of $1/6 \text{ e}$ (elementary charge) located at the centre of a quark (i.e. at the centre of its green-cube geometry); thus the net electric charge of an up quark is $+5/6 - 1/6 = +2/3 \text{ e}$.

Similarly a **down quark**, consisting of two outwardly pointing positive polarity CESs and four negative polarity CESs, resulting in a net electric charge of $-1/3 \text{ e}$. Thus the electric charge estimates derived from the E2M model correspond with experimentally determined electric charge values of up and down quarks.

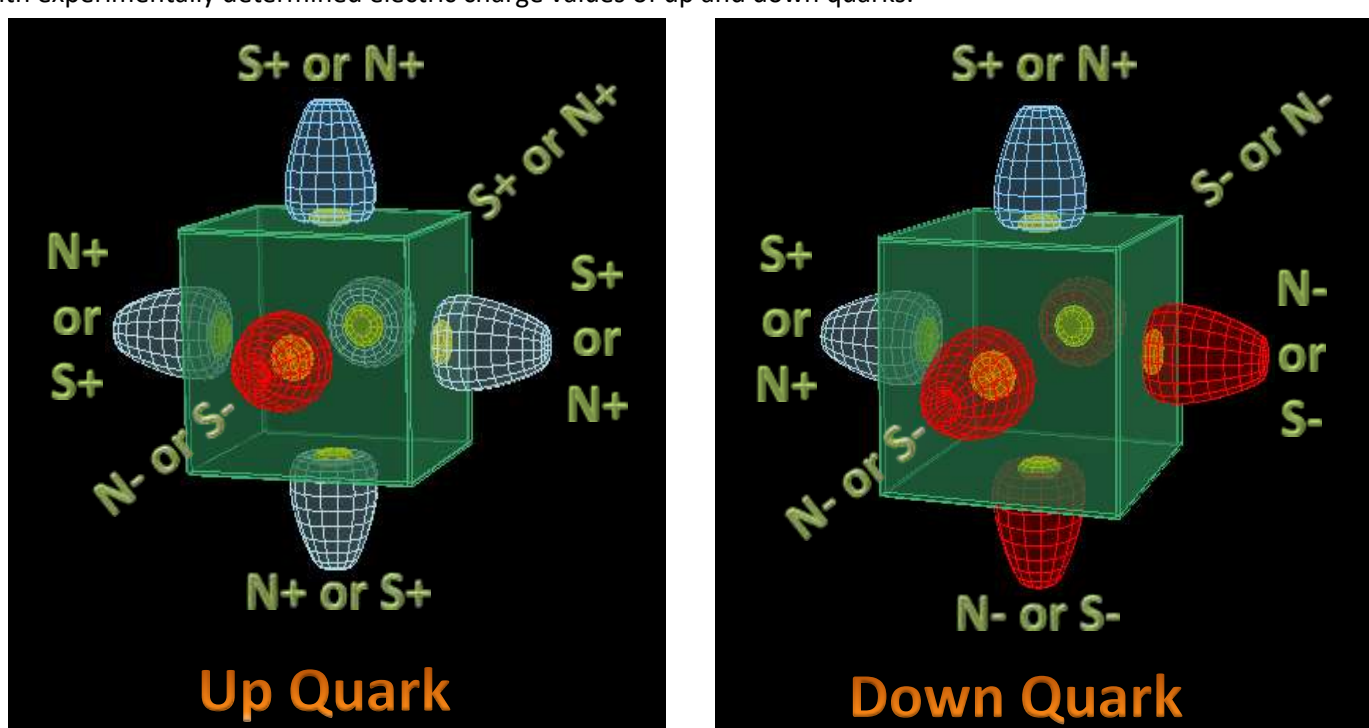


Figure 4: Up and Down Quark Structure and Electromagnetic Pole Patterns

The Nucleons

A **Proton** consists of two up quarks and one down quark, and a **Neutron** consisting of two down quarks and one up quark. Both nucleons have an 'L' shaped form, as shown in figure 5 ('I' or bar form nucleons are discussed under the heading [Atomic Structure of the Elements of the Periodic Table](#)).

Note that the strong force joins between the up and down quarks provide for the 2-way movement of electromagnetic energy between quarks, thus providing an energy balancing mechanism between nucleon quarks.

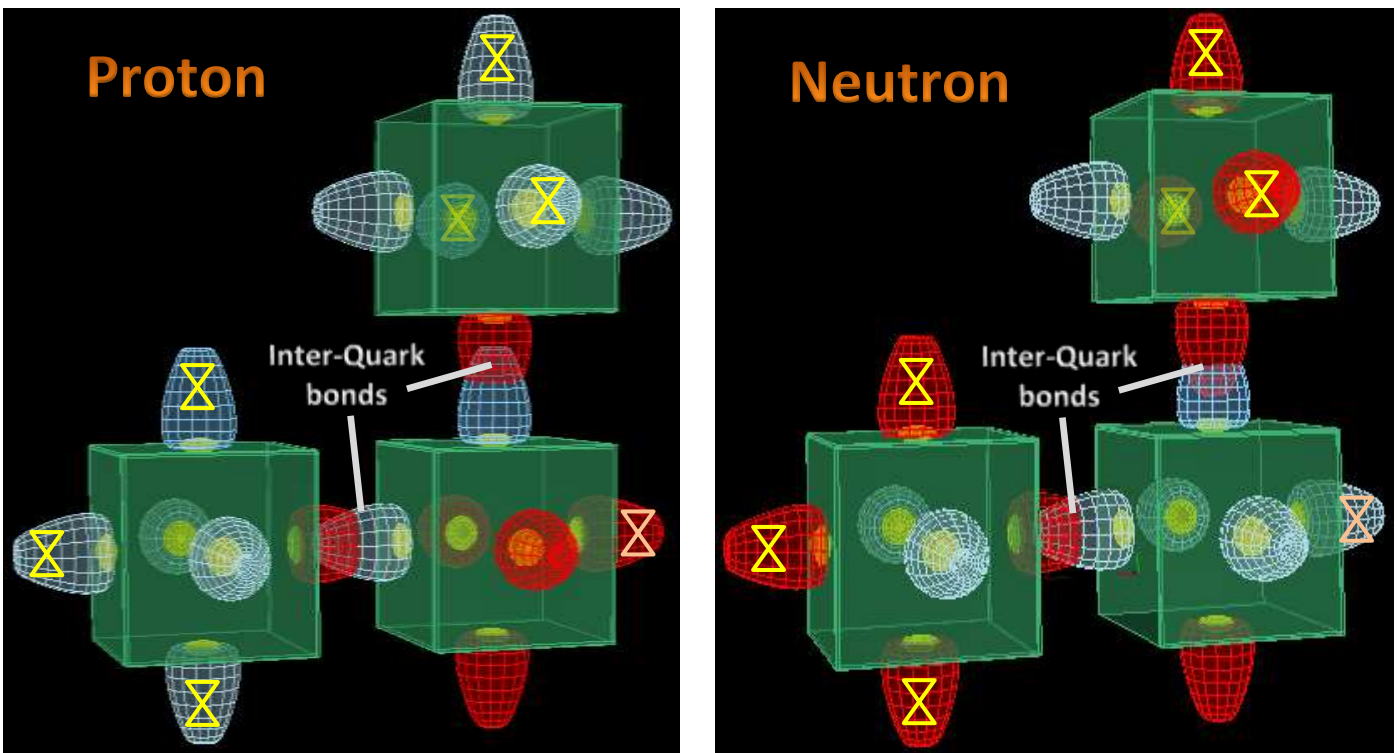


Figure 5: 'L' Form Proton and Neutron Structure

Protons consist of two up quarks ($+2/3 e^-$) and one down quark ($-1/3 e^-$), resulting in a net electric charge of $+1e$, whereas the Neutron, consisting of two down quarks and one up quark, is electrically neutral.

An important characteristic of the nucleon structures relates to those CESs annotated with a yellow hourglass symbol in figure 5 act as **flip triggers**: should any one of these 6 flip trigger tori be flipped (from a positive outward electric field to a negative one or vice versa), they cause the other five, plus the one within the central quark annotated with an orange hourglass, to flip automatically. CES torus flipping provides nucleons with the ability to instantaneously convert from a proton into a neutron or vice versa: this capability is very important for atom-building and transformation processes.

Electron-Positron Annihilation

Electron–positron annihilation occurs when an electron (e^-) and a positron (e^+), the electron's antiparticle, collide. In a majority of cases, the result of the collision is the annihilation of the electron and positron, and the creation of gamma ray photons: $e^- + e^+ \rightarrow \gamma + \gamma$. The Wikipedia diagram for the annihilation is shown in the top of figure 6 (with a Feynman diagram insert). Each electron, positron and gamma ray photon represent an energy of $0.511 \text{ MeV}/c^2$.

The E2M explanation for electron–positron annihilation is shown in the bottom part of figure 6: as the electron and positron approach each other, their magnetic fields attract causing them to accelerate towards each other. As they get really close to each other, almost touching, their electric field repulsion intensity increases dramatically and the two particle explosively separate pushing each other away in opposite directions. Comparable with two solid incompressible objects in a head-on collision, the tori fly off in opposite directions (i.e. 180° to each other) at close to the speed of light and start free-spinning at a frequency corresponding to that of **Gamma (γ) radiation**.

(Note that the Gamma radiation is a form of EMR has been represented in figure 6 by a helical solenoidal structure of a photon: photon structure will be covered in the section heading '[Photons, Energy Transfer and Spectral Lines](#)').

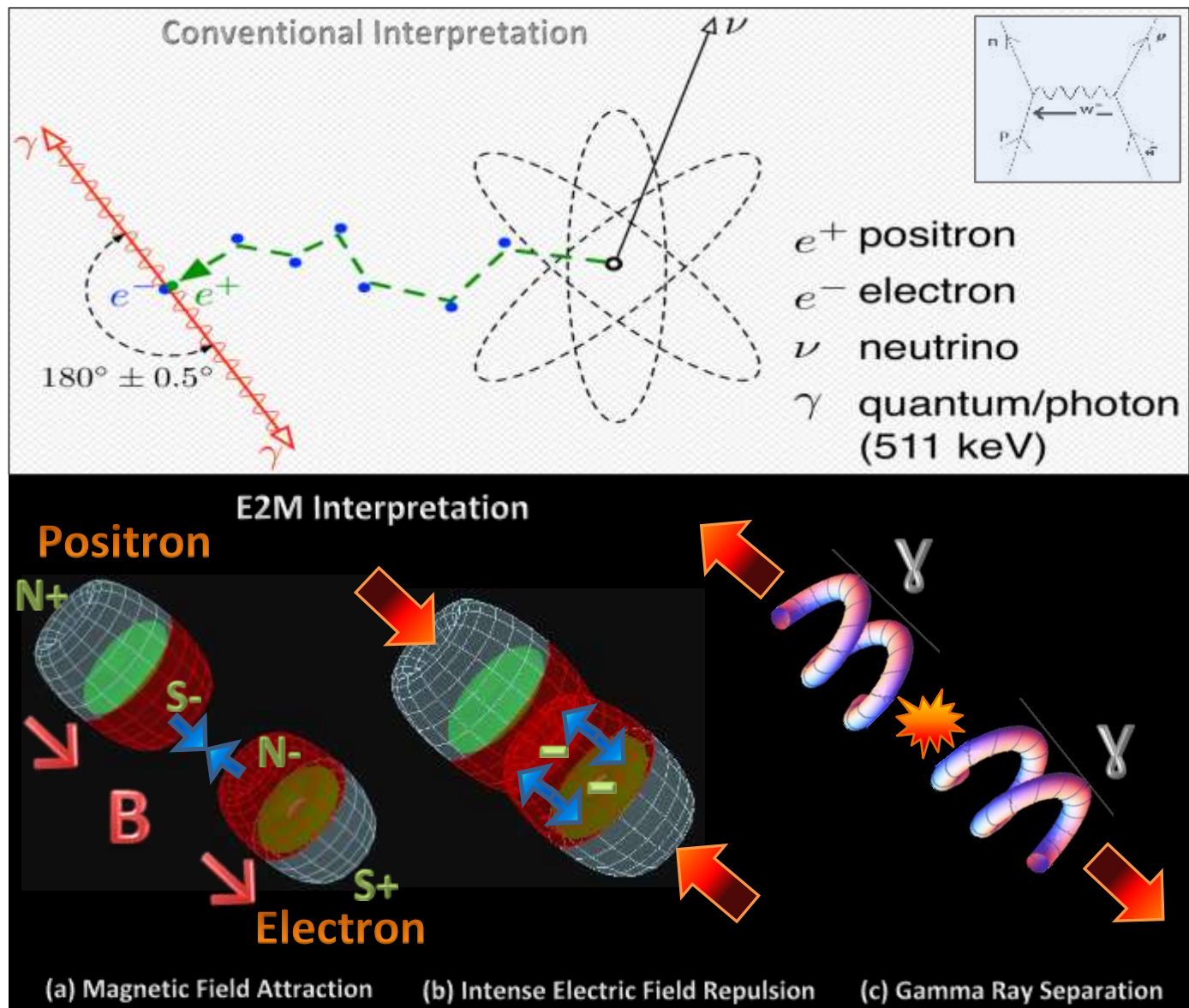


Figure 6: Electron-Positron Annihilation

Beta Decay and Electron Capture

Beta decay (β decay) is a type of ‘weak reaction’ radioactive decay in which a **beta ray** (a fast energetic electron or positron) and a neutrino are emitted from an atomic nucleus. It is quite prevalent across many elements of the Periodic Table as shown in figure 7. Stable isotopes are shown as the tenuous black line that roughly demarks the two types of decay.

Beta minus (or β^-) decay is when an ‘L’ form neutron that is loosely attached to the top or bottom layer of an atom and not forming an internal or external electron bond (see [Bonding and Free Electrons](#)) converts into a proton, increasing the atomic number of the atom concerned by 1; and **beta plus** (or β^+) decay is when an ‘L’ form proton attached to the top or bottom layer of an atom converts into a neutron, decreasing the atomic number by 1.

β^- decay is triggered when an electron internal to the atom becomes unstable and accelerates towards one of the neutron’s negative flip-triggers causing it to flip. The flip causes the neutron’s other 6 flip CESs to flip simultaneously,

converting the neutron into a proton. The flipped CES causes the electron involved to be repelled at speed away from the atom as an **electron beta ray**.

A small amount of concentrated energy is released as an anti- neutrino (Note that a **neutrino** is considered to be a low-speed torus with a rest mass of about 0.12×10^{-6} MeV/c² with the same chirality as an electron; an **anti-neutrino** has the same chirality as a positron).

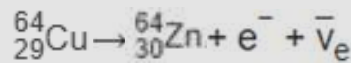
Figure 8 (a to c) shows the mechanics of β^- decay: the strong attraction of opposite magnetic and electric poles causes the acceleration of the electron towards the trigger CES, compressing and condensing the electromagnetic energy between them, forming into a neutrino torus (brown torus of 8b). Pressure from the rapidly approaching electron causes the trigger CES to flip, thus reversing its magnetic field. Neither the neutrino nor the electron are flipped, but the magnetic field associated with the newly formed neutrino is reversed (changing from +B+b to -B+b), transforming it instantly into an anti-neutrino energy pattern. The energy exchange associated with the torus flip causes the explosive and rapid ejection of the electron and anti-neutrino; the magnetic repulsion between the electron and anti-neutrino ensures that they take separate exit paths.

β^+ is essentially the reverse of β^- decay, being triggered when an energised positron within the medium containing the atom causes one of a proton's flip-trigger CESs to flip, turning the proton into a neutron, and the release of a positron beta ray and a neutrino.

Some examples of Beta decay are:

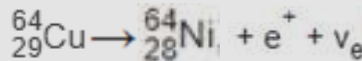
For β^- decay, a neutron is converted to a proton resulting in an electron and an electron anti-neutrino.

For $^{64}_{29}\text{Cu}$ the β^- decay equation is:



For β^+ decay, a proton is converted to a neutron resulting in a positron and an electron neutrino.

For $^{64}_{29}\text{Cu}$ the β^+ decay equation is:



Note that $^{64}_{29}\text{Cu}$ has a half-life of 12.7 hours, undergoing proton decay to $^{64}_{28}\text{Ni}$ 61% of the time (18% by beta plus decay and 43% by electron capture decay), and neutron decay by beta minus decay to $^{64}_{30}\text{Zn}$ 39% of the time.

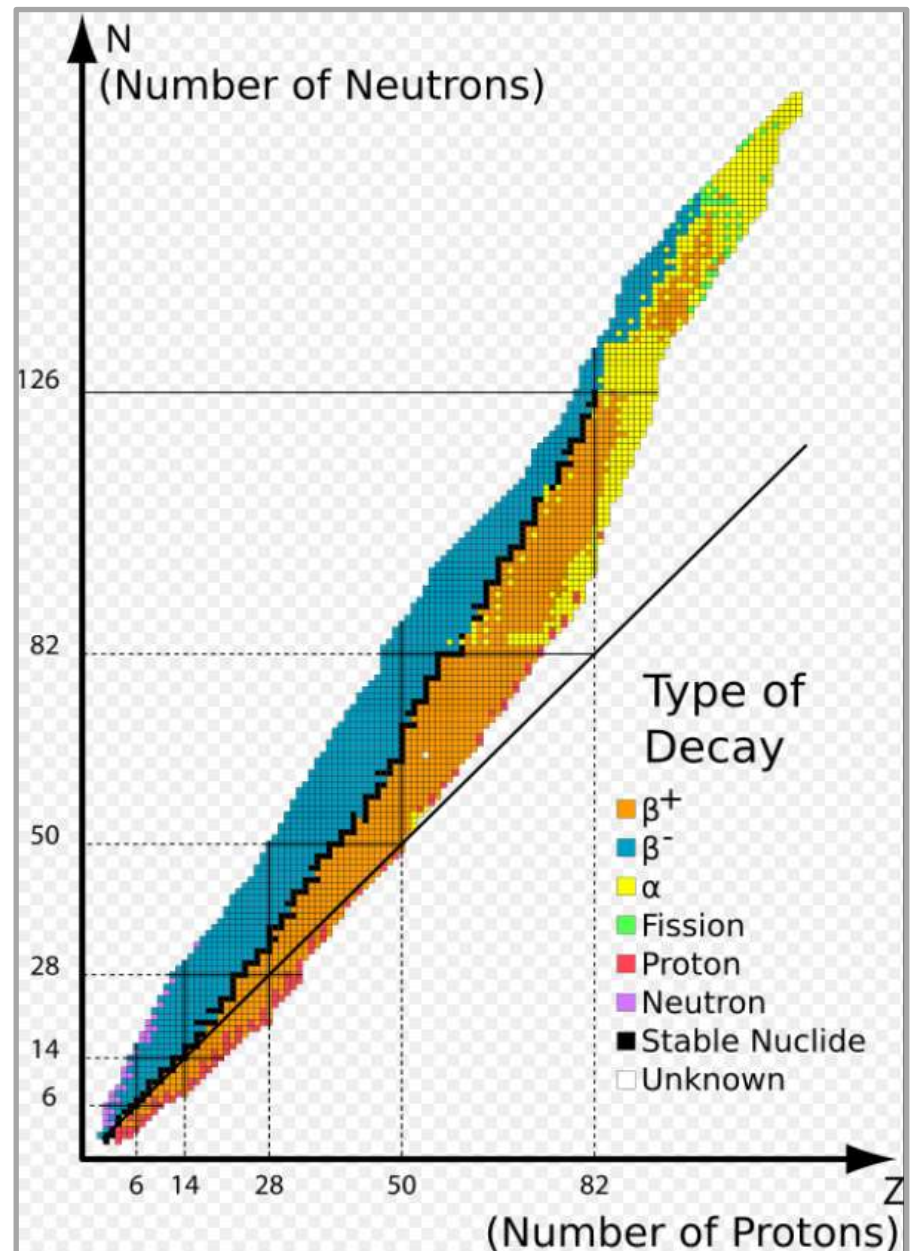


Figure 7: Plot of Beta Decay by Atomic Mass

Electron capture is very similar to β^+ decay except that the source of the positron that triggers the decay is a free positron rather than from an atom's structure. The E2M electron capture equation is: $P + e^+ \rightarrow N + \nu_e + e^+$

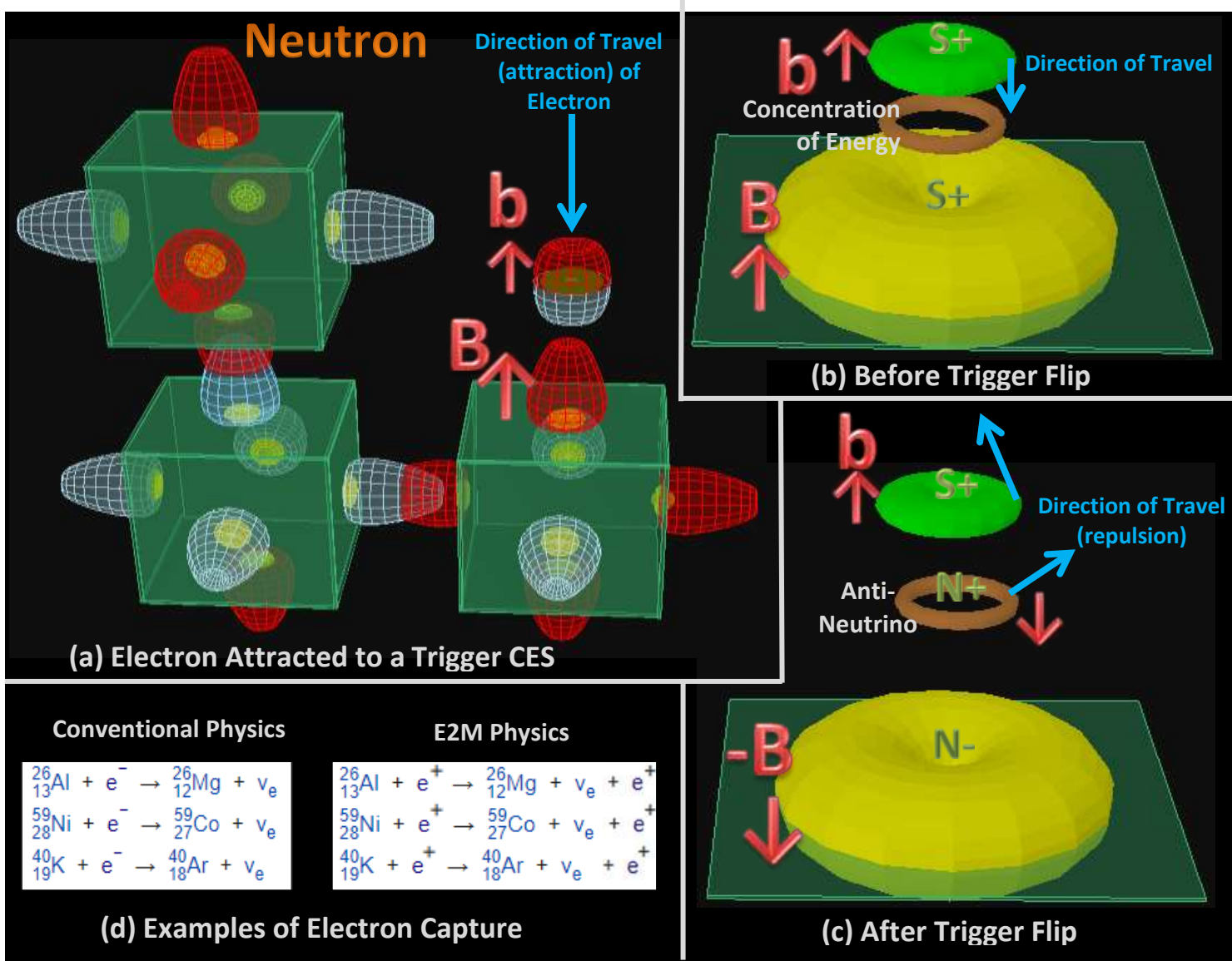
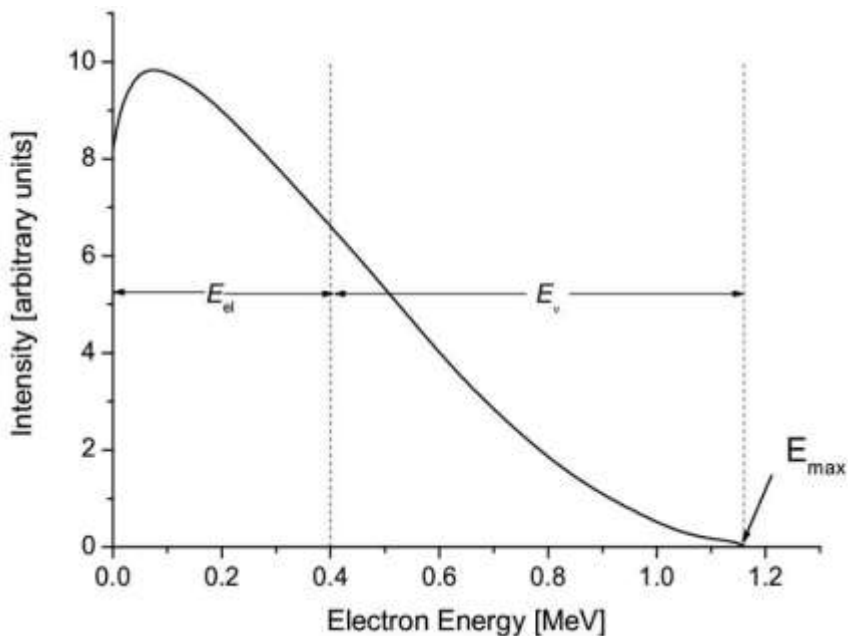


Figure 8: Beta Minus Decay and Examples of Electron Capture

For both β^+ and β^- decay the energy exchange associated with the tori flip results in the creation of an electron neutrino and anti-neutrino respectively, resulting in the energy distribution shown right. For electron capture, however, there is less momentum related energy redistribution which results in a more discreet energy profile.

The equations used to represent Beta decay and electron capture are quite deceptive because the electron being captured is shown on the left-hand side of the electron capture equation, but omitted in the beta decay equations – possibly because it is sourced from the atom itself. The conventional Physics approach involves the total exclusion of positrons from an atom's structure and from electric currents: E2M is not restricted by such constraints.



Electron and Positron Generation

As described in Appendix B, within a wire conductor electrically aligned electrons and positrons shuffle past each other, presenting as an electric current and creating a circular electromagnetic field around the wire. Although concentration of electrons (or, more accurately, the ratio of electrons to positrons) builds up on the positive side of a resistor and positrons on the negative, it is virtually impossible to distinguish between electrons and positrons within such a wire conductor, let alone separate or isolate them.

Electrons are most commonly sourced from thermionic cathode ray tubes (e.g. first generation TV tubes): those used in research settings are usually called **electron guns**. As for electric current, E2M contends that the electrons emitted from electron guns are a combination of electrons and positrons that, due to magnetic alignment (N- and N+ respectively), are deflected in the same direction and by the same amount by a magnetic field.

Low levels of positrons can be sourced from β^+ decay and Electron Capture. One practical application is **Positron Emission Tomography (PET)** which is a gamma imaging technique using radionuclide tracers that generate positrons which trigger electron-positron annihilation inside a patient's body: the resulting pair of gamma ray travel in opposite directions, and are detected allowing the tracer locations to be accurately mapped producing a high resolution image.

In order to generate larger groupings of positrons, the 'electron' beam from an 'electron' gun is concentrated and accelerated to increase the electrons' net energy; they are then used to bombard a metal film to release positrons. At CERN, the **LIL** (Large Scale Electron-Positron Collider Injector Linac) uses an 'electron' gun to assemble electrons with an energy of 80 keV; these are in turn accelerated to an energy of around 200 MeV which are then shot at a tungsten target to produce positrons that can be magnetically separated and further accelerated for particle collision purposes.

On a smaller scale, in their 2013 paper titled '[Table-Top Laser-Based Source of Femtosecond, Collimated, Ultra-relativistic Positron Beams](#)', by G. Sarri et. al. report the generation of a positron beam using a laser-driven particle acceleration setup (see figure 9). A petawatt (10^{15} W) laser was fired at a sample of inert helium gas, creating a stream of electrons (and, most likely, positrons) moving at very high speed, which were directed at a very thin sheet of metal foil: the resulting collisions produced a stream of electron and positron (and gamma ray) emissions which could be separated using magnets.

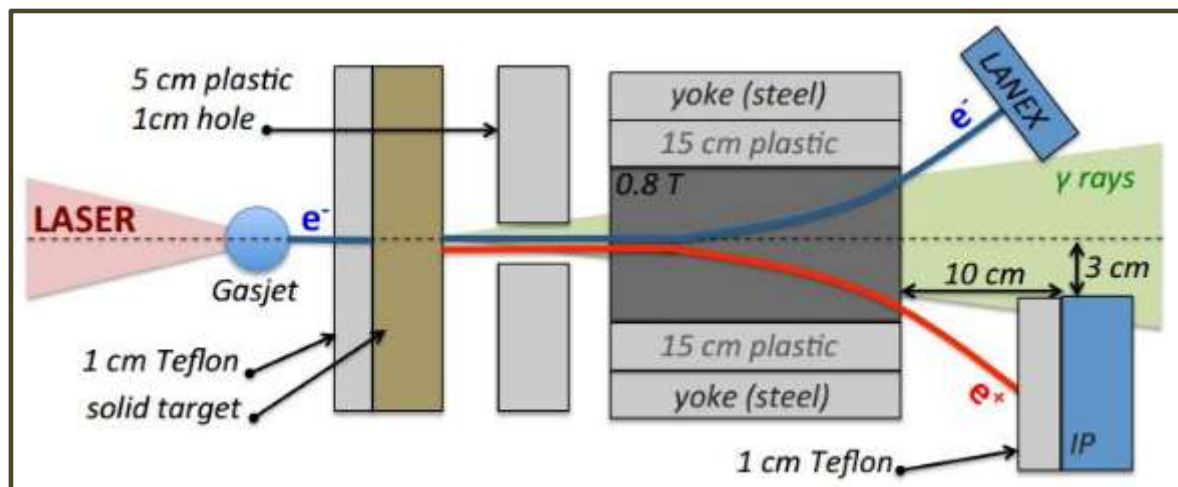


Figure 9: Laser Generated Electron and Positron Generation Setup

There would seem to be a great deal of commonality between both these examples of larger scale positron generation using energised 'electrons' and **electron-positron pair production** using high energy EMR (principally gamma radiation): both involve the bombardment of a metal target by highly energised particles. For the 'electron' gun approach (i.e. CERN and the table-top examples) the energy levels of the 'electrons' are significantly higher than that of the photons of the gamma rays, resulting in many more positrons being released. For EMR of even less energy, such as EMR in the visible light range, electron-positron pair production is called the **photo-electric effect**.

On the speculative side, it would seem that the mechanics of electron-positron pair production is analogous to that of electron-positron annihilation, except that resulting electrons and positrons are more restrained, resulting in particle velocities less than that of gamma radiation (i.e. the speed of light), and without the associated particle spin.

Atomic Structure of the Elements of the Periodic Table

As explained earlier, protons (U-D-U) consist of 2 up quarks and 1 down quark (a total of 18 CESs). Neutrons (D-U-D) consist of 2 down quarks and 1 up quark (figure 10).

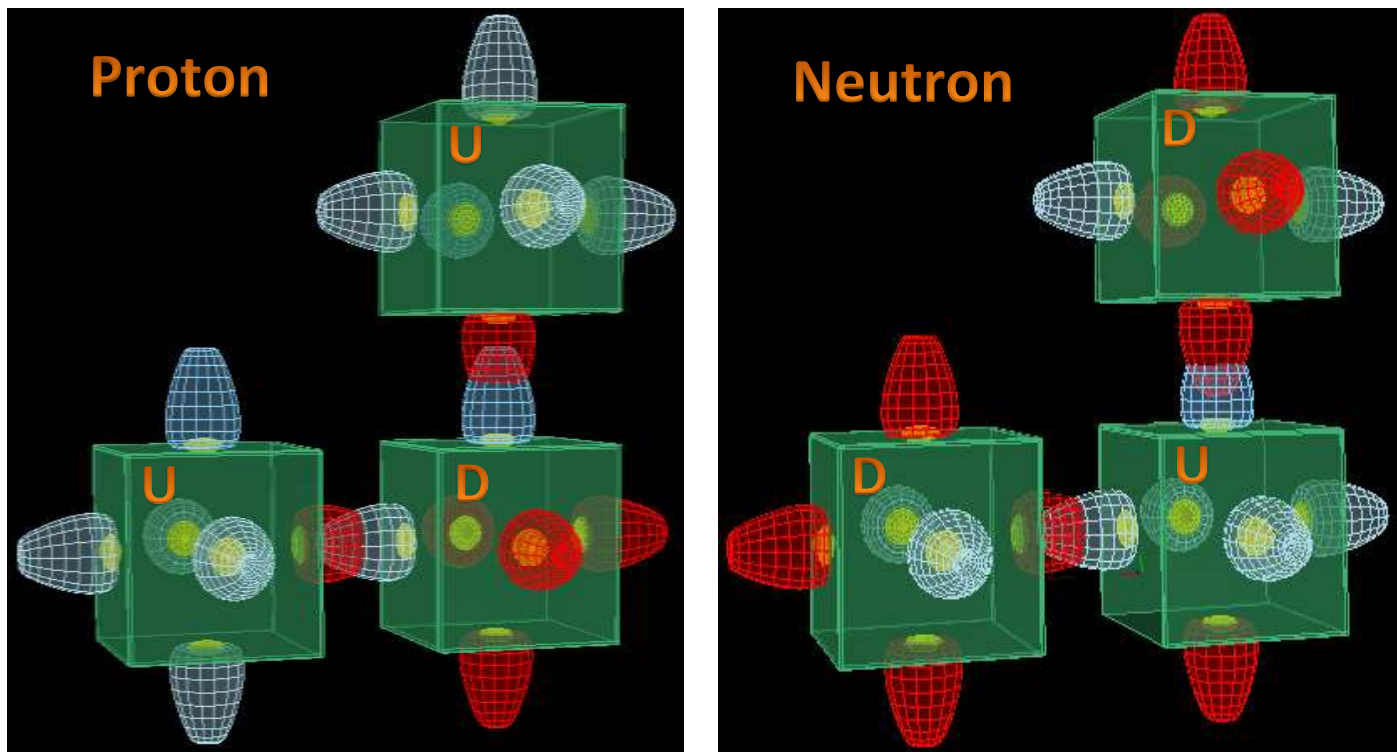


Figure 10: 'L' Form Proton and Neutron Structure

Hydrogen is the first element in the Periodic Table having an atomic number of 1. Its nucleus consists of a single proton. The **Standard Model** (SM) considers that, in its diatomic H₂ molecular form, it covalently shares two electrons.

The E2M view is that the H₂ molecule consists of two protons that are bonded internally by a pair of electron bonds. Figure 11 shows two configurations: one with the free up quarks on opposite side of the electron bonds, and the other with them both on the same side: both configurations are equally likely. Note also that the top and bottom up quarks are free to rotate around their vertical axis (as shown) and, as they are unrestrained, most likely do so.

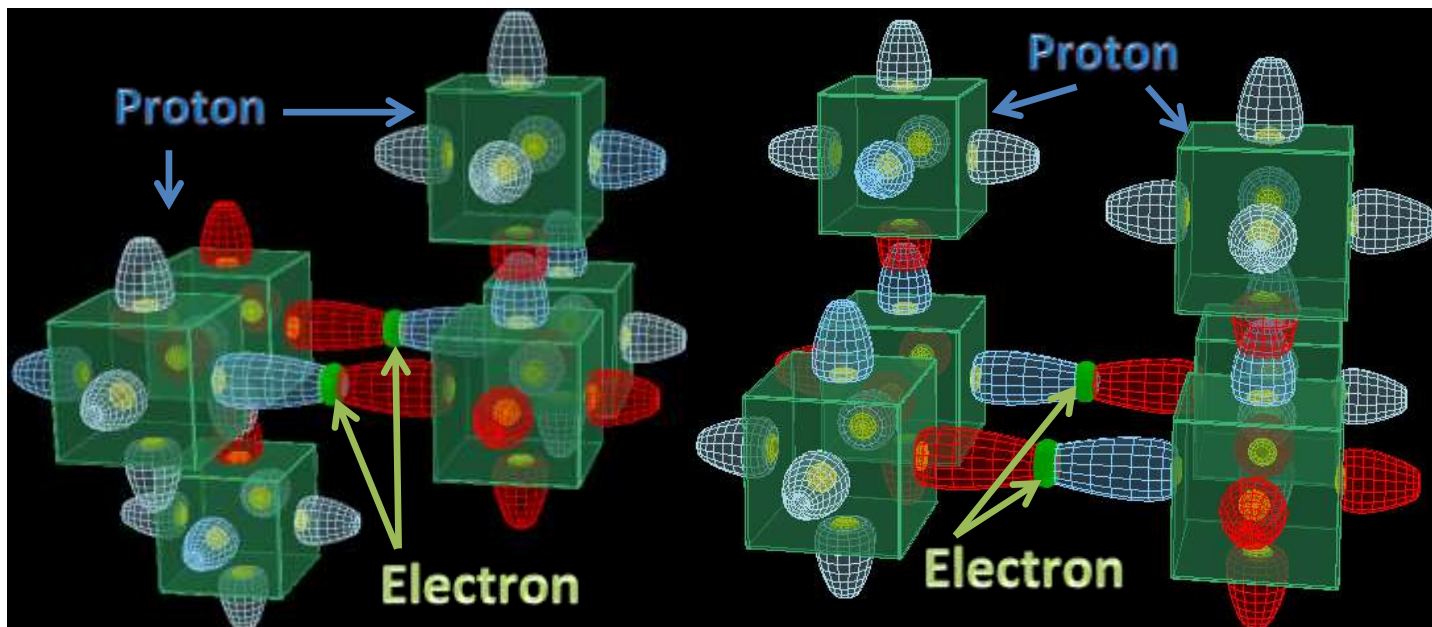


Figure 11: Models of Diatomic Hydrogen Molecule

The most striking feature of the E2M model for the H₂ molecule is that the electrons are part of the internal structure holding the protons together rather than being in a covalent 's' orbital around the protons.

The E2M view is that most of an atom's electrons are held internally, bonded between a pair of oppositely charged CESs, forming an integral part of the structure of the nucleus and adding strength to it. Some of an atom's electrons are external to the nucleus bonding atoms together to form molecules, ions and a wide range of chemical compounds. The internally bound electrons are considered to be an integral part of the nucleus's structure, whereas the outward facing bond-hook electrons can be gained, lost and/or exchanged dynamically and dictate valency options and bonding patterns.

The SM view is that electrons are external to the nucleus, orbiting at the speed of light around the nucleus in mathematically defined '**spdf**' orbital patterns as point charge particles or a wave-like form. A major problem for this model is that no electrons have ever been located in the claimed orbital zones (not even for larger atoms supporting 100's of orbital electrons). Quantum Mechanics formalises the inability to confirm the physical presence of electrons in orbital zones by invoking **Heisenberg's Uncertainty Principle**, which essentially means that any attempt to observe them in a particular location (e.g. in an orbital) lessens the chance of locating them, let alone determining their momentum and related characteristics. This uncertainty principle is in effect a version of the statistical 'accuracy' versus 'precision' argument extended to the height of absurdity: even an imprecise observation of an orbital electron would be a plus to adding credibility to the stochastic model.

The other argument justifying the lack of physical evidence of orbital electrons is the **Observer Effect**, wherein the act of observing such electrons is considered to change their behaviour, presumably from particle to wave or vice versa.

The Observer Effect and Uncertainty Principle, in isolation or in combination, represent pretty unconvincing explanations for the lack of physical evidence relating to orbital electrons. For E2M electron orbitals around the nucleus are not needed, whereas the SM needs them to balance the charge of a positively charged nucleus.

As can be seen from the simplest of atomic structures such as for H₂ of figure 11, with only 2 protons (consisting of 36 CESs and their associated electromagnetic fields) 3D models quickly become quite complex: this worsens considerably with increasing atomic number. Fortunately, within the nucleus 'L' shaped nucleons combine, interlocking as shown in figure 12 to form layers of 'I' form protons and neutrons: the upper layer has the U-D-U (Up-Down-Up) quark pattern of protons, and the lower layer as shown has the D-U-D pattern of neutrons. Also note that whereas the nucleon layering is shown as a chain in figure 3, within the nucleus the layers form into closed polygonal forms (eg. figure 4).

Thus, rather than the complicated geometries of interlocking 'L' form nucleons, the structure within the nucleus can be represented more readily by proton and neutron layers consisting of overlapping bar-shaped 'I' form nucleons. Using a 'bar' notation to represent 'I' form nucleons the 3D models of the nucleus are simplified, making them more manageable and easier to understand.

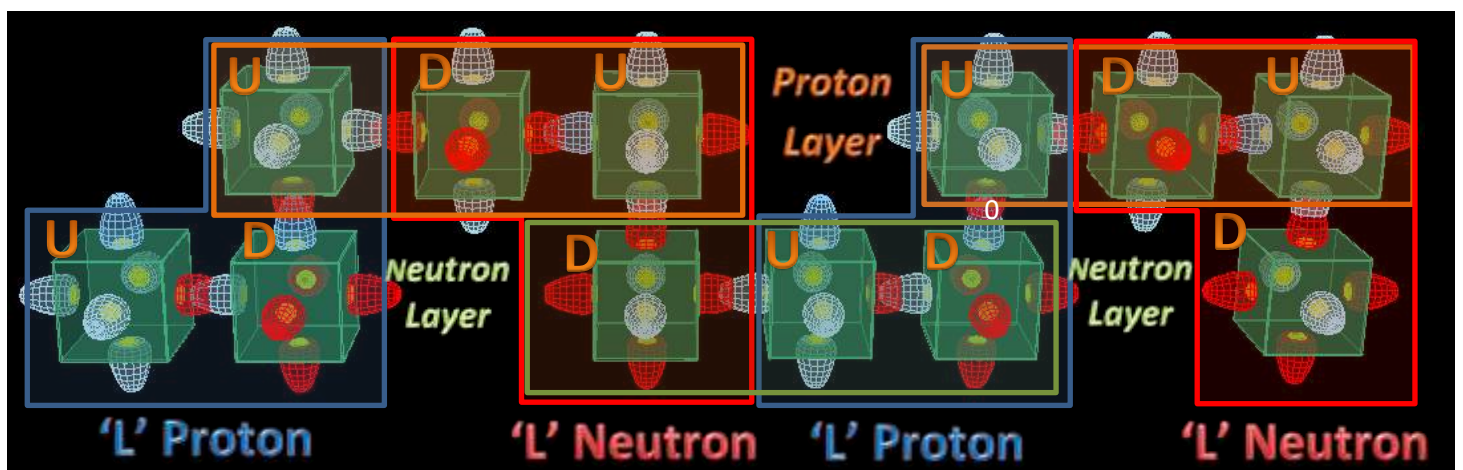


Figure 12: 'L' form Protons and Neutrons Interlock to create 'I' form Proton and Neutron Layers

The convention adopted is to represent '**I**' **protons** by **Golden-Yellow** bars and '**I**' **neutrons** by **Mid-Green** bars as shown in figure 4 for **Helium**. The 'bar' notation considerably reduces complexity due to excessive detail, allowing the nucleus geometry to be appreciated.

The second element in the Periodic Table is **Helium**, which is a colourless, odourless, tasteless, non-toxic, inert, monatomic gas, the first in the **noble gas** group in the periodic table.

He-4 consists of two 'L' form proton and neutron pairs inter-locking to form a 2 proton 'I' form and a 2 neutron 'I' form layer, and made stronger by 3 electron bonds as shown in figure 13.

The compact geometry of helium-4 results in a high binding energy (see graph right) compared with He-3, which consists of 2 'L' form protons, 1 'L' form neutron and only 1 electron bond (it has been generalised in terms of 'I' form nucleons in figure 4).

As **alpha radiation**, the nucleus of He-4 can be quite damaging to other matter over short distances.

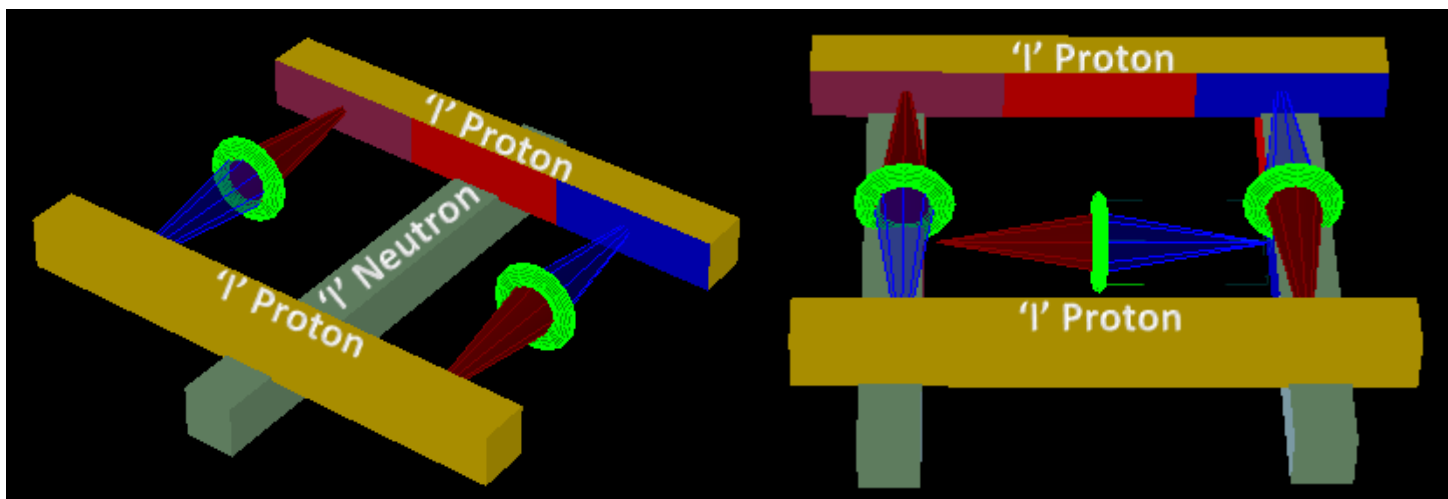
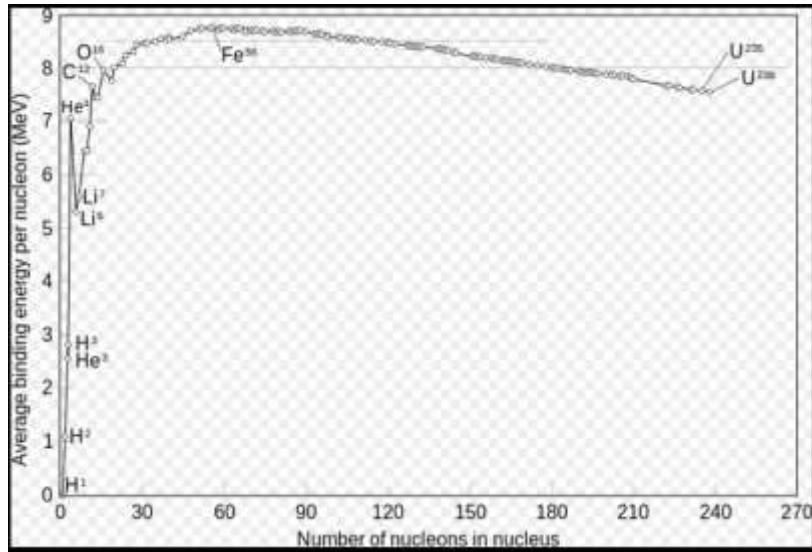


Figure 13: Bar Model of He-3 and He-4

E2M considers that He-4 contains 3 electrons that are internal to the nucleus rather than 2 electrons in the external $1s^2$ orbital as claimed by the 'spdf' model. He-3, on the other hand, is considered to contain 2 internal electrons.

The forth element in the Periodic Table is **Beryllium**, which is a divalent element only occurring naturally in combination with other elements within minerals. As a free element it is a steel-grey, strong, lightweight and brittle alkaline earth metal.

Primordial Beryllium predominantly consists of only one stable isotope, Be-9 (left in figure 14), and thus can be considered monoisotopic. On the other hand, radioactive cosmogenic Be-10 (right in figure 14) is produced in Earth's atmosphere by the cosmic ray spallation of oxygen to accumulate on surface soil. It has a half-life of 1.36 million years, with one of its two extra neutrons beta-decaying (as described earlier) into a proton, converting Be-10 into boron-10.

The extra neutrons of Be-9 and Be-10 are most likely 'L' form neutrons that attach in a variety of electromagnetically favourable positions around the nucleus: certainly a lot more work is required to determine their preferential positions, orientation and behaviour. In the meantime they are colour-coded (a brighter green than a neutron that is part of a neutron layer) to indicate that they are transitional or partially formed I-form neutrons.

Similarly, the relative length of electron bonds and the size of the electron tori are notional to highlight geometry rather than to indicate absolute or relative scale.

Be-9 and Be-10 are very interesting, as they display patterns repeated in elements throughout the Periodic Table. They demonstrate the way in which electron bonds can act as pillar and post supports holding nucleon layers together. For Be-9 there are more likely only 4 inter-layer bonds, with the other 2 neutron-to-neutron bonds being within the neutron layers. Thus the inter-layer bonding of Be-9 is weaker than that for Be-10 (that has 6 inter-layer bonds) and consequently, should it violently lose its extra neutron, the atom readily decays to Helium-4 in the form of alpha radiation.

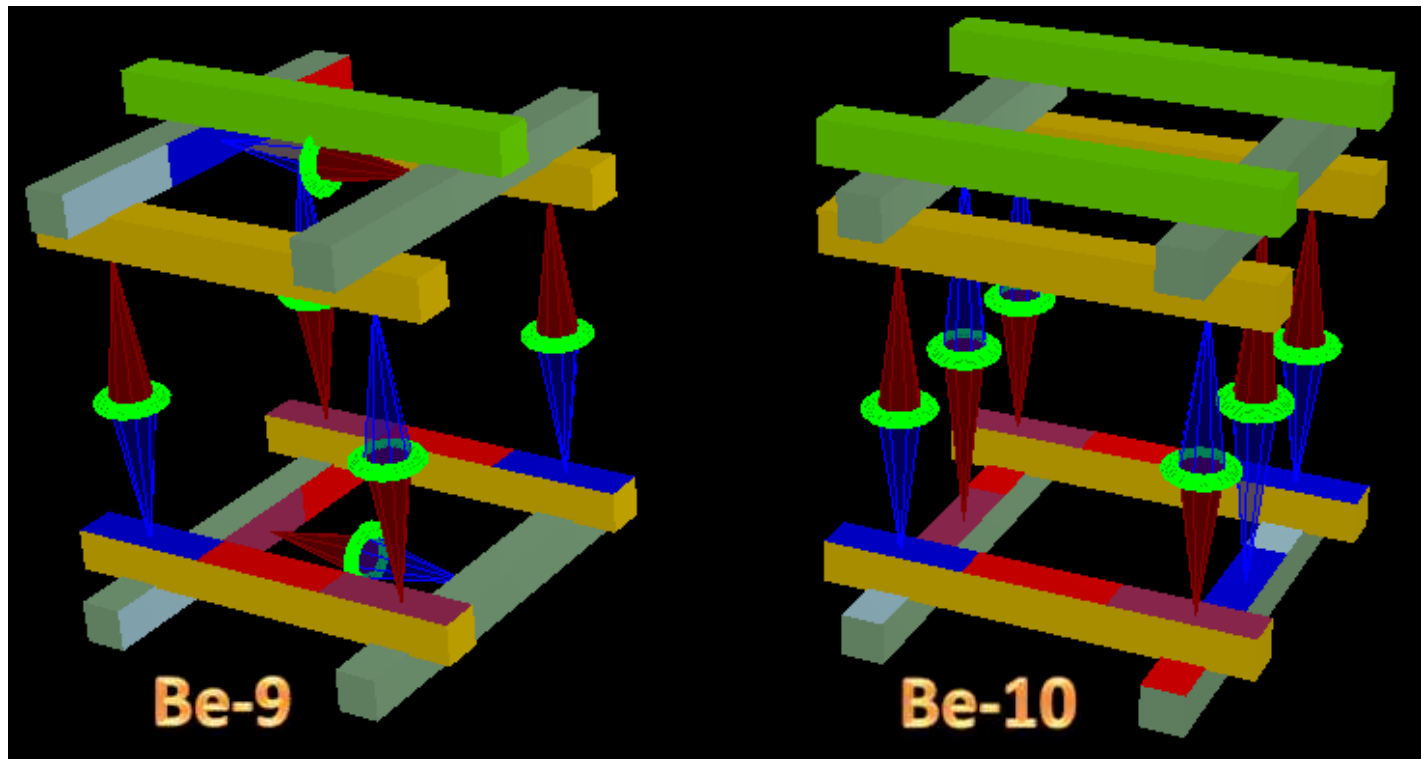


Figure 14: Bar Model of Beryllium-9 and Beryllium-10

For larger atoms further up the Periodic Table, the use of pairs of proton-to-proton (PP) and neutron-to-neutron (NN) bonding to hold nucleon layers together and to hold one polygonal form embedded within another become common features of nucleus structure. Polygonal form embedding will be discussed in more detail shortly.

Also, as the Atomic number of elements increase, so does the size and number of polygonal nucleon layer shapes possible and thus the number of forms an element can take: Carbon 12 is a good example of such **allotropy**.

Carbon is the sixth element in the Periodic Table, and Carbon-12 has two allotropic forms: one hexagonal presenting as **Graphite**, and the other tetragonal form presenting as **Diamond** (figures 15 to 17).

Graphite's nucleus consists of two hexagonal layers each made from 6 overlapping 'I' form nucleons: three neutrons and three protons. The two layers are joined (vertically as shown in figure 15) by nine internal electron bonds: three connecting matching neutrons and six connecting matching protons.

Graphite commonly occurs in sheets wherein external electron bonds (horizontal inter-atom bonding of figure 16) to create a larger-scale hexagonal sheet pattern. Graphite is soft and layered as dictated by its nuclear structure.

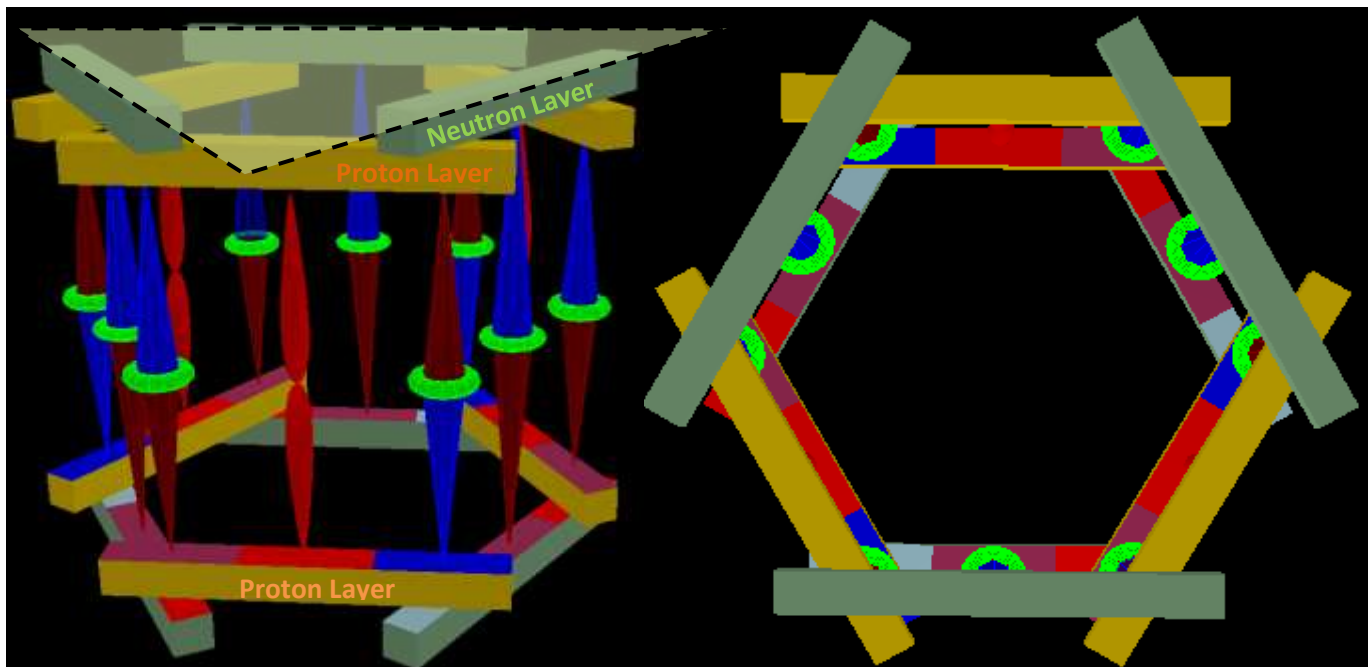
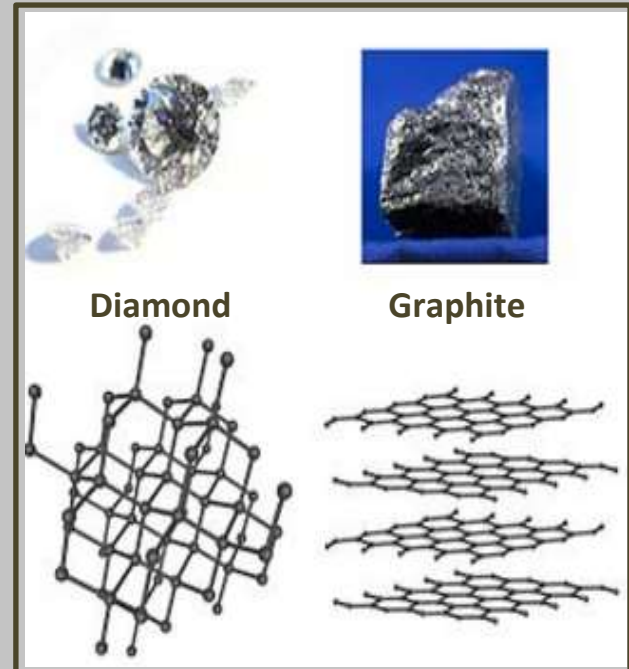
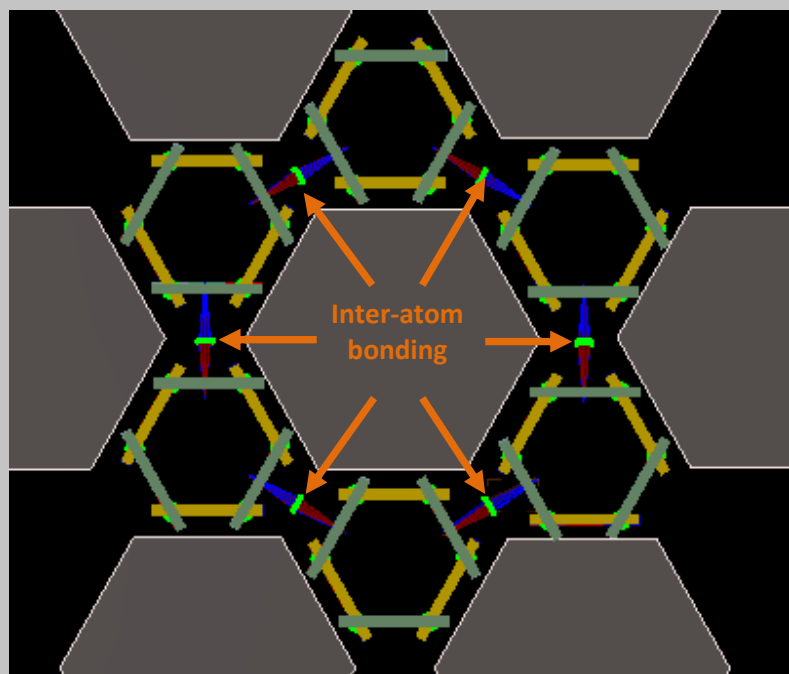


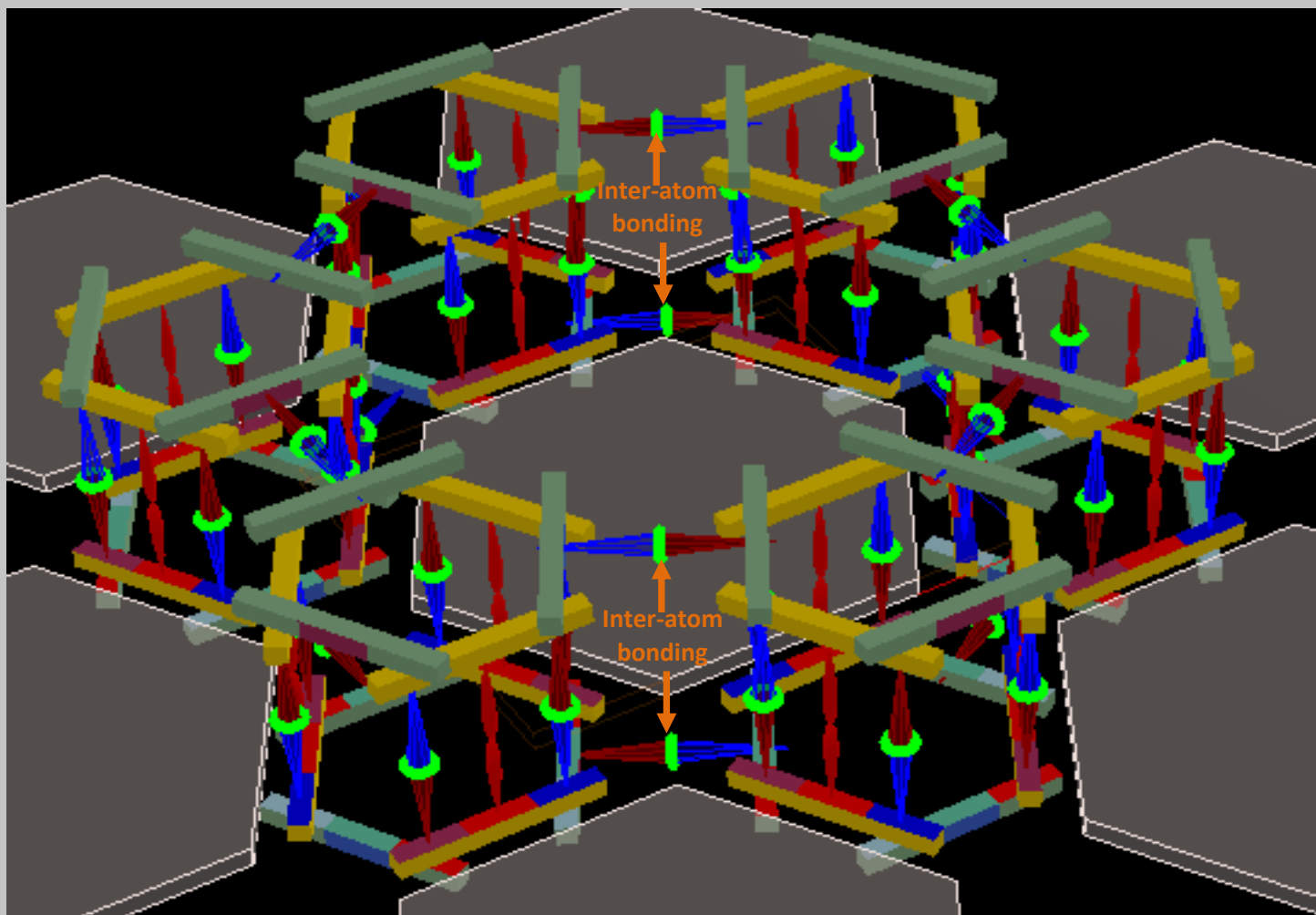
Figure 15: Bar Model of C-12 Graphite: Side and Plan Orthographic Views



Carbon C-12 : Allotropic Forms



Plan View of Graphite C-12 In-Layer Co-Joins



Oblique View of Co-Joined Graphite C-12 Sheets

Figure 16: C-12 Allotropic Forms and Bar Models of Graphite Sheets

The Diamond nucleus, on the other hand, consists of a tight, strong tetragonal structure with nine cross-lashing internal electron bonds, as shown in figure 6. It forms into a cubic-form crystal system resulting in one of the hardest elements in the Periodic Table.

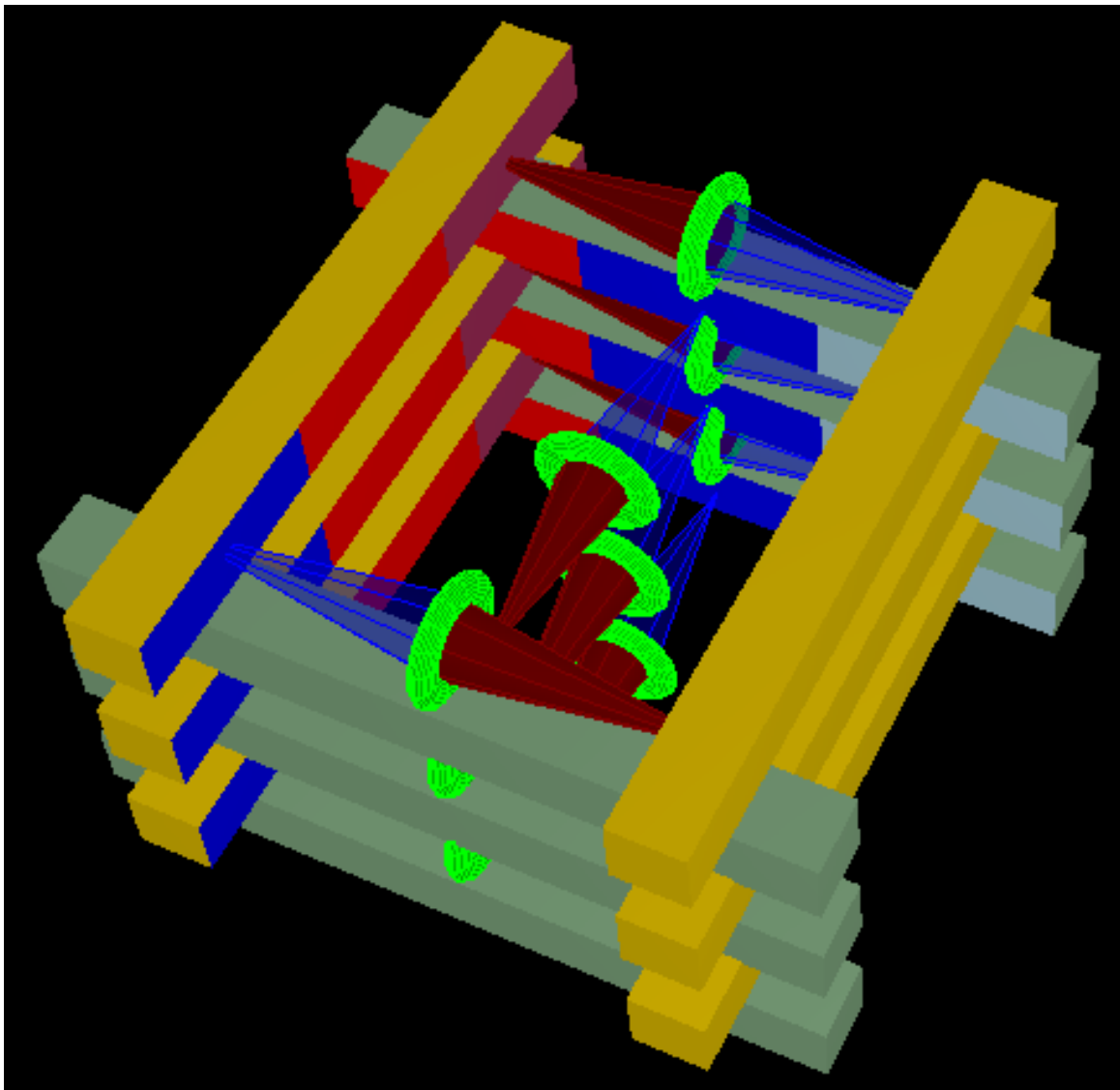


Figure 17: Bar Model of C-12 Diamond

The contrast between the physical characteristics of these 2 allotropic forms of C-12, which have the same nucleon count and internal electron count, is extreme: Graphite is a layered, grey material that is soft enough to be used for pencil 'lead', whereas Diamond is clear and hard enough to cut glass.

E2M contends that the nucleus structure of all of elements in the Periodic Table defines their physical and chemical characteristics.

Thus the key differences in the physical properties of the C-12 allotropes diamond and graphite are considered to be directly attributable to differences in nucleus structure.

Whereas nucleon layers for Carbon-12 can have a tetrahedral or hexagonal form, those for the Oxygen atom have an octagonal form. As atomic number increases, the maximum number of sides that a polygonal nucleon layers can adopt increases, but the polygonal forms for nucleus layers can only be in even side number increments, as they are formed by linked L-form nucleons (or inter-locked L-formms) of adjacent proton and a neutron layers. Polygons with an odd number of sides can only appear as a subset of a larger polygon with an even number of sides (e.g. pentagon geometries can only be a subset of a decagon geometry). The range of polygonal possibilities and their layer count (per pattern per element) can be seen in the arithmetic progressions of the figure 10 tabulation.

The 8th element of the Periodic Table is **Oxygen**, which is a highly reactive non-metal and oxidizing agent that, by mass, is the third-most abundant element in the universe after hydrogen and helium. At standard temperature and pressure, two atoms of the element oxygen bind to form dioxygen, a colourless and odourless diatomic gas with the formula O₂, which constitutes 20.8% of the Earth's atmosphere. As compounds, including oxides, the element makes up almost half of the Earth's crust.

The **Oxygen** atom has 12 electrons as 8 proton and 4 neutron inter-layer bonds. **Dioxygen** (O₂) has 24 electrons (22 well protected inter-layer electrons and 2 covalent bond electrons) as shown in figure 18.

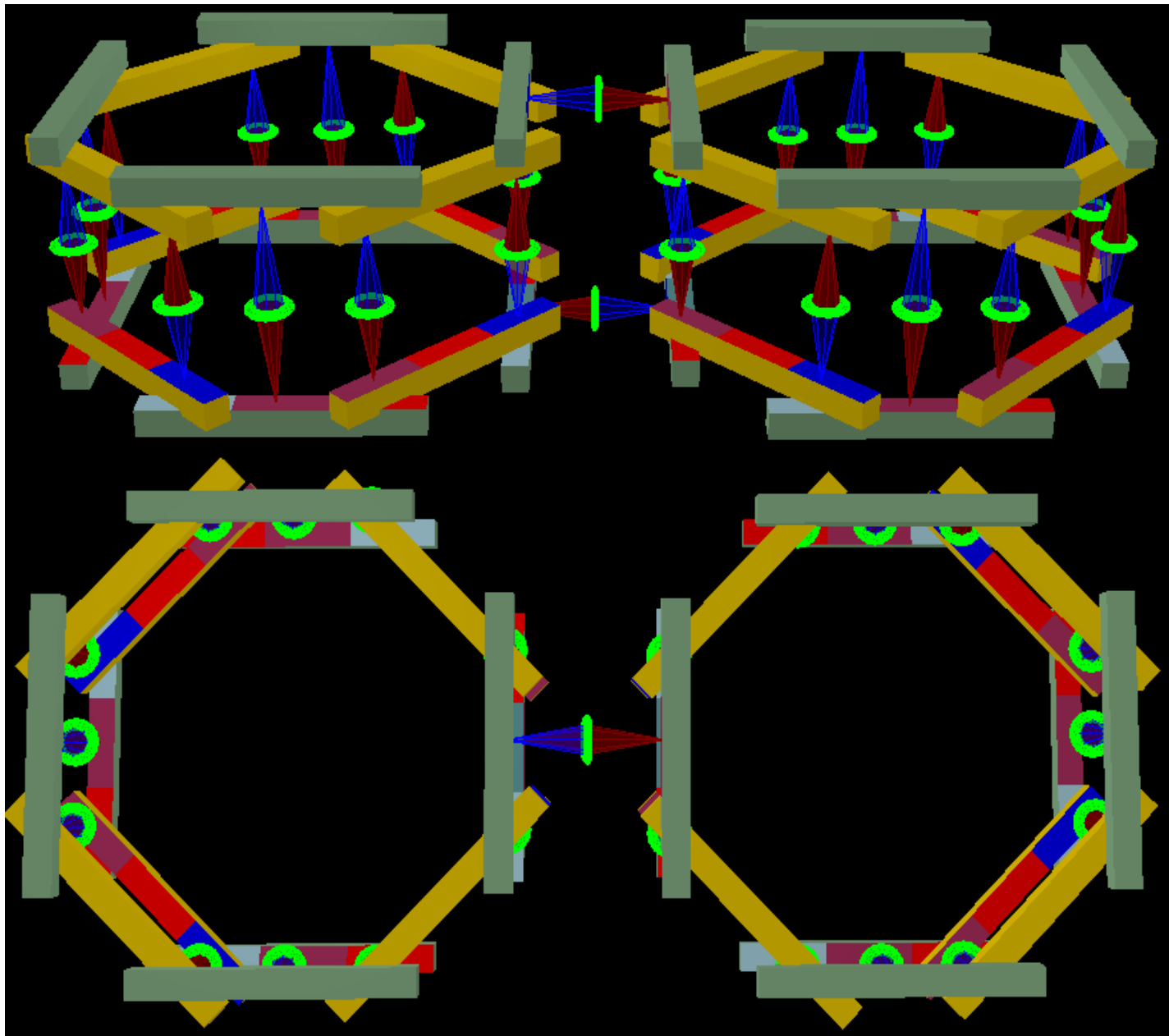


Figure 18: Bar Model of Dioxigen (O_2)

As well as the development of larger polygonal forms, the increase in atomic number of elements within the Periodic Table is also accommodated by the embedding of one polygonal form within another. Such embedding of one atomic structure within another starts at the lower end of the Periodic Table with Beryllium-9, which contains two embedded He-4 molecules and continues with larger polygonal forms further up the Periodic Table.

Elements of the 3rd period are transitional embedding tetragon forms within octagon forms (figure 11 and ↓ in table right).

By the 4th and 5th period the hexadecagon (16-gon) form is added (lower figure 24 graphic), with the triacontadigon (32-gon) by the 6th period.

Similar embedding of hexagon forms within the dodecagon (12-gon) form is possible, even extending to the tetracosagon (24-gon) form.

Framework Geometry	Period Number						
	1	2	3	4	5	6	7
Tetragon				↓	↓	↓	↓
Octagon				↓	↓	↓	↓
Hexadecagon					↓	↓	↓
Triacontadigon						↓	↓

Periods 1 to 3 Potential Nucleus Structures

	----- Polygon Names/No. Sides of Polygon/External Angles/Level Adjacent Face Angles -----																
	D	H	T	r													
	d	x	t	i													
	T			e			t			r			i			c	
names	T	H	O	D	d	o	a	D	e	a	c	o	s	a	d	i	
# polygon sides	4	6	8	10	12	14	16	18	20	22	24	26	28	30	32	34	36
# protons	2	3	4	5	6	7	8	9	10	11	12	13	14	15	16	17	18
External Angle Degs	90	60	45	36	30	25.71	22.5	20	18	16.36	15	13.85	12.86	12	11.25	10.59	10
Level Adjacent Angle	180	120	90	72	60	51.43	45	40	36	32.73	30	27.69	25.71	24	22.5	21.18	20
AN Element	----- Possible Nuclide Geometries and Layer Counts -----																
H																	
2 He	1																
3 Li	1																
4 Be	2 1+1 1																
5 B	1+2 1+1 1																
6 C	3 2 1															Magnesium Diborate (MgB ₂) = Hexa	
7 N	2+1 1+2 1															Decaborane (B ₁₀ H ₁₄) = Hexa	
8 O	4 2 1+3 1															Racetams (drug class) and Pyrrolidine/tetrahydropyrrrole (CH ₂) ₄ NH, NH ₃ = Deca	
9 F	3 1															Tetrahydrofuran (THF)	
10 Ne	5 2 1																
11 Na																1	
12 Mg	6 4 3 2 1																
13 Al																1	
14 Si	7 5 4 3+4 2 1															Siloles (silacyclopentadienes) = Deca	
15 P	5 3 1															1	
16 S	8 4 3+1 2 1															1	
17 Cl																1	
18 Ar	9 6 3 2 1															1	

Figure 19: Nuclei Polygonal Forms for Periods 1 to 3 of the Periodic Table

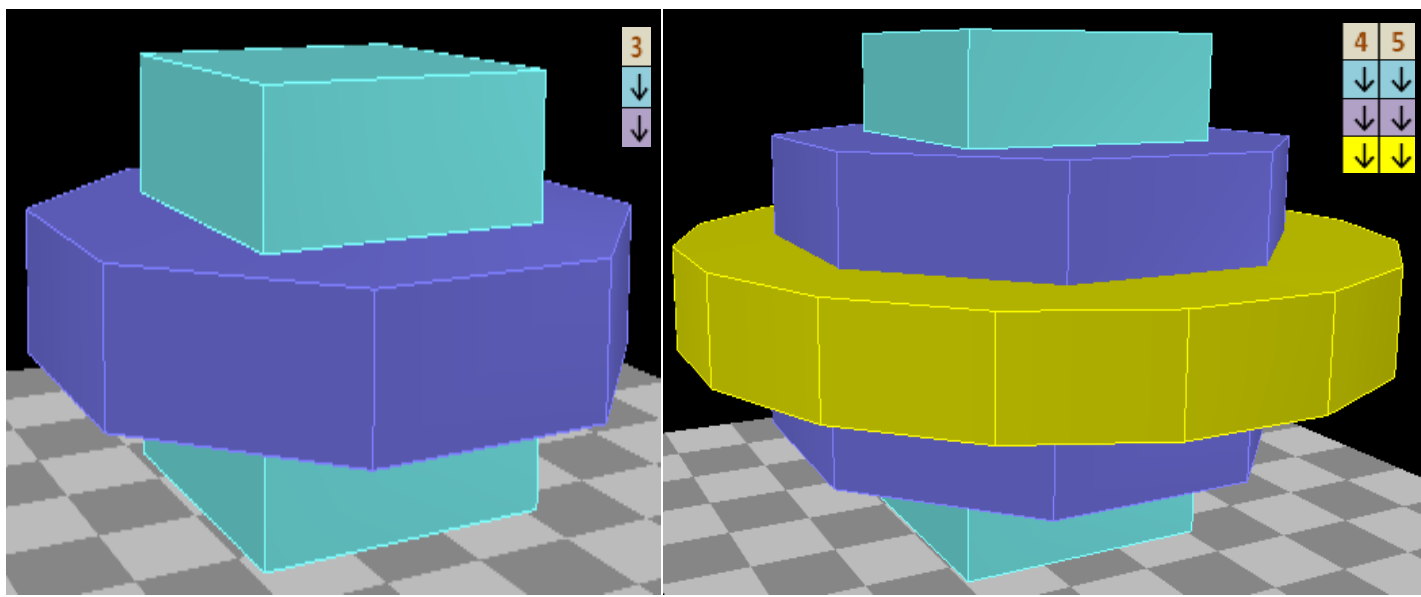


Figure 20: 4-8-16 Polygonal Embedding of Nuclei (Period 3 and Onwards)

The embedding of polygonal forms is well demonstrated by comparing the atomic structure of Copper, Silver and Gold in group 1B spanning periods 4 to 6 of the periodic table and having atomic numbers 29, 47 and 79 respectively.

Figure 21 shows nested tetragon, octagon and hexagonal proton/neutron layers for Cu-63 and the SM equivalent (insert of figure 21). The larger outer ring structure consists of 2 hexagonal nucleon layers separated and supported by a combination of proton and neutron electron bonds (vertical as shown). The octagonal layers are attached to the enclosing hexagonal layers by 16 proton electron bonds (4 sets of 4 shown as horizontal offset by 90° to each other). The nested tetragon is more rigidly attached to the enclosing octagon by neutron electron bonds.

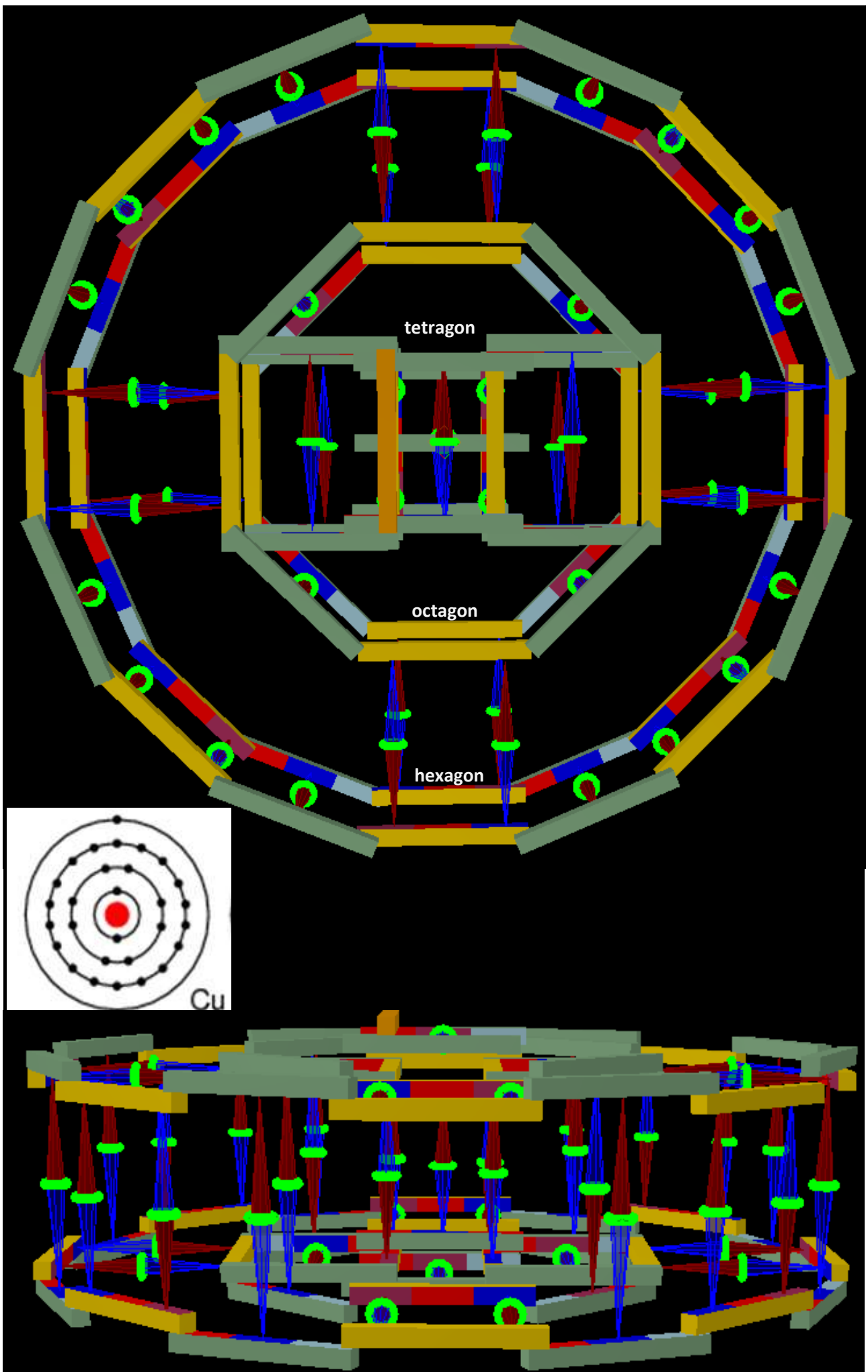


Figure 21: Bar Model of Copper-63

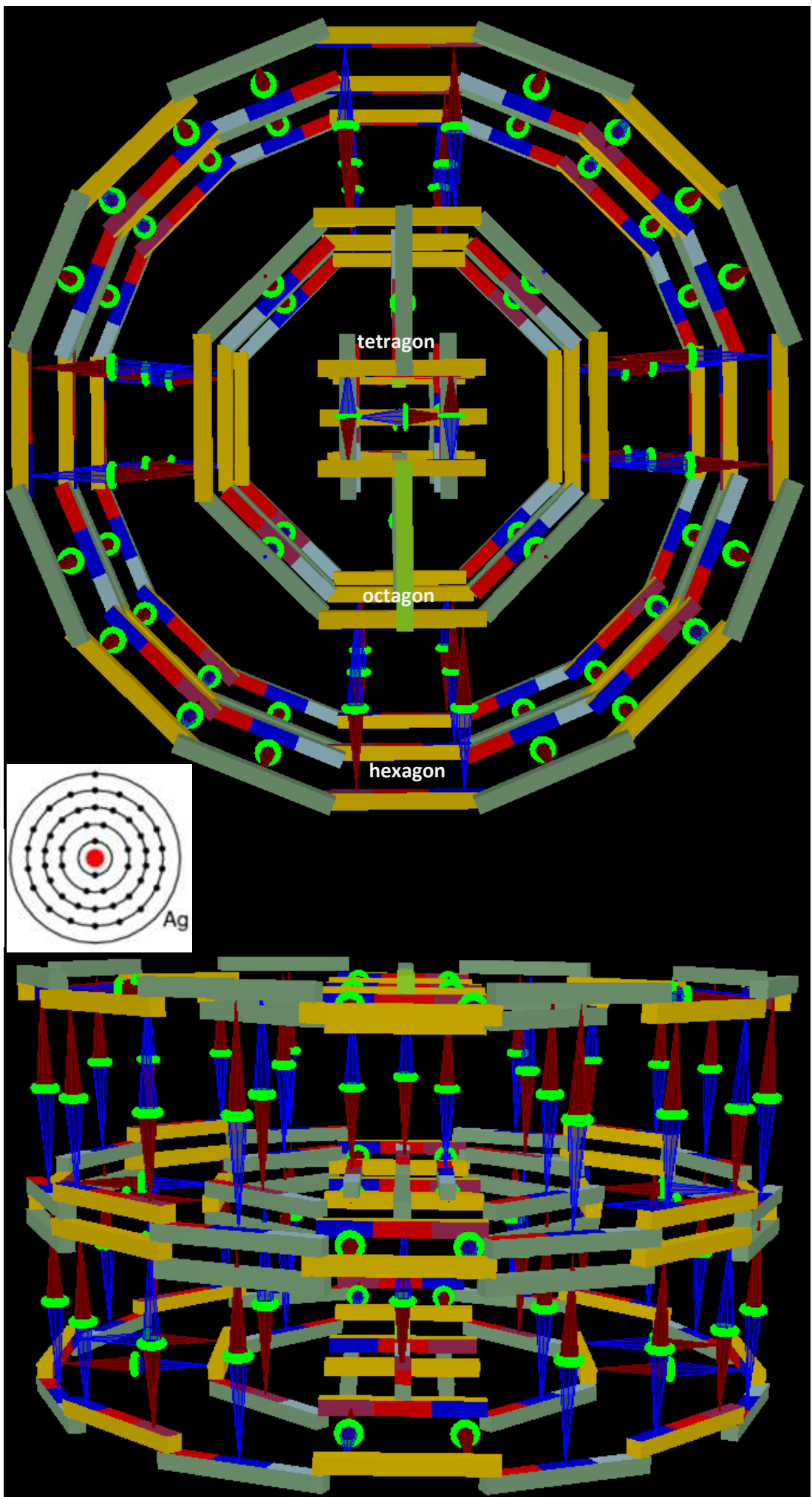


Figure 22: Bar Model of Silver-107

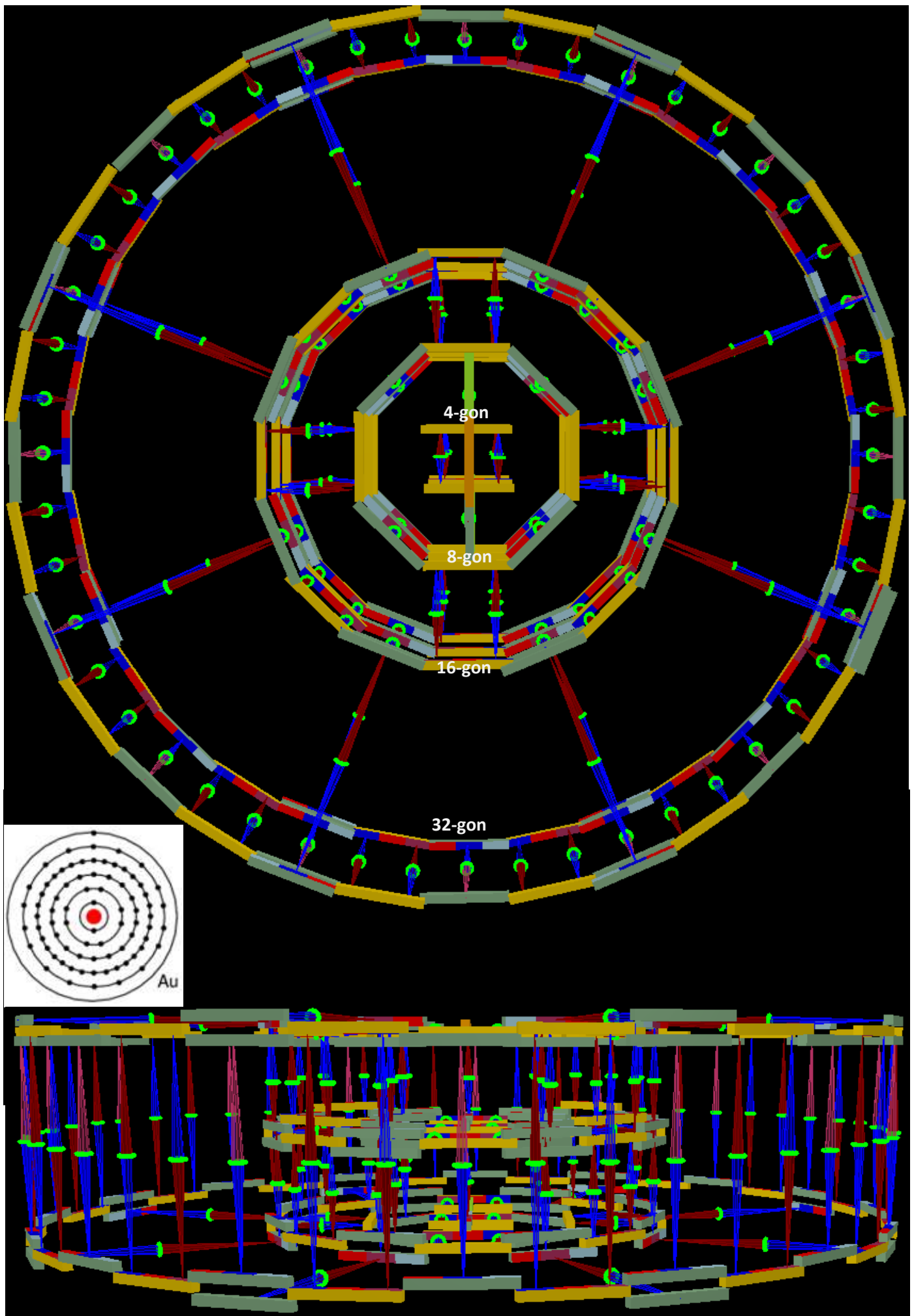
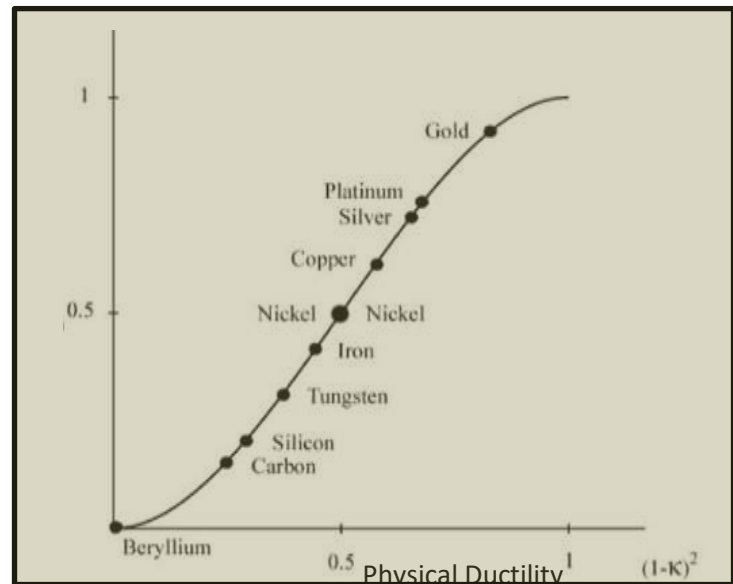


Figure 23: Bar Model of Gold-197

The physical characteristics of Copper, Silver and Gold match quite well to the E2M atomic model for them. Gold's two triacontadigon (32-gon) layers (figure 23) overlap its central hexagon layer contributing to its malleability - Gold is the most malleable of metals, followed by Silver, Aluminium and Copper.

Gold and Silver are also the 2 most ductile of metals (see graph right) with Copper being the 6th behind Platinum, Iron and Nickel. Also, the Shear Modulus of Copper is 48 GPa, reflecting its more compact form, compared with 30 and 27 GPa for Ag and Au respectively.

The SM represents the nucleus as an amorphous conglomerate of nucleons with no particular structure of note apart from size. E2M, on the other hand, claims that the unique structure each atom's nucleus contributes towards its physical form and characteristics. Even for large atoms such as Copper, Silver and Gold, each proton and neutron is needed and accounted for within their structure, as shown in their 3D bar models and summarised in the table below.



Metal Isotope	Level 1 (Top)		Level 2 (Middle)		Level 3 (Bottom)		Totals	
	Protons	Neutrons	Protons	Neutrons	Protons	Neutrons	Protons	Neutrons
²⁹ Cu-63	14+1	17	-	-	14	17	29	34
⁴⁷ Ag-107	15	15+1	18	28	14	16	47	60
⁷⁹ Au-197	30+1	46	18	26	30	46	79	118

Nucleons cannot just be added to the nucleus arbitrarily here and there to build up nucleon numbers and to transform one element's structure into that of another that might be structurally similar (e.g. from a Copper atom to Silver to Gold): there are changes in structure that have proven to be quite subtle and non-intuitive. For example:

- an additional neutron layer to support the central hexagonal layer in Silver and Gold;
- an additional neutron layer to support Gold's two triacontadigon (32-gon) layers;
- a weakening of the tetragon structure for Gold from that for Copper and Silver; and
- the staggered neutron bond supports between the tetragon layers within Gold.

Importantly, there is little room to vary the nucleon geometry for a particular isotope of an element. Apart from Carbon allotropes, the nucleon count corresponds to only one geometry, making it unique. However, the geometry may include several polygonal forms that resemble the nesting of other elements of a smaller atomic number. Should one or more nucleons be different or out of place, then you have a different element or isotope that may or may not be stable.

Bonding and Free Electrons

Bonding between CESs within up and down quarks can only occur when the facing poles have the opposite electric charge, thus having the same circular electromagnetic energy flow direction. Should the pole charge be opposite then should the magnetic poles also be opposite, then a strong bond, such as those holding the up and down quarks together to form the nucleons, is formed; otherwise an electron or positron bond is formed should the facing magnetic poles be the same, as shown in the table right. No bond is formed for any other combination.

Bond Type	CES1	CES2
Inter-quark bond (Strong Force)	N+	S-
	S+	N-
Bitron (Electron/ Positron) bond	N+	N-
	S+	S-

The bonds holding up (U) and down (D) quarks together to form 'L' form protons (U-D-U) and neutrons (D-U-D), and binding 'L' form nucleons together to create 'I' form nucleon layers are strong **inter-quark bonds**. As well as being very strong, inter-quark bonds act as two-way conduits (blue or orange flow directions in figure 24a) to distribute energy evenly throughout nucleons and nucleon layers.

When two CESs having opposite chirality are held in close proximity, an electromagnetic stability or bond results. Should their North poles (N^+ and N^-) or their South poles (S^+ and S^-) be facing each other, their swirling electromagnetic fields overlap so as to concentrate energy between them as a torus-shaped structure called a **bitron**, resulting in a **bitron bond**. The bitron is a tentative toroidal concentration of electromagnetic energy that is a precursor to the generation of an electron or a positron. Its maximum contained energy is the same as that of an electron, but its concentrated energy has a circular rather than a solenoidal flow pattern (typical of an electron or positron), as shown by the alternative blue and orange flow direction arrows of figure 24b.

It is only as it is physically removed from the bond field that the energy flow pattern of a bitron takes on a solenoidal (i.e. with small radius spin) flow pattern as a free electron or positron. The chirality of the solenoidal flow is dictated by which side of the bond field (i.e. the CES1 or CES2 side) that the bitron exits: statistically a bitron has equal probability of becoming an electron or a positron. (Note: so far in this article a **bitron bond** has been loosely referred to as an **electron bond**).

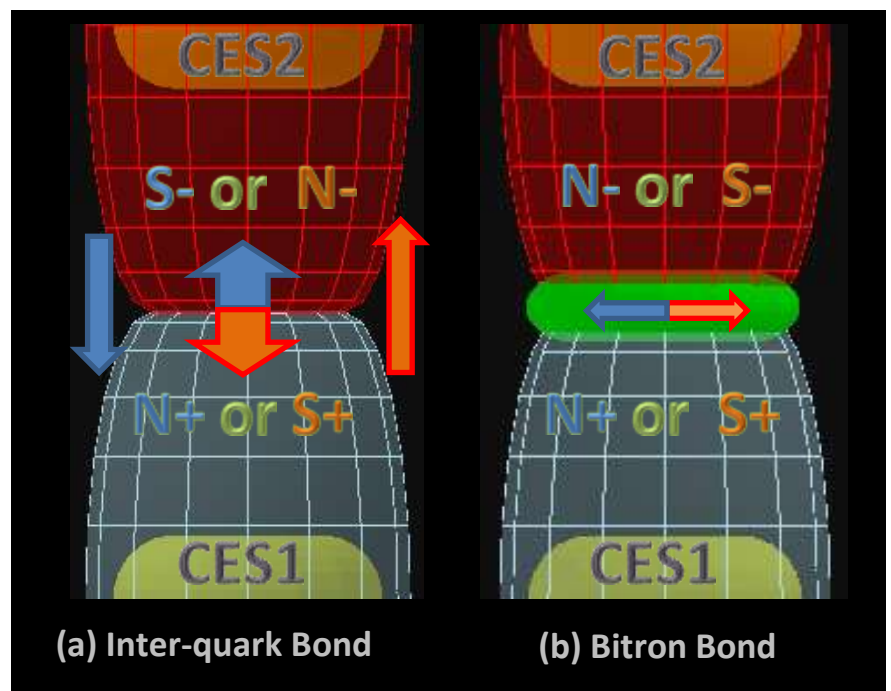


Figure 24: Inter-Quark and Bitron Bonding

The central postulate of E2M is that there is only one fundamental source of electromagnetic energy from which normal matter is formed, and that source is the CES. Thus all other energy manifestations, including electrons, positrons, neutrinos, anti-neutrinos, quarks, nucleons and photons, are derived directly or indirectly from CESs.

Free electrons and **free positrons** can be created by the electromagnetic bump-release of the bitron from a bonded pair of CESs; or by radioactive decay; or by chemical reactions (wherein bitron bonds are formed and/or re-assigned).

When an electromagnetic force (emf) is applied across a conductor (most metals), free electrons and positrons are aligned and induced to move as a current (see [Appendix B](#)). When the emf is removed, the free electrons and positrons are randomly aligned by the electromagnetic fields of nearby bitron bonds and to un-bonded outward facing CES tori of nearby atoms.

For **catalysis** (a pre-cursor to many chemical reactions), some **enablers** (chemicals involved in a starter chemical reaction) can induce free electrons and positrons to become loosely attached to the outward-facing side of an un-bonded CES. Such attachment extends the strength and reach of that CES's electromagnetic field, and thus its potential to attract and bond with other atoms and partake in chemical reactions. This process is referred to as **nucleon electron capture**: it should not to be confused with β decay related electron capture [described earlier](#).

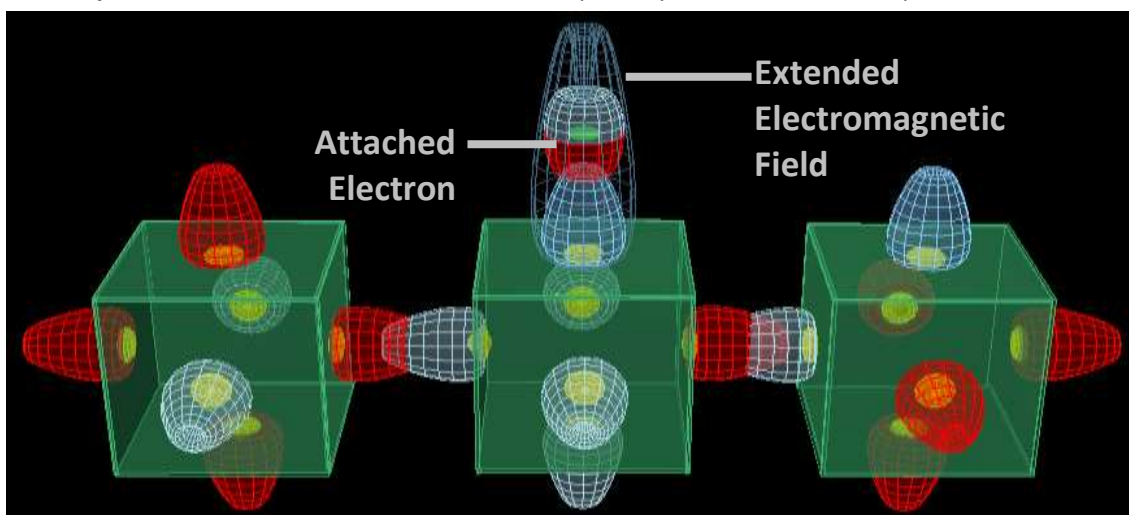


Figure 25: Free Electron Attachment to an 'I' form Neutron

Complex Chemical Compounds

A chemical compound is composed of atoms from more than one element held together by chemical bonds. For E2M chemical bonds result from bitron bonds or electromagnetic adsorption (e.g. oxygen adsorption). Conventional and E2M descriptions for specific types of chemical compound formation are summarised in the table:

Compound Type	Conventional Description	E2M Description
<u>Molecules</u>	An electrically neutral group of two or more atoms held together by chemical bonds (electron transfer or sharing).	An electrically neutral group of two or more atoms held together by bitron bonds.
<u>Ionic Compounds</u>	An electrically neutral chemical compound composed of ions held together by electrostatic forces between positively charged ions (cations) and negatively charged ions (anions).	An electrically neutral group of two or more atoms held together by bitron bonds. As separate ions (e.g. in solution) cations have a majority of their out-facing CES poles being a positive (N^+ or S^+), and a negative (N^- or S^-) majority for anions.
<u>Intermetallic Compounds</u>	Composed of definite proportions of two or more elemental metals wherein electrons form what may be termed an "electron sea" in which valence electrons are free to move from one atom to another to create a bonding effect.	Composed of definite proportions of two or more elemental metals, which pack due to the size and geometry compatibility of their nuclei that allows their atoms to inter-lock with possible electromagnetic adsorption between nuclei.
<u>Coordination Complexes</u>	Consists of a central atom or ion (often a metal) called the coordination centre, and a surrounding group of ligands (bound molecules or ions).	Consists of a central atom or ion (often a metal) called the coordination centre, and a surrounding group of ligands (bound molecules or ions) held by bitron bonds.

Electromagnetic **adsorption** occurs when atoms are aligned so that the bitron bonds supporting their nucleon layers interact, bending each other to create a bond, which, for oxygen adsorption, is only slightly less strong than bitron bonding. With bitron bonds under stress, many bitron tori are released as free electrons and positrons, resulting in high electrical and thermal conductivity.

Interstitial alloys provide examples of where adsorption is the main type of bonding. Figure 26 shows Cu-Au adsorption for Rose (or Russian) Gold, which is an interstitial alloy (e.g. 18K rose gold is 75% gold, 22.25% copper, 2.75% silver). For **substitution alloys** (e.g. bronze and brass, where some Cu atoms are substituted with either Sn or Zn atoms respectively) the size and electromagnetic structure of the base metal and alloying agents must be compatible.

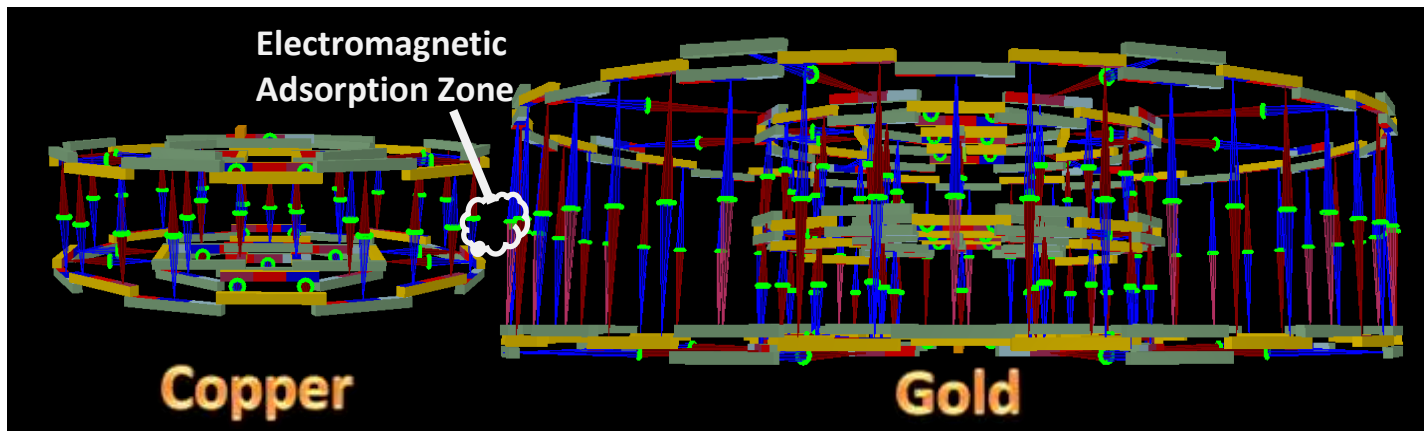


Figure 26: Electromagnetic Adsorption between Copper and Gold Atoms

As a noble metal, gold does not electron bond with oxygen. The top part of figure 27 shows two alternative models of oxygen (within water molecules) adsorption patterns for gold nanoparticles. Both patterns are compatible with the E2M model for gold, with water molecule potential bonding locations for each adsorption pattern shown by the symbols \otimes and \oplus . For oxygen such adsorption is only slightly less strong than that of bitron bonding.

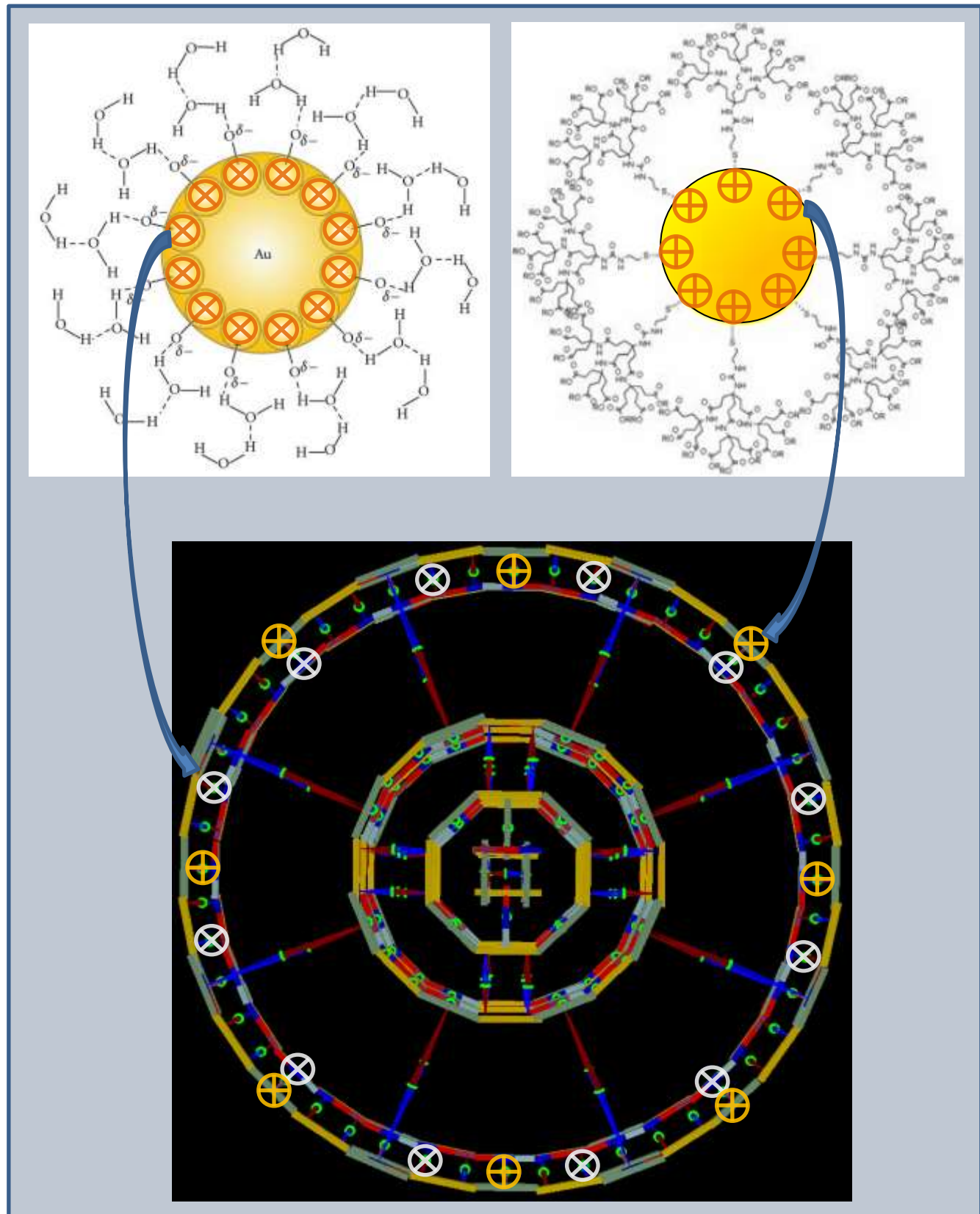


Figure 27: Models for Gold Nanoparticles in Water

As well as nucleon electron capture as already described, some catalysis enablers (chemicals involved in a starter chemical reaction that is reversed by the end of the main reaction) can induce the inter-layer bonds of reactant molecules to bend and stress to breaking point. Thus such enablers are active in the formation of reactant ions, which chemically interact to create molecular and ionic compounds via the formation of the appropriate bitron bonds.

Adsorption is the bond-like attraction between certain elements and compounds that can act as a pre-cursor to facilitate a chemical reaction that involves the breaking of inter-layer bitron bonds, the freeing of electrons and/or positrons, and the creation of new bitron bonds and accompanied by related energy transfers. Whilst not the only effective adsorption mechanism, water based oxygen adsorption is quite strong and widespread, enabling many chemical reactions, particularly those involving ions in aqueous solutions.

Bitron bonding also commonly occurs on the top and bottom nucleon layers of an atom. Nucleons not locked into a complete nucleon layers (i.e. are attached as an 'L' form nucleon), and excess neutrons in particular, are excellent candidates for chemical reactions involving bitron bonding with other elements, molecules or compounds. Most molecules and compounds have one or more top/bottom bitron bonds.

For the Standard Model, the **valency** (or **oxidation state**) of an element (figure 28) is determined by the number of outer shell (valence) electrons, and for polyatomic ions (such as SO_4^{2-}) is the charge associated with the ion. For E2M valency relates to the total number bitron bonds formed via adsorption of external inter-layer bitron supports (as in figure 26 plus bitron bonds involving nucleons on the top and bottom nucleon layers. Atoms may display multiple valencies depending upon the degree of adsorption of outer vertical bitron supports, and upon the top and bottom nucleon layer landscape (i.e. the preferential bond sites), and to which side (i.e. top or bottom) of the atom that other elements and compounds attach.

Compound	NH_3 Ammonia	NaCN Sodium cyanide	H_2S Hydrogen sulfide	H_2SO_4 Sulfuric acid	Cl_2O_7 Dichlorine heptoxide
Diagram	$\begin{array}{c} \text{H} \\ \\ \text{H}-\text{N}-\text{H} \end{array}$	$\text{Na}-\text{C}\equiv\text{N}$	$\begin{array}{c} \text{H} \quad \text{S} \quad \text{H} \\ \quad \backslash \quad / \\ \text{H}-\text{S}-\text{H} \end{array}$	$\begin{array}{c} \text{O} \\ \\ \text{HO}-\text{S}-\text{OH} \\ \\ \text{O} \end{array}$	$\begin{array}{c} \text{O} \quad \text{O} \\ \diagup \quad \diagdown \\ \text{O}=\text{Cl} \quad \text{O}-\text{Cl}=\text{O} \\ \diagdown \quad \diagup \\ \text{O} \quad \text{O} \end{array}$
Valencies	Nitrogen: 3 Hydrogen: 1	Sodium: 1 Carbon: 4 Nitrogen: 3	Sulfur: 2 Hydrogen: 1	Sulfur: 6 Oxygen: 2 Hydrogen: 1	Chlorine: 7 Oxygen: 2

+1		Valency Table						0	
H	Be	B	C	N	O	F	He		
Li	Mg	Al	Si	P	S	Cl	Ne		
Na	Ca	Ga	Ge	As	Se	Br	Kr		
Rb	Sr	In	Sn	Sb	Te	I	Xe		
Cs	Ba	Tl	Pb	Bi	Po	At	Rn		
Fr	Ra								
1 group	2 group	3 group	4 group	5 group	6 group	7 group	8 group		

transition metals

Members of this group of metals display a number of valencies

Figure 28: Valency Groupings and Diagrams

The geometry of chemical compounds is greatly influenced by the polygonal shape of the nucleon layers. Looking at an atom from the top or bottom perspective, lateral bitron bond angles are dictated by the polygonal shape of an atom's nucleon layers. Vertical (or near vertical) bitron bonds are dictated by the top and bottom layer landscape.

All bonded groupings will adjust their position in space in accordance to the net electromagnetic field generated by all attached atoms. The net electromagnetic field acting on vertical members is always symmetrical and provides them with strength and stability. Lateral bonds, on the other hand, are usually formed by the central up quark of an 'I' form neutron, which provides for rotation in a vertical plane, and are thus able to move vertically up and down to adjust to the net electromagnetic field around them.

Using Methane (CH_4) as an example, the C-12 atom has three bitron bonds firmly securing a Hydrogen atom (i.e. a proton) above its top nucleon layer as shown in figure 29, connected to the three neutrons in the upper nucleon layer. The corresponding three neutrons in the lower nucleon layer are each attached laterally to single hydrogen atoms via single bitron bonds. Within the original intact single C-12 atom the 3 pairs of neutrons would have originally been

bitron bonded together, acting as vertical supports: however these were broken and re-assigned to bond with hydrogen atoms to form methane as shown.

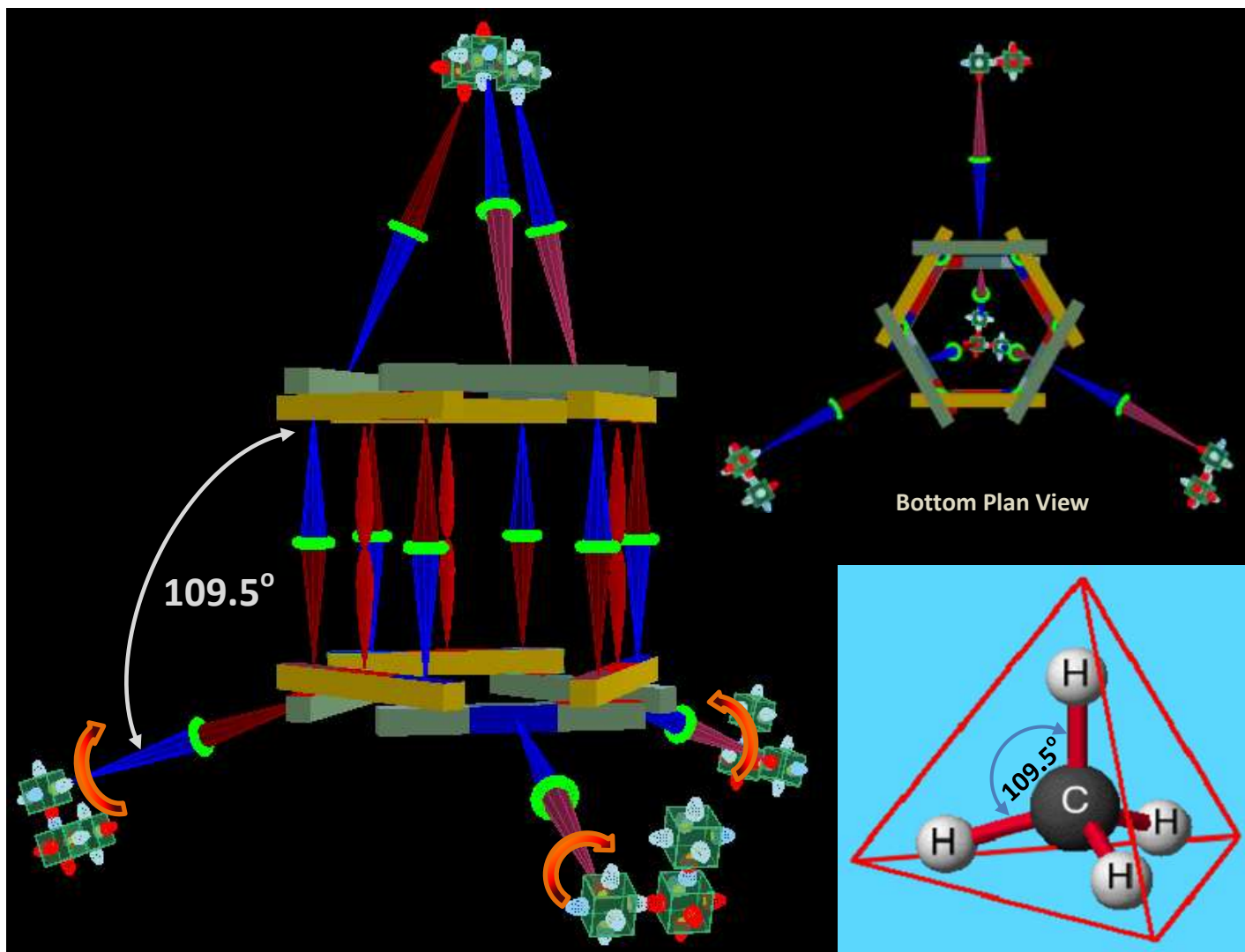


Figure 29: Bar Model for Methane (CH_4)

Within nucleon layers, down quarks within 'I' form neutrons have the ability to rotate when they are not rigidly bonded to another neutron layer within an atom's structure. In methane, the three lateral bonds with hydrogen atoms are free to swing in a vertical plane, hinged by their 'I' form neutron. The hydrogen atoms (i.e. protons) spin about their bitron bond's long axis quite rapidly to create a uniform electromagnetic field around each of the lateral hydrogen atoms. The vertical hydrogen atom, on the other hand, is rigidly held aloft by the three top nucleon layer's bitron bonds with little chance of movement or rotation.

The net result is a stable equilibrium resulting in a strong structure with the three lateral bonds being equal spaced and separated by 120° when viewed in plan projection, 109.5° to each the vertical bitron bond and to each other, forming a tetrahedral geometry.

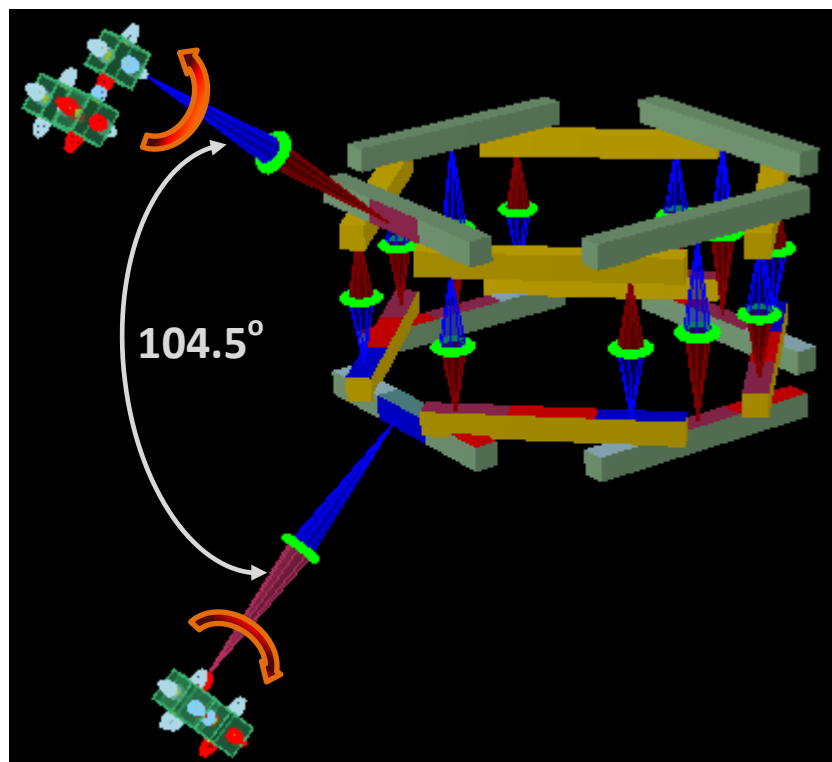


Figure 30: Bar Model for Water (H_2O)

For water (H_2O) the two hydrogen atoms are bitron bonded to a pair of neutrons in the top and bottom nucleon layers of an oxygen atom, as shown in figure 30. The free swivel action of these bitron bonds means that in the gaseous state the angle between them and the length of the bonds vary, or more accurately, vibrate around the mean angle of 104.45° and 0.9584 \AA (see graphs and notes of figure 31 which are from the [World of Molecules](#) web site).

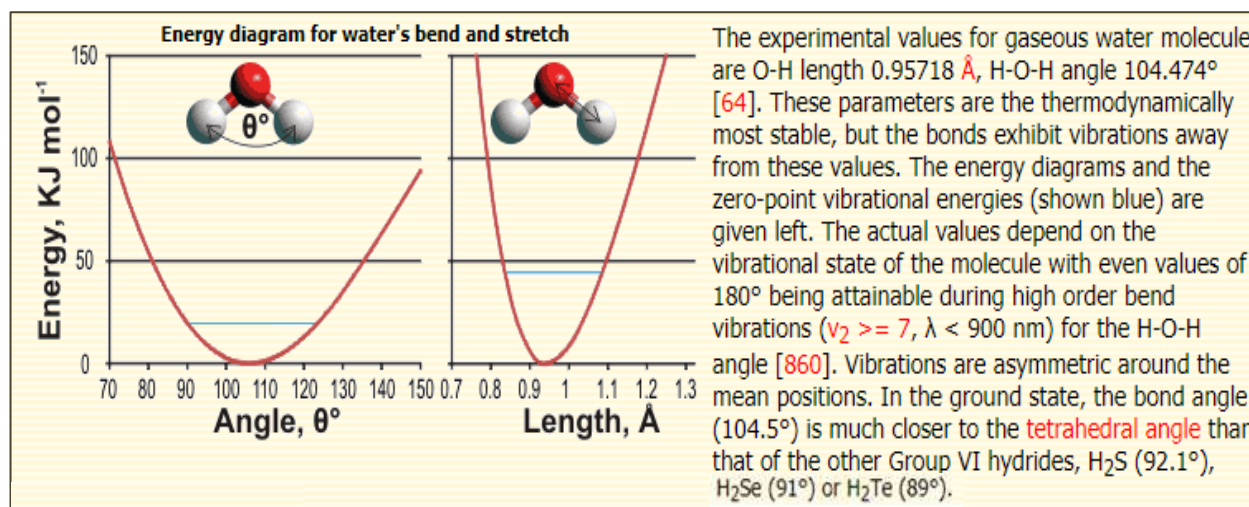


Figure 31: Bond Variation of Gaseous Water (steam)

Figure 32 shows examples of two-coordination (linear bonding) to six-coordination bonding: all examples show vertical bitron bonds (one top and/or one bottom). The trigonal planar, tetrahedral and trigonal by-pyramidal geometries (the 3 to 5-coordination examples) require hexagonal nucleon layers, whereas the others could correspond to tetragonal, hexagonal, octagonal or larger polygonal nucleon layers.

Shape	Geometry	Examples
Linear		BeCl_2 , HgCl_2 , CO_2
Trigonal planar		BF_3 , CO_3^{2-} , NO_3^- , SO_3
Tetrahedral		CH_4 , PO_4^{3-} , SO_4^{2-} , ClO_4^- , TiCl_4 , XeO_4
Trigonal bipyramidal		PCl_5 (with bond lengths: axial Cl 214 pm, equatorial Cl 202 pm, axial-P-Equatorial angle 90°, Equatorial-P-Equatorial angle 120°)
Octahedral		SF_6 , WCl_6

Figure 32: Atomic Geometry of Chemical Compounds

Whereas conventional science struggles to explain the bonding geometry of chemical compounds by complicated scenarios involving the sharing of orbital electrons, E2M provides uncomplicated and logical explanations involving the polygonal form of nucleon layers and the flexibility (albeit somewhat restricted) of neutron-based bitron bonds.

Photons, Energy Transfer and Spectral Lines

The wave nature of EMR has allowed the [allocation of wavelengths for the complete EMR spectrum from Gamma to long radio wave](#), complete with a detailed colour map of EMR by wavelength in the visible light range. From the colour of light, its wavelength can be determined and, using Planck's constant and the speed of light, the formula $E=hc/\lambda$ allows the corresponding energy of photons to be calculated.

E2M considers the photon to be particle formed by concentrated energy travelling as a helical solenoid (as in figure 33) and thus having wave-like characteristics. It is thus compatible with the Quantum Mechanic's particle-wave duality concept, as supported mathematically by the Schrödinger and Dirac equations, and is not far removed from the vibrating string concept of String theory. The E2M model for atomic structure as presented in this thesis can provide a simple feasible mechanism for the generation and emission of photons that is considerably different to the electron orbit-jumping mechanism based upon conventional Science's orbital nuclear model.

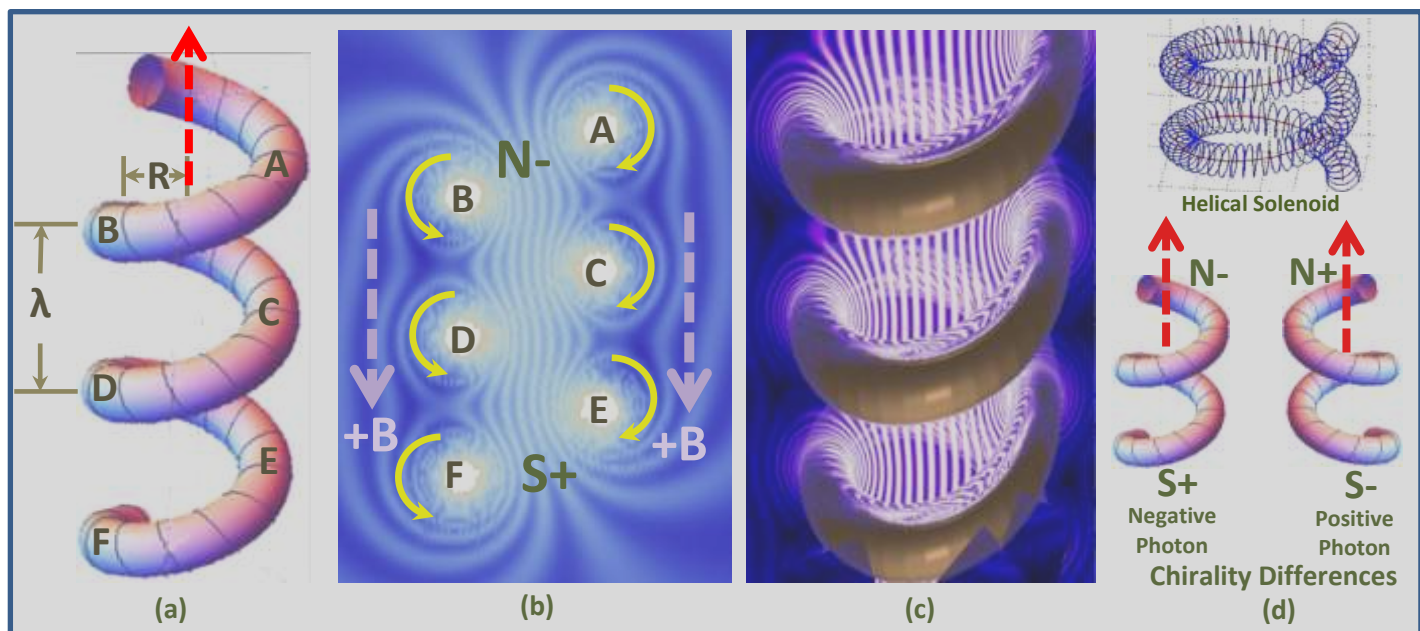


Figure 33: A Photon as a Helical Solenoid

Although Oliver Consa, in his 2018 paper '[Helical Solenoid Model of the Electron](#)', uses the helical solenoid model for the electron and, in a later paper, to preons, E2M considers that it only applies to the photon, with the toroidal solenoid structure being applicable to the electron, positron and preon (CES). The electromagnetic compatibilities of electrons/positrons and photons are attributed to compatibilities between the toroidal and helical solenoid models.

The helical solenoidal form of a photon can be considered to be broken torus solenoid, which is then stretched out in the torus's spin-axis direction and spinning to form a helical spiral. The concentrated energy swirls in a solenoidal pattern within helical coil's tube (with small radius r), and the helical coil rotates around the central axis that corresponds to the direction of movement (dashed red arrow) of the photon. There is no re-circulation of energy as there is in a toroidal solenoid: the concentrated energy keeps swirling forwards as the photon spins its way forwards.

The wavelength (λ) of a photon is shown in figure 33a. A beam of light consists of multiple positive and negative photons traveling in unison leading with their magnetic North poles.

Electron (and a positron) has a rest mass of $0.511 \text{ MeV}/c^2$, but the rest mass of a photon is so small that it cannot be directly measured, although satellite measurements of planetary magnetic fields infer that it is in the order of $3 \times 10^{-33} \text{ MeV}/c^2$. For practical purposes, a photon is usually considered to be massless. And as can be seen in figure 33b, laterally it is electrically neutral (3 positive and 3 negative electric fields A, C, E and B, D, F respectively), which explains why, unlike electron emissions, light photons are not deflected by even strong large-scale magnetic fields acting close to perpendicular to their direction of travel.

E2M contends that photons are emitted by un-bonded out-facing CESs within the nucleons. Nucleons consist of three up/down quarks (U-D-U for protons and D-U-D for neutrons), and are thus made up of 18 CESs: 2 pairs of CESs form inter-quark bonds as shown in figure 5, leaving 7 outward facing North Pole CESs and 7 outward facing South Poles (neutrons have 7 outward-facing positive and negative poles, and protons 10 out-facing positive poles and 4 negative).

Photons, however, can only be ***created by and emitted*** as EMR from out-facing South Pole CESs as shown in figure 34a. When the energy-return funnel of a CES with an out-facing South Pole cannot cope with the amount of electromagnetic energy being drawn towards the centre of the torus (south-heading), congestion builds up to form an embedded torus (as shown by the purple torus). The embedded congestion-torus expands outwards until it reaches a critical point that causes it to be caught by the outer electromagnetic field (north-heading), causing it to be ejected at the speed of light as a photon, partially unravelling, outer edge first, into the helical solenoidal form of as it exits.

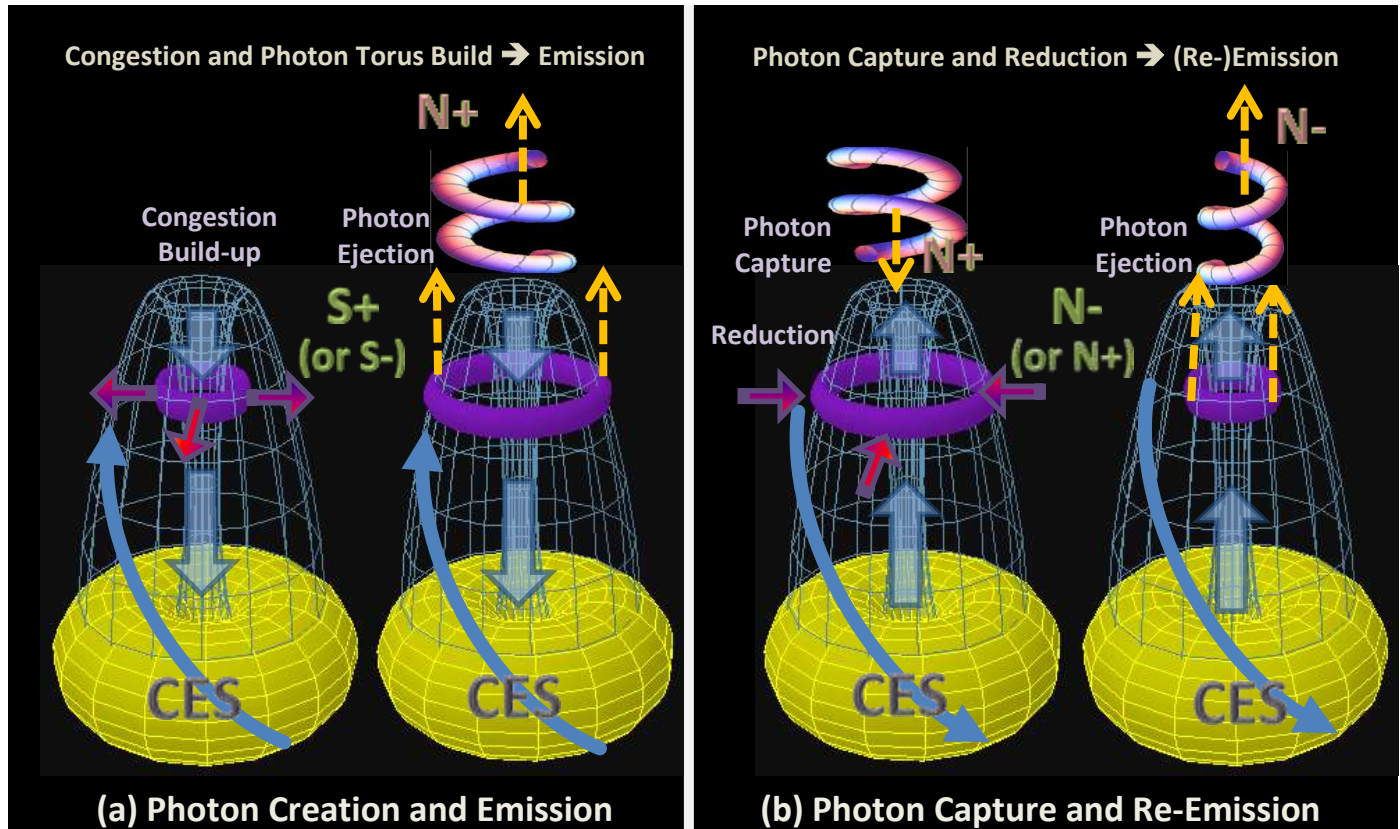


Figure 34: Photon Creation/Emission and Capture/Re-Emission

Photons can be ***captured and re-emitted*** as EMR of a different wavelength by out-facing North Pole CESs (as shown in figure 34b). When a N- photon encounters an outwards-facing N+ CES, it can be captured by the CES's outer electromagnetic field and its helical form is concertinaed to a torus form (the larger purple torus). The captured photon can be temporarily held in limbo before being released as a photon of approximately the same energy level and frequency, but with **reverse helicity**. This involves minimal energy transfer between EMR and matter.

Alternatively, particularly in a highly energised environment, energy exchange between photons and atoms is more likely than the hold-and-release scenario. Here the captured photon starts to lose energy to the CES's southwards-heading outer zone electromagnetic field, thus reducing in energy level and large radius size. The shrinkage of the torus's large radius continues until it is completely consumed by the CES (total absorption), or until it is picked up by the inner funnel of the CES's electromagnetic field (northwards moving) and ejected. The ejection process causes the embedded torus to partially unravel, inner edge first, into the helical solenoidal form of a photon, travelling with the **reverse helicity** to that of the captured photon and with **reduced energy and frequency**.

The frequency of the helical solenoid form of a photon is proportional to $R/(r.N)$. Assuming that the number of turns per unit length (N) and the small radius (r) of the captured and re-emitted photons are approximately the same, then the reduced large radius (R) means that the frequency of the re-emitted photons is reduced (i.e. has an increased wavelength λ). The increased effective wavelength is analogous to the **Compton Effect**, wherein the wavelength of X-rays and other energetic electromagnetic radiation is increased when elastically scattered by electrons.

The emission spectra of elements and compounds provide excellent examples of the photon creation and capture/re-emission processes. Each element in the Periodic Table is capable of creating and emitting EMR with one or more

wavelengths which are dictated to geometry of their atomic structure: these are collectively referred to as their **base EMR**. Along similar lines, each element can only capture photons of particular wavelengths as dictated by the geometry of their atomic structure and re-emit them as lower-energy photons of increased wavelength with reverse chirality: these are collectively referred to as **rebound EMR**. The combination of base and rebound EMR create the multiple bands of specific wavelength combinations that present as emission spectrum that are unique for each element, examples of which are shown in figure 35 (Note: the rightmost colour bands reflect increased rebound EMR).

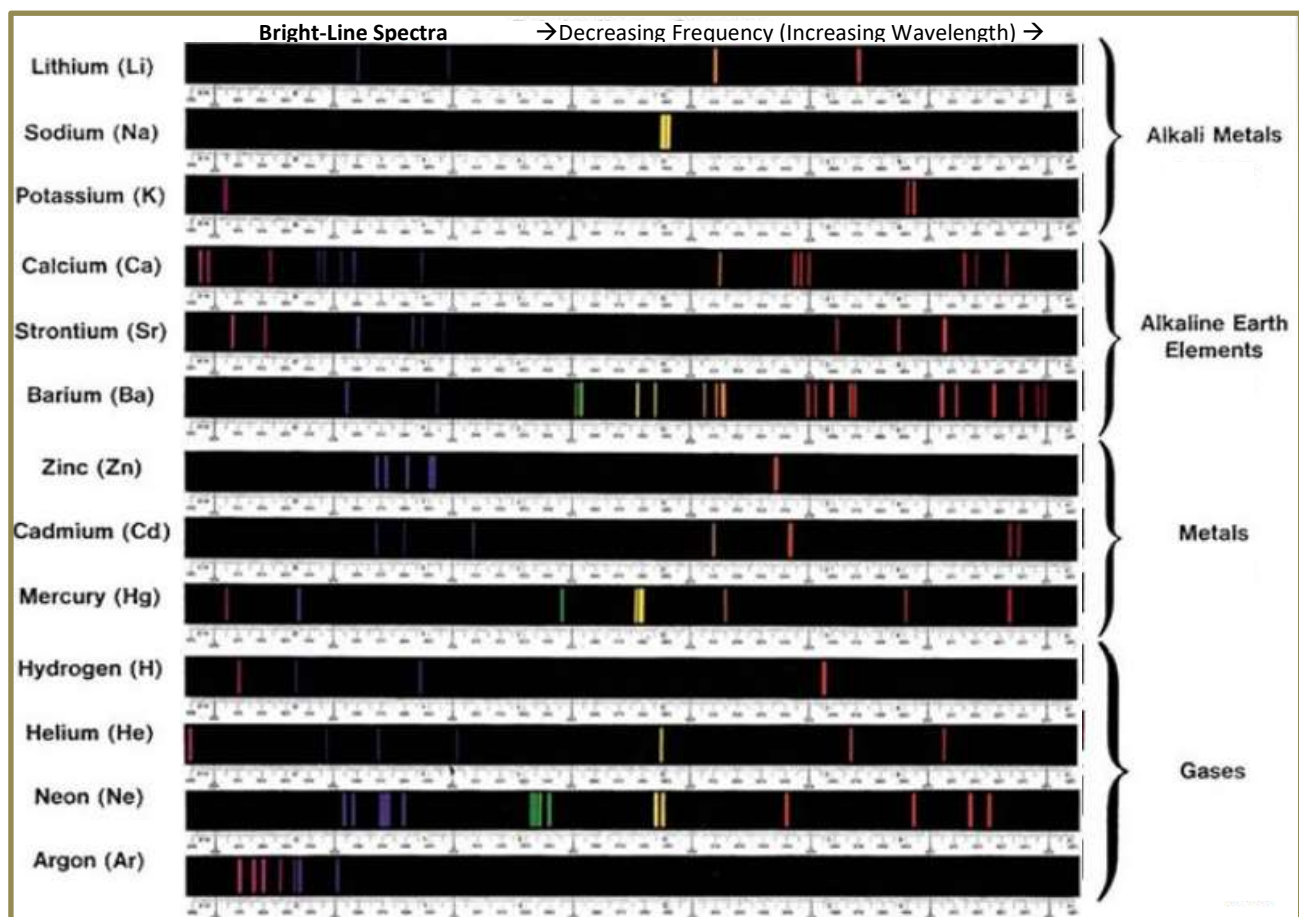


Figure 35: Emission Spectra for Common Element Groupings

The base, capture and rebound photon frequencies are quantum-like and unique to and related to the atomic structure of each element. For some elements, rebound photons can be re-captured and emitted several times, so increasing the number of re-bound bands visible. The base and re-bound frequencies are related to the strength and orientation of CESs, which are dictated mainly by the geometry and related net electromagnetic energy capacitance of their nucleon layer. The energy capacitance of nucleon layering is related to its geometric shape (which dictates layer size), the number of the connected layers and the nature of the connectivity (i.e. inter-quark or bitron connected). The geometry of each layer and its inter-connectedness with other layers thus result in the unique range of quantum-like base and re-bound frequencies of elements and compounds.

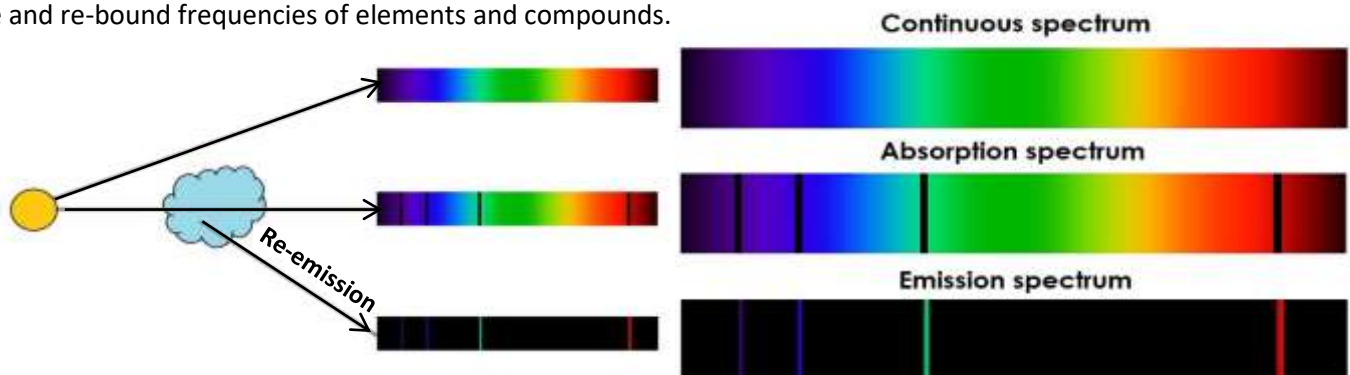


Figure 36: Absorption and Re-Emission Spectra

A spectacular example of the hold-and-release scenario is **spectral line absorption**, wherein photons with the optimum quantum frequencies are captured from incident light and held by the material involved. This produces dark bands in the absorption spectrum corresponding to the captured photon frequencies. The captured photons can in turn be released with energy levels and frequencies very close to their pre-capture state, appearing as solitary bands in the material's emission spectrum, as demonstrated by gaseous cloud example as represented in figure 36.

EMR represents a major way in which energy (radiant) is transferred between bodies. Some photons from incident EMR are electromagnetically repelled (reflected) or diverted (refracted); others become attached to or absorbed by nucleons. Bodies gain energy by capturing photons and partially or partly absorbing photon energy and releasing lower energy re-bound photons. The extra energy acquired feeds back into the atom's nuclear nucleon layers, adding to the net energy level of the atoms involved. When in an excited state, atoms create and release energy as EMR to reduce their net energy level. In balanced environments atoms are more likely to hold-and-release photons with very little energy exchange between the two.

A **beam of light** is Electromagnetic Radiation (EMR) within the visible light frequency range, consisting of multiple North-facing positive and negative photons. Within a beam of light adjacent positive and negative photons have a propensity to move away from each other (analogous to parallel wires carrying electric currents moving in opposite directions repel), whereas those of the same charge to move closer each other (analogous to wire attraction between parallel wires carrying electric current in the same direction). Also, positive photons have a propensity to align and keep in line when they are end-on-end adjacent, and similarly for negative photons. These combined factors marshal photons into linear strand-like groups of positive photons or negative photons that results in a light beam that is more robust and stable than could be expected from a random group of independent photons.

Figure 37 shows how the in-phase sinusoidal electric and magnetic fields associated with unpolarised light are generated. Referring to the yz -plane cross-section of the unpolarised negative photon moving down the z Axis (37a), the first electrical maximum after point G passes by is at point B of the photon helix.

Looking from above, point B can be represented by a small disc-like piece of the photon's concentrated energy. Looking from above (37c), the disc's magnetic field ($-b$) points back to the xz -plane. It is perpendicular to the negative electric field (37d is view from the front). The electromagnetic fields at B plot as perpendicular fields in (37b).

The next electrical maximum after point B is point C, which is a positive charge, and, because the electromagnetic energy is moving in the opposite direction to that at Point B, the magnetic field direction is reversed ($+b$). The electrical and magnetic fields reduce in sinusoid fashion from B and C to the zero values at points G and H and to the mid-point between B and C to complete one complete cycle as shown in (37b).

Photons can be packed together with their helical spirals entwined to form **Optical Vortex Light** (figure 38a). Optic vortex light is associated with **Orbital Angular Momentum (OAM)**, which is sufficient to rotate and manipulate nanoparticles (figure 38b). The electromagnetic fields of the entwined helical solenoidal photons interfere with each other to generate circular zones of interference when viewed end-on (leftmost in 38a).

Optic vortex light can be produced by a range of techniques including Spiral Phase Plates (SPP), Q-plates, pitch-fork holograms and cylindrical mode converters.

To entwine the photons must have the same chirality, which dictates the left- or right-handedness of the optic vortex light, with the ' ℓ ' factor (38a) indicating the number of photons entwined together to form each super-photon.

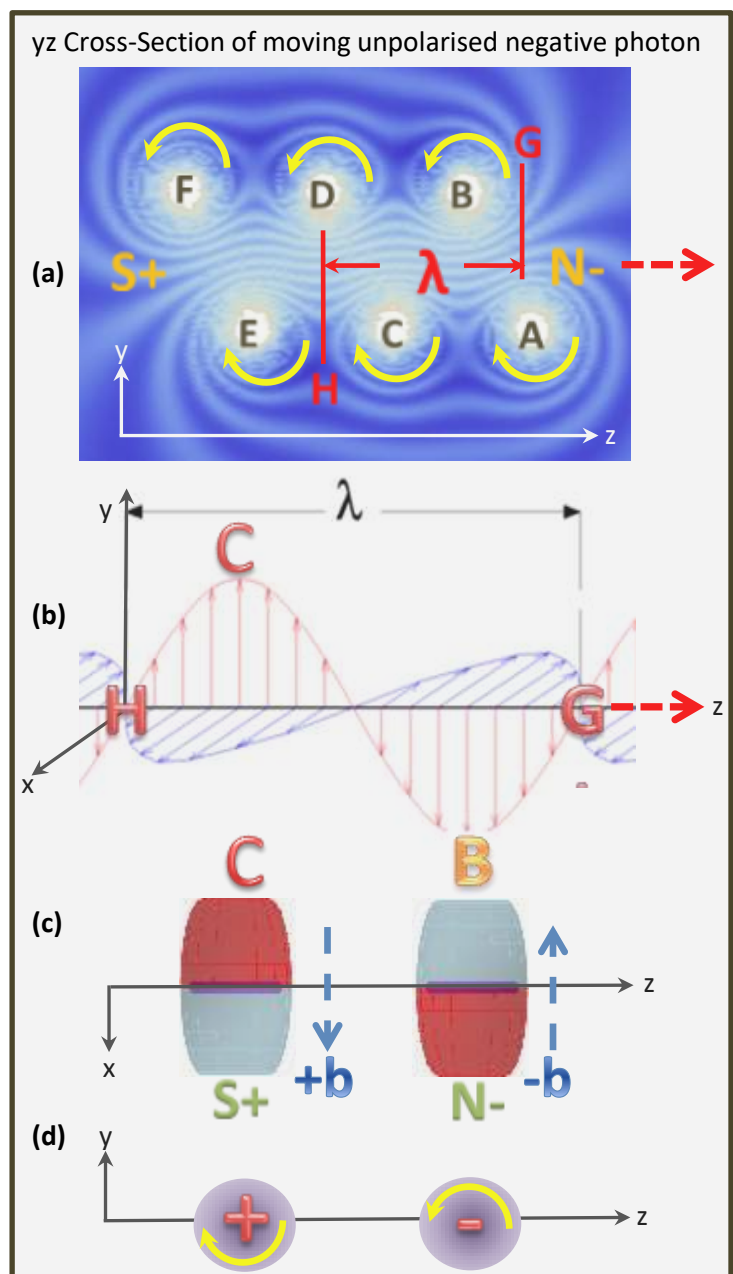


Figure 37: Electromagnetic Fields of an Unpolarised Photon

More common and less exotic than optical vortex light is **polarised light**. The helical solenoidal structure of photons is quite fragile, and can easily be mechanically uncoiled into polarised light by the process of reflection by a polished non-metallic surface (e.g. glass) or by transmission of unpolarised light through polarising materials.

Considering reflection option (38d), as the leading head of an unpolarised photon reaches the reflecting surface the concentrated energy tube of helical solenoidal is simply uncoiled and transformed into a sinusoidal planar form of is **linear (or planar) polarised light**, oscillating perpendicular to the I-R plane (the plane containing the incident and reflected light paths). This results in sinusoidal electric fields perpendicular to the I-R plane and magnetic fields perpendicular to and in phase with the electric fields, forming a pattern similar to that for unpolarised photons, albeit a somewhat attenuated one. Thus, although unpolarised and polarised photons have different energy forms, their electromagnetic footprints are similar.



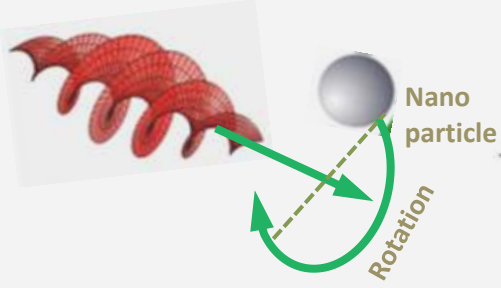
$\ell=1$

$\ell=2$

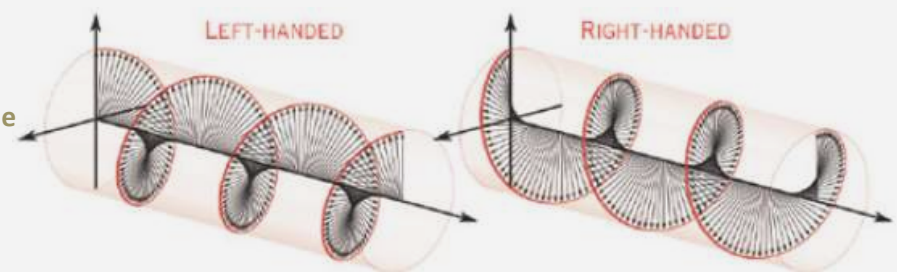
$\ell=3$

$\ell=4$

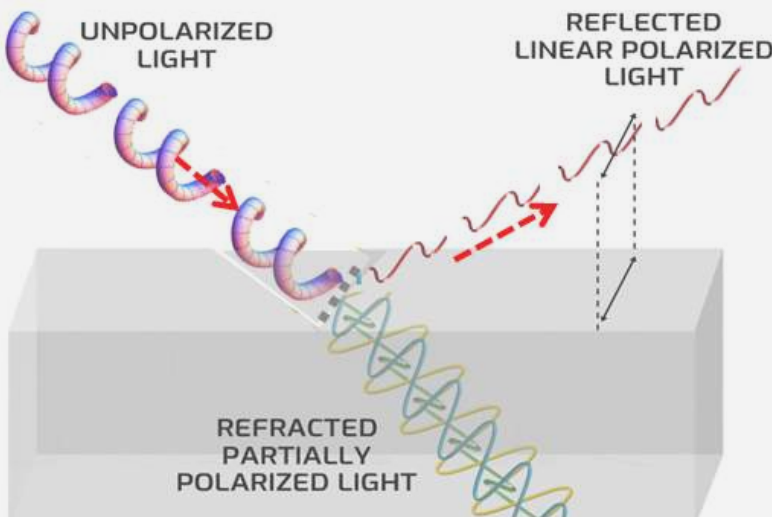
(a) Optical Vortex Light Photons



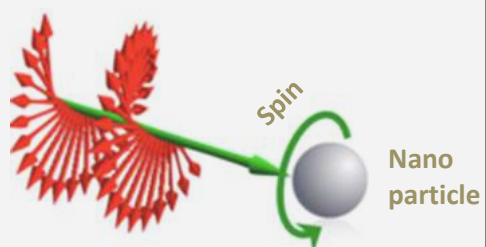
(b) OAM Nanoparticle Rotation



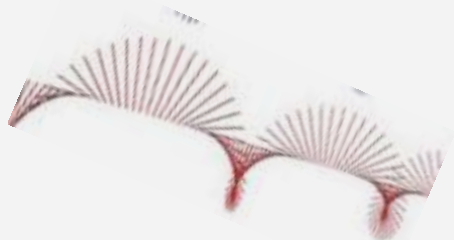
(c) Circular Polarised Light Electric Field



(d) Creation of Linear (or Planar) Polarised Light by Reflection



(e) SAM Nanoparticle Spin



(f) Elliptical Polarised Light Electric Field

Figure 38: Optic Vortex and Linear, Circular and Polarised Light Forms

Circular polarised light occurs when photon groupings whose polarisation planes are perpendicular to each other, equal in amplitude and have a phase difference of $\pi/2$ are combined to create an electric field that rotates in a circle around the direction of propagation with a left- or right-hand rotation effect (38c) resulting from the chirality of the component photons. Circular Polarised Light is associated with **Spin Angular Momentum (SAM)**, which while not being as strong as the OAM of optical vortex light, is sufficient to cause nanoparticles to spin (38e).

As for unpolarised light, when a circular polarized light beam is reflected by a conventional (or regular) mirror, the mirror reverses the beam's spin state, so that the light it reflects back out has the **opposite** spin or chirality as the light

that enters (figure 39a). A chiral meta-mirror, on the other hand reflects circular polarized light with the **same** spin of the incident beam, but only for one spin state: a beam with the opposite spin is completely absorbed. Chiral meta-mirrors are available to reflect either right (39b) or left (39c) circularly polarized light, and do so without a change of chirality, but each can only reflect light of one chirality, with any light having the opposite chirality being absorbed.

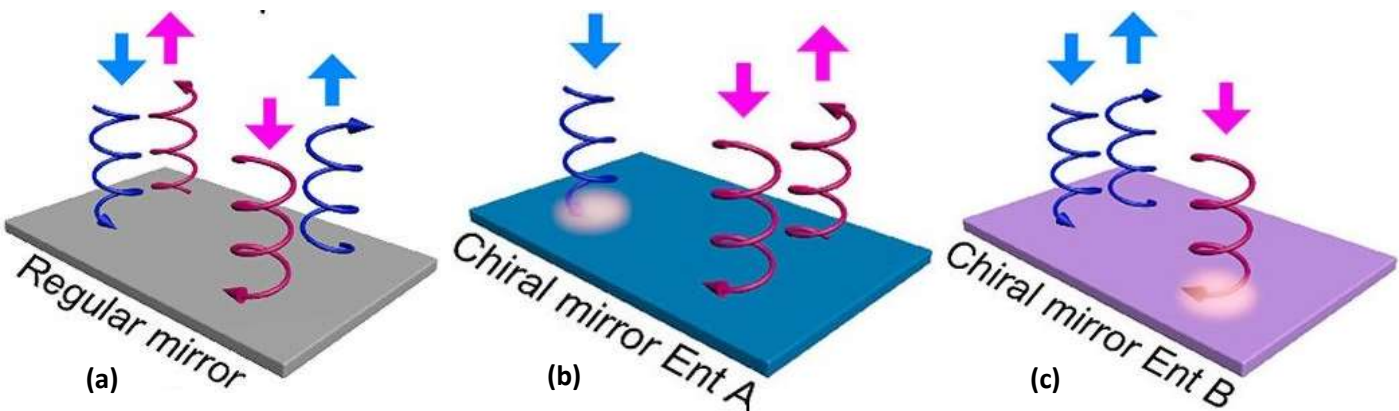
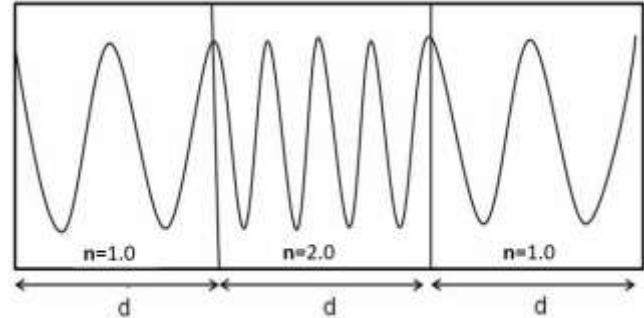


Figure 39: Reflection of Circular Polarised Light

Elliptical polarised light (38f) is a more general form of circular polarised light with the combination of 2 perpendicular linear polarised light components with differing amplitudes and a phase difference of $\pi/2$.

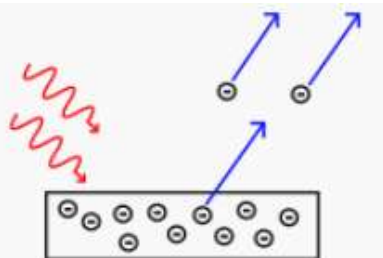
Light **refraction** occurs when light passes from one medium into another with a different **refractive index**. When light passes from a fast medium (e.g. air with $n=1.0$) to a slow medium (e.g. $n=2.0$ as in the figure right), the denser medium axially compresses the photons, thus reducing their wavelength and forward speed: the net result is that their frequency remains unchanged. The reverse takes place when they pass into a medium with a lower index of refraction, and the wavelength increases.



In order to reduce bulk in the body of this thesis, discussion of micro and radio Waves, destructive and constructive interference, the Michelson Interferometer and the double-slit experiments have been delegated to [Appendix A](#).

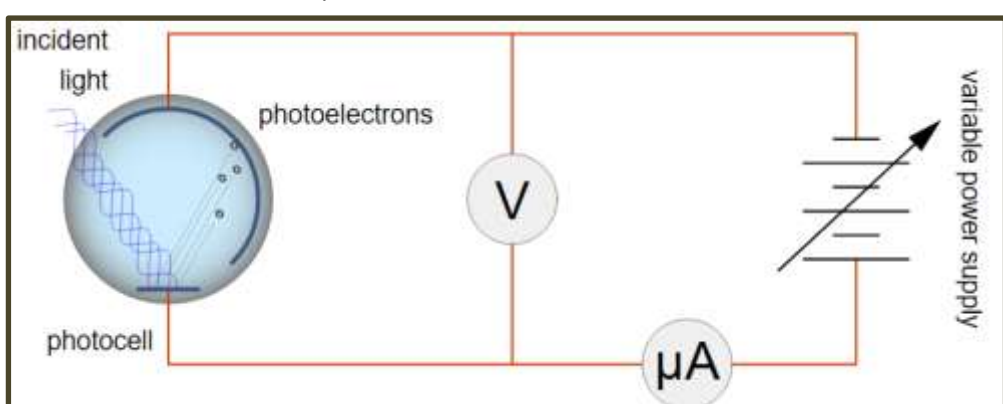
The Photoelectric Effect

The **photoelectric effect** is the release of electrons by Incident light. The photons arriving at the surface of the incident medium can be a) polarised and reflected; b) absorbed retransmitted as photons of a different frequency; or c) cause the emission of electrons (the photoelectric effect). The first two effects have been described in the previous section. The ensuing discussion about the photoelectric effect assumes an understanding of the E2M model for electricity (see [Appendix B](#)) involving the synchronous source-to-sink movement of electrons and positrons.



The photoelectric effect occurs when a photon of sufficient energy strikes a bitron within an inter-layer bitron bond, causing the bitron to be ejected from the bond. Many of the ejected bitrons have sufficient momentum to escape the host incident medium and others become free electrons or positrons within the incident host medium.

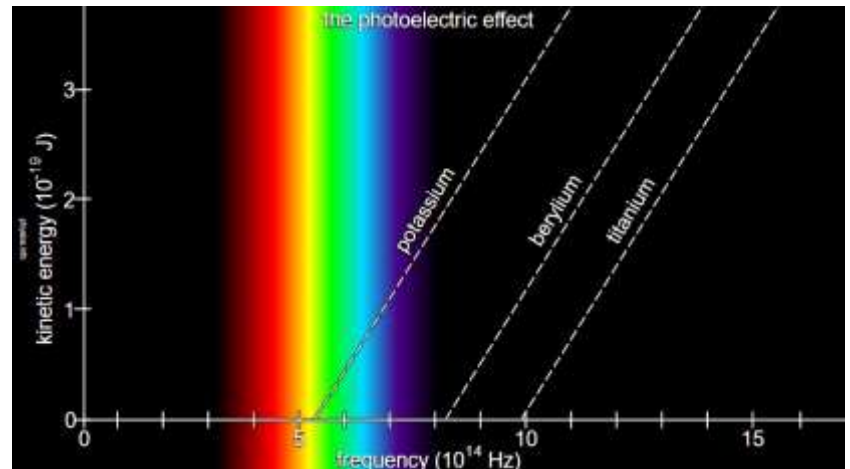
The figure right represents a simple form solar photocell with a stopping current setup, that is typical of those used for photoelectric demonstrations. More elaborate [experimental setups](#) involve light filters to control the wavelength of the incident light.



Incident photons that have a frequency above the **threshold frequency** of the incident medium's surface layers and strike a bitron cause the release of approximately equal numbers of positrons and electrons, but only electrons created by direct-hit bitrons can acquire sufficient momentum to escape the incident medium. Those electrons created by oblique or glancing bitron blows gain insufficient momentum to escape the surface or insufficient kinetic energy to reach the receiving plate should they escape. However, no positrons so created can gain sufficient kinetic energy to escape the residual positive charge of protons within the atomic structure of the incident plate regardless of the directness of the photon hit (it should be noted that, as discussed in the section [Electron and Positron Generation](#), a high energy particle accelerator can provide sufficient energy to eject positrons from the incident medium).

The inability of positrons to escape results in an increase in the positron-to-electron ratio within the incident medium, which, with the accumulation of captured electrons at the receiving plate, creates an emf that aligns electrons and causes them to start shuffling from the receiving plate (electron source) towards the incident plate (electron sink); and movement of positrons from the incident plate (positron source) towards the receiving plate (positron sink).

By applying an opposing emf, electron build-up increases at the receiving plate which, at the **stopping voltage**, can prevent even the most kinetically energetic of the ejected electrons from reaching it. This allows the maximum kinetic energy of the emitted electrons for a given EMR frequency to be determined. Such measurements confirm a linear relationship between maximum kinetic energy and photon frequency that varies depending upon the incident plate surface medium as shown in the graphs right.



The E2M approach explains electric current in terms of the synchronous source-to-sink movement of electrons and positrons that is different to the conventional science model of monopole electrons moving from a negative to a positive charge area. E2M also contends that atoms can re-build displaced bitrons: thus regardless of how extensive and intensive that EMR bombardment might be, a healthy supply of target bitrons is always available. Because electrons are continually lost without replacement according to the conventional Science model, outer orbital electron depletion (and consequential ionisation) can be expected from extensive and intensive EMR exposure: the lack of evidence of such depletion is thus a problem. However, in spite of their differences, both approaches are compatible with the experimental evidence and mathematics associated with electricity generation and distribution.

Plasma and Cosmic Radiation

Plasma is formed by super-heating matter, which causes electrons to be stripped from the atomic structure to yield a mixture that is rich in electrons and ions. Over 99% of the matter in the visible universe is believed to be plasma. An important source of plasma formation in space is **photoionization**, wherein photons from stellar EMR are absorbed by an existing gas mixture, causing electrons to be emitted.

Closer to Earth, lightning, naked flames, welding arcs, neon/fluorescent tubes, neon signs, plasma (some TV and computer screens), plasma lamps and globes involve the generation of plasmas; and the Earth is surrounded by a dense plasma called the **ionosphere** and impacted by the Sun's solar wind plasma.

Plasma can also be created in the laboratory by super-heating a neutral gas or subjecting it to a strong electromagnetic field to the point where it is ionised. At lower temperatures radiant EMR energy is acquired and managed by the energy transfer and balance mechanisms as described in the previous section.

The temperature and degree of chaotic buffeting within a gaseous mix increases as the energisation levels increase, and the bitron within external bitron bonds start being released as a fast moving electron or a positron, depending upon which side of the bond the bitron exits. In such a highly energised environment, when one bitron is released another quickly forms: this bitron form-and-release and re-form process represents a much higher energy transfer rate than that of photon absorption and re-transmission. Importantly, it results in a rapid increase of electron and positron release that greatly increases the electrical conductivity of the mix, the generation of extensive long-range electromagnetic fields and production of gamma radiation (resulting from electron-positron annihilation collisions).

As the energisation continues to increase, external bitron bonds start to fail and the plasma mix becomes increasingly ionized. For Hydrogen ionization starts at about $7,000^{\circ}$ K and by around $10,000^{\circ}$ K it is completely ionized.

When temperatures rise to well above the 10^4 K range, such as achieved by active stars, the bitron bonds supporting nucleon layers within atoms (i.e. atoms more complex than Hydrogen) start to fail, facilitating the separation of nested polygonal forms and the creation of atoms lower down the Periodic Table. The very fabric of the original compounds has commenced to break down, with any semblance to the original atomic structures being lost. Cooling of the plasma cloud would now result in a completely different mix of atoms and compounds.

Should energisation continue even further, nucleon layers would be further separated with the destruction of any remaining inter-layer bitron bonds, and the layers then broken down into their component nucleon and/or quark parts: such utter destruction and decomposition most likely only occurs in the crush within the bowels of a black hole or collapsing neutron stars.

For Hydrogen, the most elementary and widespread form of plasma in the universe, the ionization process takes place from about $7,000^{\circ}$ K, with the bitron bonds of Hydrogen molecules being stripped away, creating a mix rich in electrons, positrons and protons (hydrogen nuclei). At this stage some interesting things start to happen:

- Firstly, because the in and out energy flow of protons is not restricted unless bitron bonded to another atom, no accumulation of excess energy occurs at outward facing South Pole CESs within the rising number of protons. As the protons no longer emit EMR (the same comments also apply to neutrons) Hydrogen drops out of emission spectra for the plasma mix: any spectral lines are thus attributable to other contaminants.
- Secondly, because highly energised free electrons and positrons abound, protons are being toggled into neutrons via β^+ decay (see earlier) and then back again into a proton via β^- decay. This ongoing circular process generates a large number of beta rays, neutrinos and anti-neutrinos.
- Thirdly, the ongoing toggling of nucleons between proton to neutron and back again generates a mix of free protons and neutrons in close proximity, which allows them to combine and form new atoms, principally Helium, which, in such a highly energised environment, present as alpha radiation.

Cosmic radiation, the high-energy particles arriving from outer space from distant galaxies, consists mainly of protons (89%), Helium (10%) and a mix of heavier nuclei (about 1%), plus abundant levels of high-energy neutrinos, anti-neutrinos and gamma radiation: a content compatible with that of a completely ionized Hydrogen plasma mix.

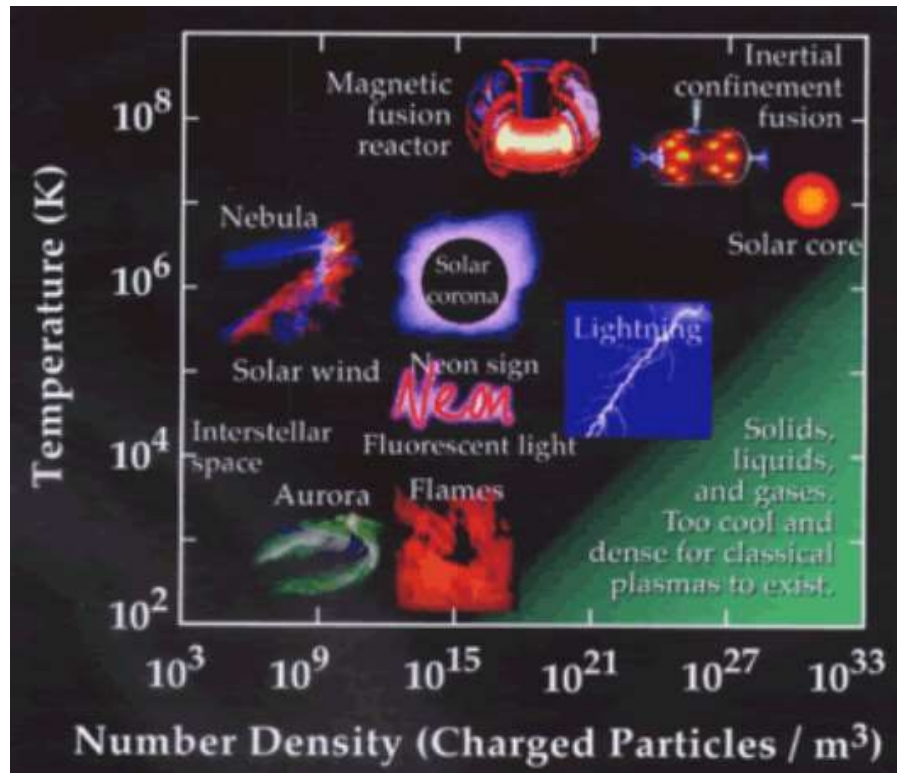


Figure 40: Plasma Temperature/Density Distribution

Spin and the Orbital Nuclear Model

Central to the E2M approach is that all concentrated energy sources (CESs) have spin, and that low level electromagnetic energy spirals around them in sync with their spin, with the circular divergent and convergent flows presenting as positive and negative charge electric fields, and the lengthwise flow presenting as a magnetic field. As electric and magnetic fields are formed by the same electromagnetic energy, they are only differentiated by their flow pattern and characteristics associated with those patterns, with E2M there is no need to balance the notional positive and negative point charges to achieve electrical neutrality: only magnetic moments need to be accounted for.

For the conventional Science approach based upon an orbital nuclear model for atomic structure, the combination of charge and spin has proven to be more problematic. In the early 1920's the Standard Model consisted of a Bohr-styled

model for atomic structure consisting of negatively charged electrons orbiting a positively charged nucleus. **Orbital angular momentum** was accounted for by integer quantum numbers, but it was soon realised that the orbiting electrons possessed magnetic moments associated with their axial spin, which has been called **intrinsic angular momentum**. In the late 1920's Paul Dirac's equations, which factored in relativistic theory, allocated fermions (including electrons) quantum spin 1/2, 3/2 etc. to cater for intrinsic angular momentum, with anti-particles having a corresponding negative half spin number.

The **Stern–Gerlach experiment** is used to illustrate that an orbital electron possesses intrinsic angular momentum due to electron spin. The experiment involves sending a beam of silver atoms through an inhomogeneous magnetic field and observing their deflection as shown in figure 41.

Due to random thermal effects in the oven used for the experiment, the magnetic dipole moment vectors of the silver atoms are considered to be randomly oriented in space. Based on classical physics theory, a continuous spread of the atoms in the z direction corresponding to the random spread of magnetic moments could be expected (a lip-like pattern filled with atom hits as shown in the top-right insert of figure 41): instead the experimental results had no central hits resulting in the open thin-lip distribution as shown.

Originally the thin-lip distribution of the atom stream was interpreted that as being due to integer quantised angular momentum as per the quantum theory that then (1922 to 1925) existed. Upon the arrival of Dirac's equations in the late 1920's, the experimental results were re-evaluated and conclusions changed: the deflection pattern was now explained in terms of the intrinsic angular momentum of orbital electrons. According to the orbital model, silver atoms have one unpaired 5s electron, with all others being paired. Thus, as the 5s electron is considered to be in a zero orbital-derived angular momentum state, its quantum spin-1/2 results in an up or down state, resulting in an even splitting of the electron stream in the z direction.

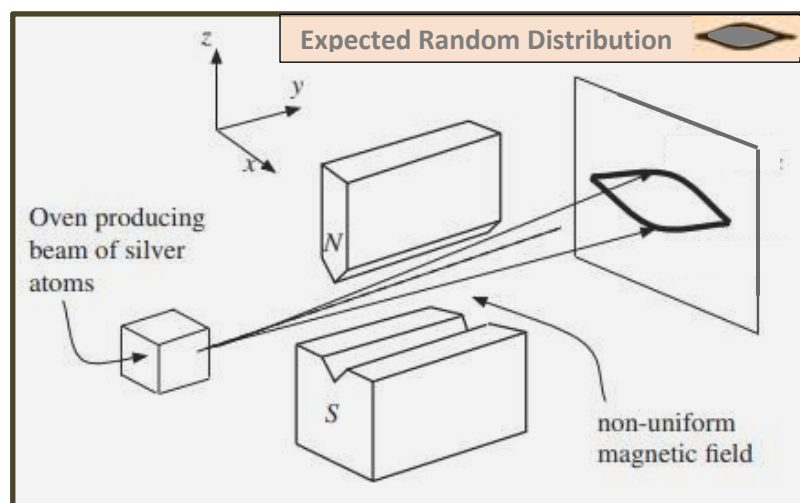


Figure 41: The Stern–Gerlach Experiment Setup

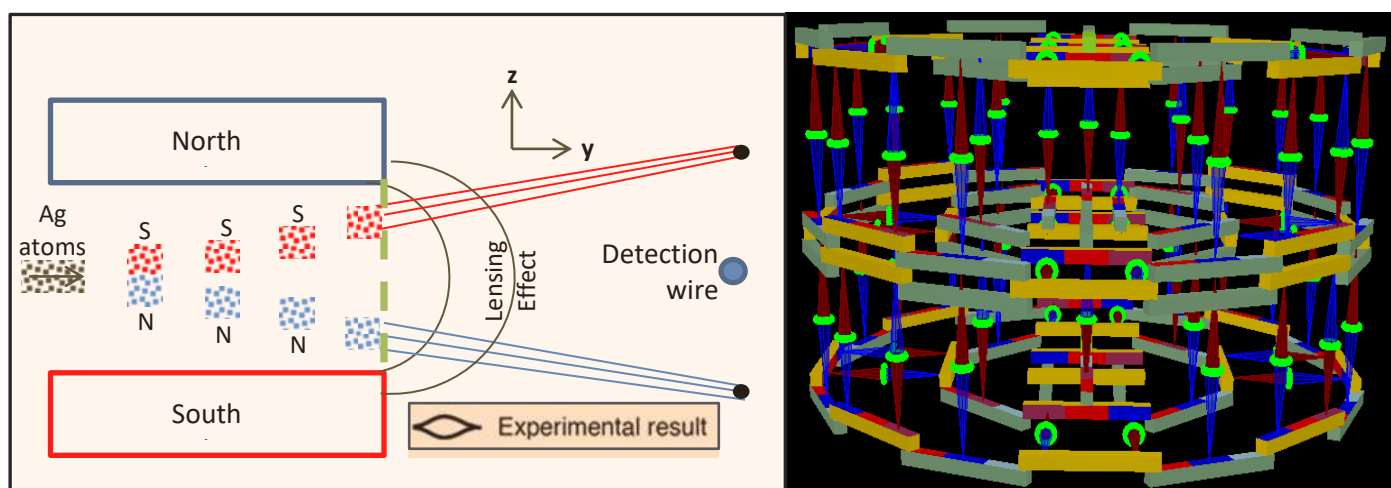


Figure 42: The Stern–Gerlach Experiment - Silver Atom Structure and Deflection Pattern

The E2M model for a silver atom (see right in figure 42 the electromagnetic field of the outer bitron bonds quickly align the atoms as they enter the applied magnetic field so their North-South axial alignment is vertical (i.e. parallel to the z direction). The outer bitron fields are magnetically balanced, but the neutron attached to the top (or bottom) nucleon layer represents unbalanced magnetic fields that cause the atom to move up or down in the z direction, separating into two groups around the central xy plane.

The silver atoms would be expected to spread in a fairly concentrated lens-like distribution band with no atoms centrally, thus producing an open lip-styled pattern. Also, in a manner not dissimilar to the optic focusing effect of a convex lens with light, the convex shape of the outer magnetic field at the atom exit-end of the magnet (dashed olive-green line in figure 39) would have a lensing effect causing the atoms to converge further into thinner lines.

Conclusions

The energy-centric approach to atomic structure as presented in this thesis paper is based upon a **toroidal solenoid** model for electrons, positrons and CESs, and a **helical solenoid** model for photons. It results in atomic structures that are significantly different to those of conventional Science's orbital nuclear model, and provides feasible explanations for many physics and chemistry related phenomena, including:

- The physical characteristics of elements
- Different allotropic forms of elements
- Bonding geometry within molecules and chemical compounds
- EMR wave-particle duality
- The photoelectric effect
- EMR-based radiant energy transfer and balancing
- Emission and absorption spectra for light
- Electric and magnetic field interdependency (or duality)
- Electric current flow and capacitor charge storage and discharge
- Beta decay and electron capture
- Electron-positron annihilation
- The ionization process during plasma formation and the Helium content of cosmic radiation
- Gravity and Gravity waves (Appendix C)

The toroidal solenoid model used has been postulated to consist of a torus core of concentrated energy enveloped by less concentrated energy responsible for a surrounding electromagnetic field. The nature of the flow of concentrated core energy swirling around the electron's torus is unknown: it could be a liquid-like flow or consist of fast-moving energy strands, vibrating strings or particles. All these feasible options are compatible with the characteristics of an electron as presented in this thesis.

Apart from having different chirality, **electrons** and **positrons** have the same structure and electromagnetic characteristics. At present there is no known way to distinguish between electrons and positrons when they are contained within matter, which causes problems when considering the nature of an electric current within a wire conductor or how a capacitor stores and releases charge, as discussed in Appendix B. Consequently elaborate high energy accelerators are required to extract, collimate and axially align electrons and positrons so they can be separated by a magnetic field (e.g. the desk-top positron generator represented in figure 9).

There may be subtle differences in the structure of CESs, electrons/positrons and photons that are unique to each, but, for the purposes of this thesis, they have all been considered to have a toroidal structure and display similar characteristics. CESs are the larger and more energetic, and, as **Preons**, represent the primary energy source from which other energy evolves; they are considered to have the ability to accumulate and release energy as part of the energy balancing processes within and between atoms. On the other hand, electrons and positrons are considered to be secondary or derived forms of concentrated energy which can (re-)form within bitron bonds, some of which are internal to the atom and others external between atoms. Similarly, photons are considered to be derived secondary energy concentrations which are formed by and/or captured and released by un-bonded out-facing CESs within an atom.

The four most conjectural aspects of the E2M model relate to assertions that 1) some electrons are internal to the nucleus and are (re-)generated by bitron bonds; 2) electric current is the synchronous source-to-sink movement of electrons and positrons; 3) the source of EMR emissions; and 4) Gravity. It is, however, quite possible that free electrons are captured and held by bitron bonds in the atom-building process rather than being generated from excess bitron bond energy as proposed in this thesis. Also, the explanation for Gravity is highly speculative. However, apart from the concept of some electrons being internal to the nucleus, these are considered to represent ancillary issues and, should any of these aspects require change, the basic E2M atomic model would still remain largely intact.

It is amazing that a change in assumption relating to the nature of one of the smallest known sub-atomic particles, the electron, can result in atomic models that are so radically different. The differences between the new E2M model and status quo orbital nuclear model are considerable, and both approaches cannot be correct. One has to be in essence correct (or at least in the right ball-park), or both have to be incorrect, representing totally misleading, flawed false-positives. The very real dilemma that urgently needs to be resolved relates to which of the approaches represents a false-positive, because should a false-positive model be adopted, used and relied upon, then the implications for the future of Science and mankind would be significant, costly and potentially very embarrassing.

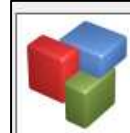
Acknowledgements and References

3D Modelling Software

3DCrafter by Amabilis Software

Technical References

Most technical detail was obtained from **Wikipedia**



3DCrafter
Freeware Edition

Version 9.3 (Build 1620)

Copyright © 1998-2015 Amabilis Software
3DCrafter is a trademark of Amabilis Software

E2M: **E2M version 13 (2018)**

- Bach R, Pope D, Liou S and Batelaan H : *Controlled double-slit electron diffraction*, New J. Physics, March 2013
- Bergman D and Wesley J : *Spinning Charge d Ring Model of Electron Yielding Anomalous Magnetic Moment*, Common Sense Science, February 2002
- Bianchi C and Melon A : *Natural and man-made terrestrial electromagnetic noise*, Annals Of Geophysics, June 2007
- Bostick W : *Mass, Charge and Current: The Essence and Morphology*, Physics Essays, 1991, v.4(1), 45–59
- Cambier J and Micheletti D : Theoretical Analysis of the Electron Spiral Toroid Concept, NASA, December 2000
- Clarke B : *'The Quantum Puzzle - Critique of Quantum Theory and Electrodynamics'*, World Scientific, June 2017
- Consa O : *Helical Solenoid Model of the Electron*, Progress in Physics, Volume 14, Issue 2, April 2018
- Consa O : *The Helicon - A New Preon Model*, Progress in Physics, Volume 14, Issue 4, October 2018
- Der-Chi, Chen L, Van Thai N and Ashrai S : *Study of Ag and Au Nanoparticles Synthesized by Arc Discharge in Deionized Water*, Journal of Nanomaterials, Vol 2010 Article 634757
- Kanarev P : *Particle Resolution*, Proceedings of the NPA, Albuquerque m 2012
- Kyriakos A : *Geometrical illustration of the electromagnetic representation of Dirac's electron theory*, arXiv:quant-ph/0407071v1, July 2004
- Lapoint D : *The Primer Fields*, videos at <http://www.rexresearch.com/lapoint/lapoint.htm>
- Lincoln D : *The Inner Life of Quarks*, Scientific American, November 2012
- Osmera P : *Fractal Dimension Of Electron*, Proceedings of MENDEL, June 2012
- Padgett M et Al : *'Photon Orbital Angular Momentum: Generation, measurement and application to QKD'*, Proceedings of SPIE, 2012
- Sarri G et al : *Table-Top Laser-Based Source of Femtosecond, Collimated, Ultra-relativistic Positron Beams*, Phys. Rev. Lett. 110, 255002, June 2013
- Shengtao M et Al : *'On-chip discrimination of orbital angular momentum of light with plasmonic nanoslits'*, Nanoscale, Royal Society of Chemistry, 8.2227, 2016
- Wayte R : *A Model of the Electron*, Progress in Theoretical Physics, July 2010
- White Paper : *Antenna Patterns and Their Meaning*, Cisco Public Information, 2007
- Williamson J and Van der Mark M: *Is the Electron a Photon with Toroidal Topology?*, Annales de la Fondation Louis de Broglie, Vol 22, No. 2, 133, 1997
- Willner M et al : *'Reconfigurable orbital angular momentum and polarization manipulation of 100 Gbit/s QPSK data channels'*, Optics Letters, Vol. 38, No. 24, December, 2013
- Yao A and Padgett M : *'Orbital angular momentum: origins, behaviour and applications'*, Advances in Optics and Photonics, 3 (2). p.161. ISSN 1943-8206, July 2012
- Zhang J, Zhang L and Xu W : *Surface plasmon polaritons: Physics and applications*, Journal of Physics, March 2012
- Zyga L : *'New mirror reflects light differently than conventional mirrors'*, phys.org, November, 2017

© David L Johnson, Perth Australia, 14th December 2018

(Note: Despite this copyright notice, this article can be freely copied and used for non-commercial purposes)

Appendix A: Electromagnetic Radiation

Micro and Radio Waves

Micro and radio waves have frequencies less than 300 GHz corresponding to wavelengths from 1 millimetre upwards. Radio and micro waves can be man-made or result from natural sources. Unlike other frequencies in the EMR spectrum, radio and micro waves have the ability to pass through Earth's atmosphere intact (see figure 43): this plus the ability for data to be encoded and decoded using frequency and amplitude modulation techniques make them invaluable for communication purposes.

The ability of man-made radio waves to pass through the Earth's atmosphere intact, whereas the rest of the EMR spectrum cannot, suggests that they could possibly be different in nature to other EMR.

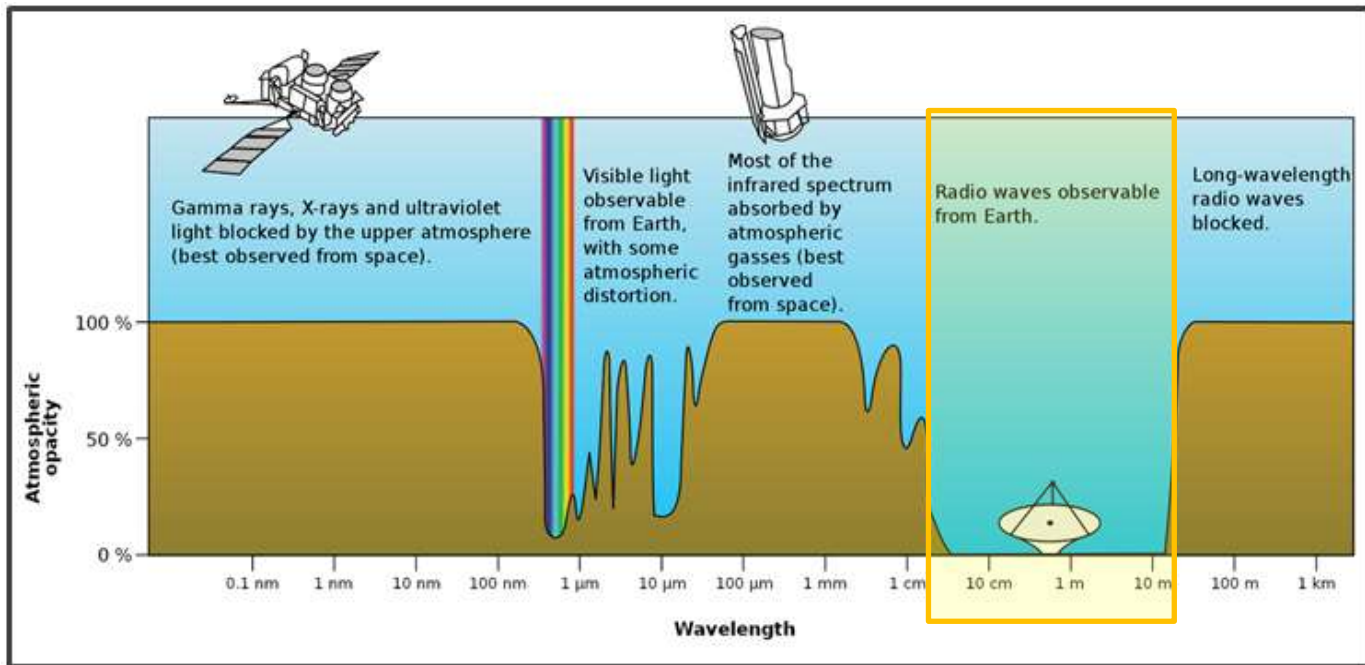


Figure 43: Electron and Positron Electromagnetic Field Patterns

Man-made micro and radio waves are generated by a capacitor and inductor loop type of circuitry that delivers an oscillating current to an aerial. It is the oscillation frequency that dictates the frequency of the emitted EMR. E2M contends that the energy-wave nature of such man-made radio/micro transmission relate to the variation in photon concentration from zero to the maximum concentration in the wave peaks, as shown in figure 44. Although a range of photon wavelengths in the micro/radio wavelength range are transmitted, it is considered to be the photon density within N+ and N- photon concentrations that defines the transmitted wave-form picked up by the receiving aerial. Man-made micro and radio waves are thus distinctly different to the 'normal' EMR such as light and X-ray radiation.

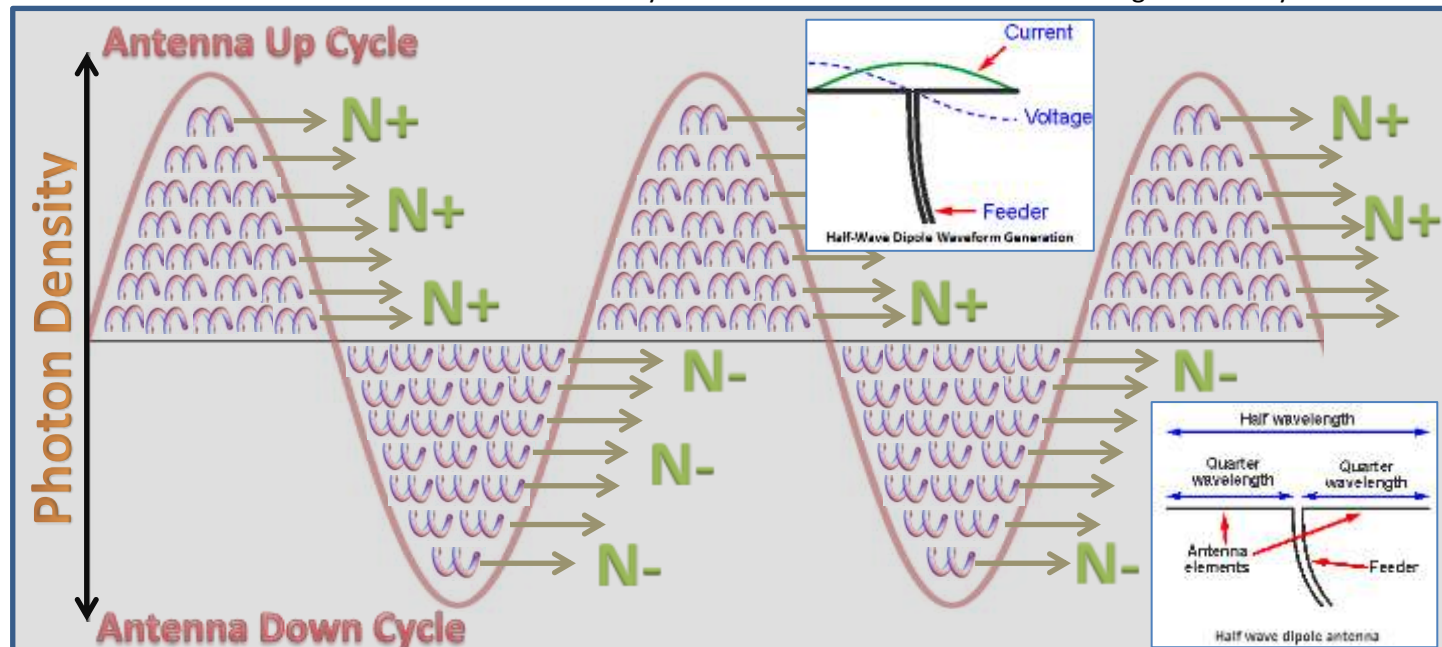


Figure 44: Man-Made Micro and Radio Waves

For a hypothetical perfect radio aerial, the transmitted wave fronts would spread as spherical sets of waves and troughs of different photon densities. Larger power transmitters are simply able to pump out more photons per cycle.

In practice, radio antennae display a range of radiation patterns. The radiating radio waves from a dipole antenna consist of electric field half-waves created by an alternating electric current applied to the antenna's two vertical metal rods. The oscillation frequency of the alternating current switches the antenna rod charge between positive (+) and negative (-), producing successive concentration bands of N- and N+ photons (highlighted in red and blue in figure 45): the animation quite clearly shows the outwardly radiating electric field waves corresponding to concentrated groups of photons (see https://en.wikipedia.org/wiki/File:Dipole_xmting_antenna_animation_4_408x318x150ms.gif).

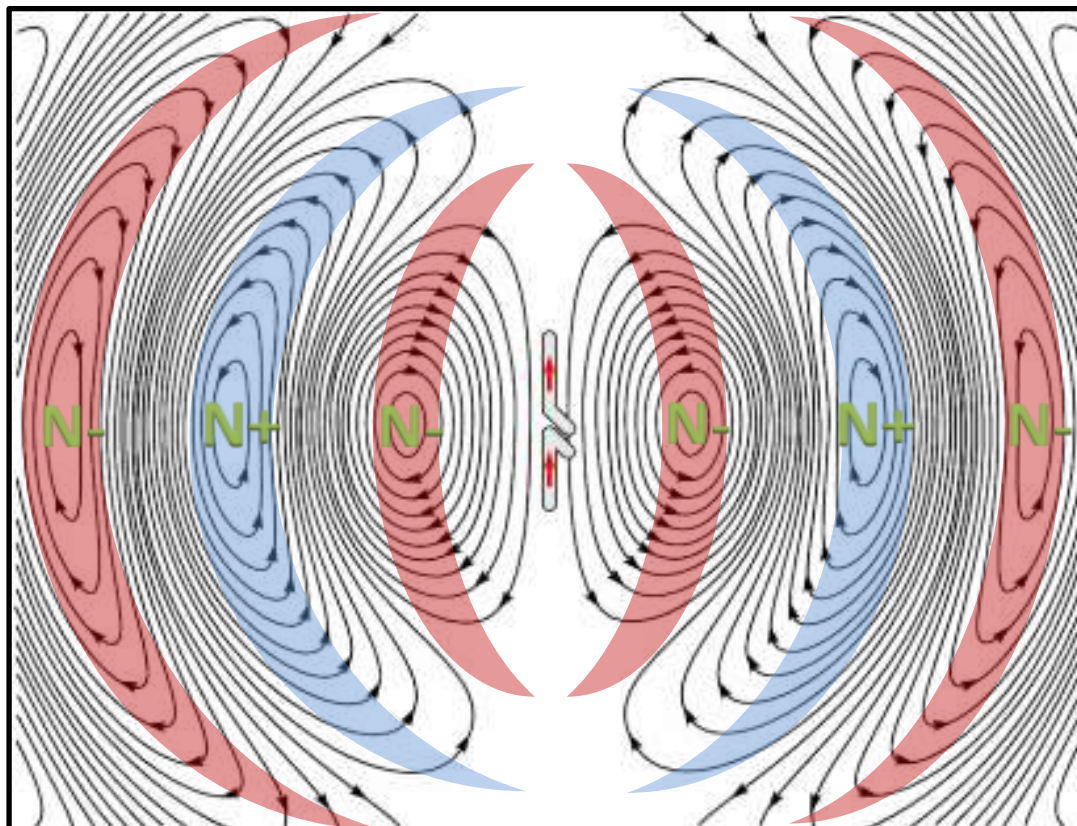


Figure 45: Electromagnetic Field Patterns for a Dipolar Antenna

As stated above, man-made micro and radio waves are considered to be different to 'normal' EMR with the corresponding frequency: they represent photons that have been concentrated into robust synthetic standing energy-waves that can be modulated to encode data, and which can be received by an appropriately tuned antenna and de-modulated to decode carried data. Apart from technologies using pulsed laser light, data packaging is only possible with man-made EMR in the micro/radio wavelength range: another indication of how different it is to 'normal' EMR.

Constructive and Destructive Interference

Constructive and destructive interference of intersecting wavefronts is well understood and documented. However, experiments involving the constructive and destructive interference of light and its extension to electrons, nucleons and molecules, need to be considered and explained in terms of the E2M model as presented in this thesis.

Starting point is the interference patterns derived from a **Michelson Interferometer** setup for parallel merged beams as shown in figure 46. A single beam of **coherent light** (i.e. light whose photons have the same frequency and a constant phase difference) is split into two identical beams by a partially reflecting mirror beam splitter. Each of the split beams travels a different path to be re-combined before arriving at a detector. The path length difference of each beam creates a phase difference between them, producing a characteristic concentric interference pattern (such as for the insert in figure 46).

At the beam-splitting mirror M, approximately half the light is reflected as linear polarised light heading towards reflecting mirror M1, where it is reflected towards the detector E. The rest of the split beam from M strikes reflecting mirror M2, where its photons' chirality is reversed and sent to the reverse side of mirror M (C1) where it is linear polarised and reflected towards the detector E. The interference patterns formed (figure 47a) are circular because the virtual images S1' and S2' of the light source form with one behind the other.

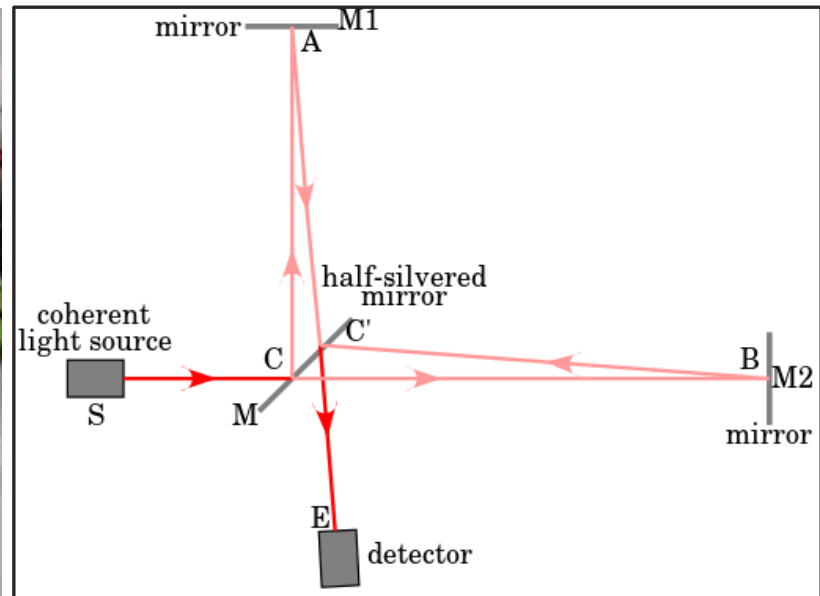
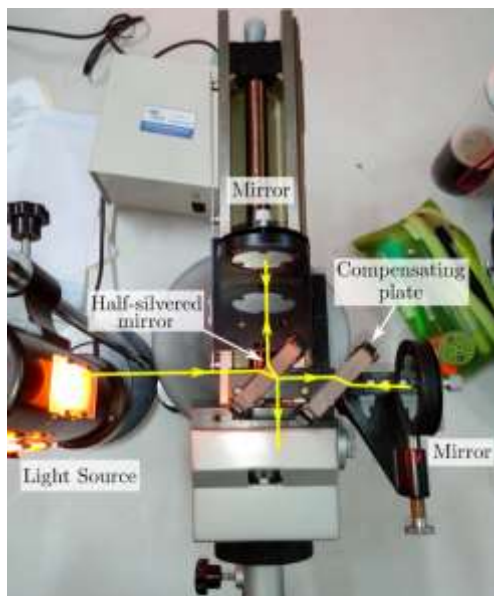


Figure 46: Michelson Interferometer setup: parallel merged beams

For the inclined Michelson Interferometer setup, a slight angle between the two returning beams caused by the inclined mirrors M₁ and M₂ results in a sinusoidal fringe pattern as shown in Figure 47b. If there is perfect spatial alignment between the returning beams, then there will not be any such pattern but rather a constant intensity over the beam dependent on the differential path length.

For the inclined Michelson Interferometer the interference patterns are formed by the side-by-side virtual image (S'1 and S'2) offset.

For the 2-slit experiments with light the main problem is an adequate explanation of why the light beams are deflected so as to cause interference patterns rather than the patterns themselves (which is a given).

The E2M explanation relates to turbulence as photons enter and leave the slits, drag on photons moving close to the sides of the slits (figure 49) and the effect of Surface Plasmons (if the barrier is metallic) as photons enter and exit the slits. The result is a curved wavefront that causes the interference from the 2nd slit's similar wavefront to create interference bands.

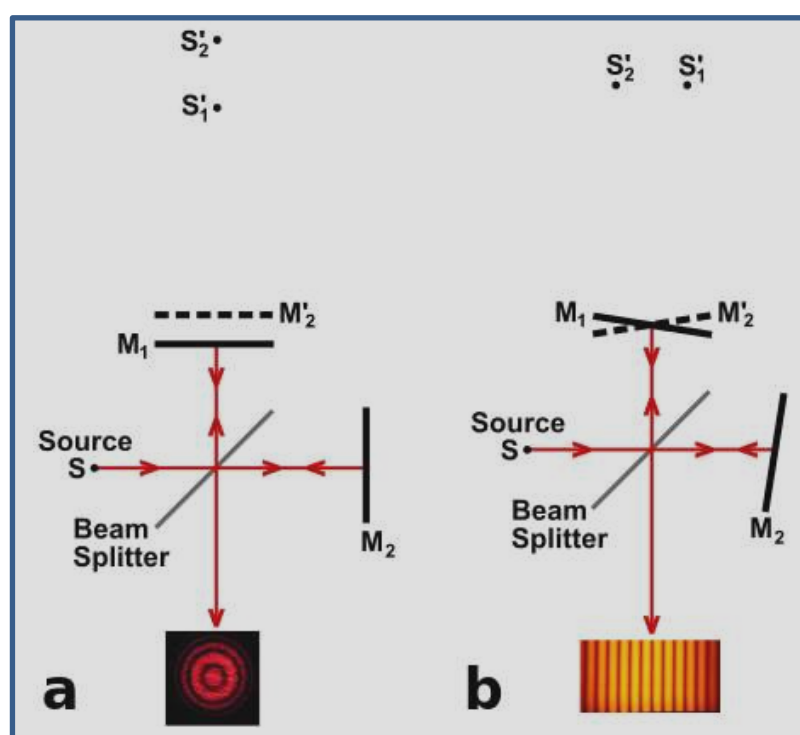


Figure 47: Michelson Interferometer Interference Patterns

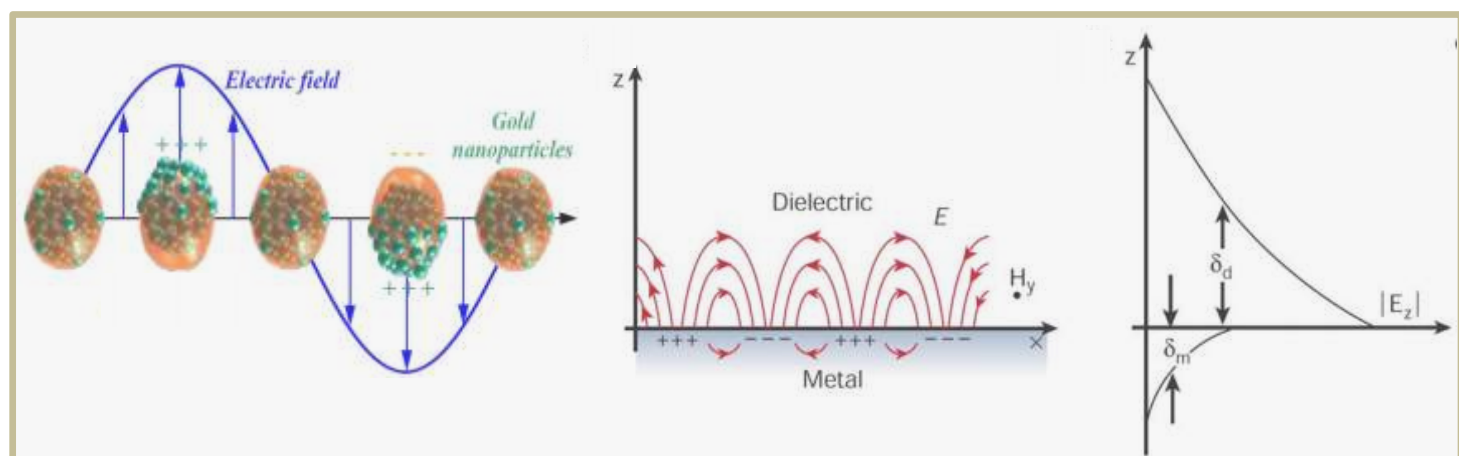


Figure 48: Surface Plasmons

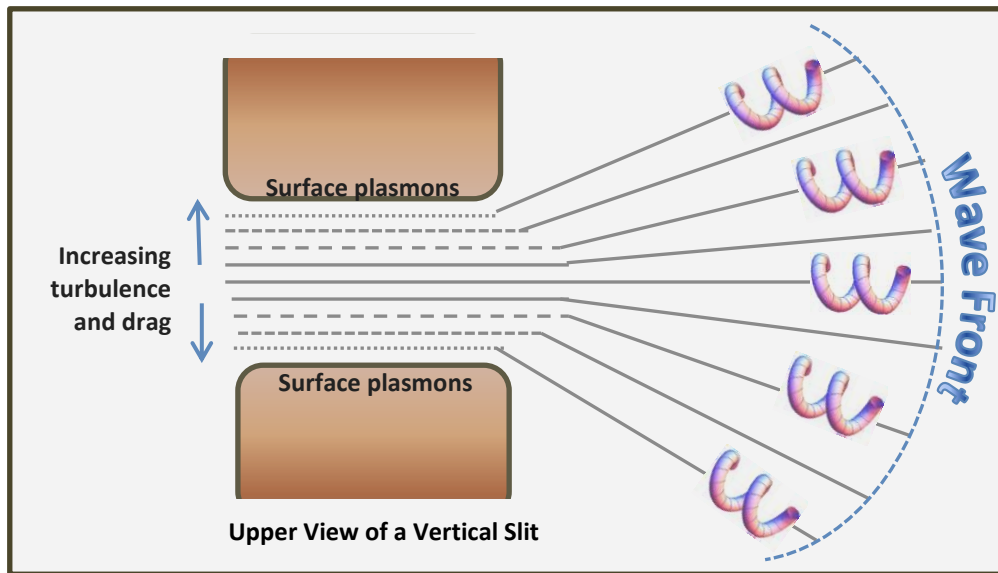


Figure 49: Light Wavefront Created by Progressive Photon Deflection

For light the 2-slit experiment is easily duplicated and the banding explained in terms constructive and destructive interference from intersecting curved wavefronts. The story for 2-slit experiments using electrons, atoms and molecules is different.

One of the better documented single and 2-slit experiments is the paper titled 'Controlled double-slit electron diffraction', by Roger Bach, Damian Pope, Sy-Hwang Liou and Herman Batelaan (New Journal of Physics Volume 15, March 2013; downloadable at <http://iopscience.iop.org/article/10.1088/1367-2630/15/3/033018>). The referenced paper provides an excellent historical overview of the most significant experimental evidence on the subject since Richard Feynman's thought experiment concept and is one of the few single/double slit experiments that provide full details (although the backstop distance is missing) of the setup for electron streams and for single electron-by-electron accumulation, together with good clear presentation of the results.

The wall and mask (bottom right of figure 50) were constructed from 100 nm thin silicon-nitride membrane coated with approximately 2 nm of gold, and the slits are 62nM wide separated by 272nM. Whenever a metal (such as gold) and a dielectric (such as air) interface a surface effect is an alternating series of micro positive and negative charges called **Surface Plasmons** (see figure 48) that will affect the electrons' path. The result of turbulence close to the slit surface and surface plasmon fields is deflection of the electrons into a wavefront pattern similar as that for light as explained above.

The result is the banded pattern P_{12} to the right of figure 50: however this is an intensity enhanced version of the electron distribution at the backstop. When the single electrons are used there is no chance of interference with each other because although their paths may cross, they are never in the same place at a given point in time. However, take the 6235 single electron distribution, as shown bottom left in figure 50, project the count to a central axis and show the results as an intensity enhanced plot, it would be the same as P_{12} , but without constructive and destructive interference being a factor. Such 2-slit experiments can in no way be construed to demonstrate a particle-wave duality for electrons.

Assuming that the electrons are deflected to form a curved wavefront pattern (similar to that for photons) that, with no constructive or destructive interference being involved, produces a series of overlapping skewed distributions of electron hits at the backstop: the electron contribution from each slit is shown in blue for the upper slit and red for the other. The net distribution of electron hits is shown by the dashed green line plot: it corresponds well to the 6235 stage of the progressive plots for single electrons as shown bottom left in figure 50.

Most likely for the continuous streaming of electrons (as opposed to the single electron firings), some electrons will be deflected when their paths cross. The resulting deflection and electrical interference between them is far removed from pairs destructively eliminating each other: when an electron and positron so meet electron-positron annihilation takes place with the generation of gamma radiation. The claim that electrons, atoms molecules can constructively and destructively interfere with each other due to a their claimed particle-wave nature, as suggested by mathematical modelling, would not seem to be supported by any of these 2-slit experiments.

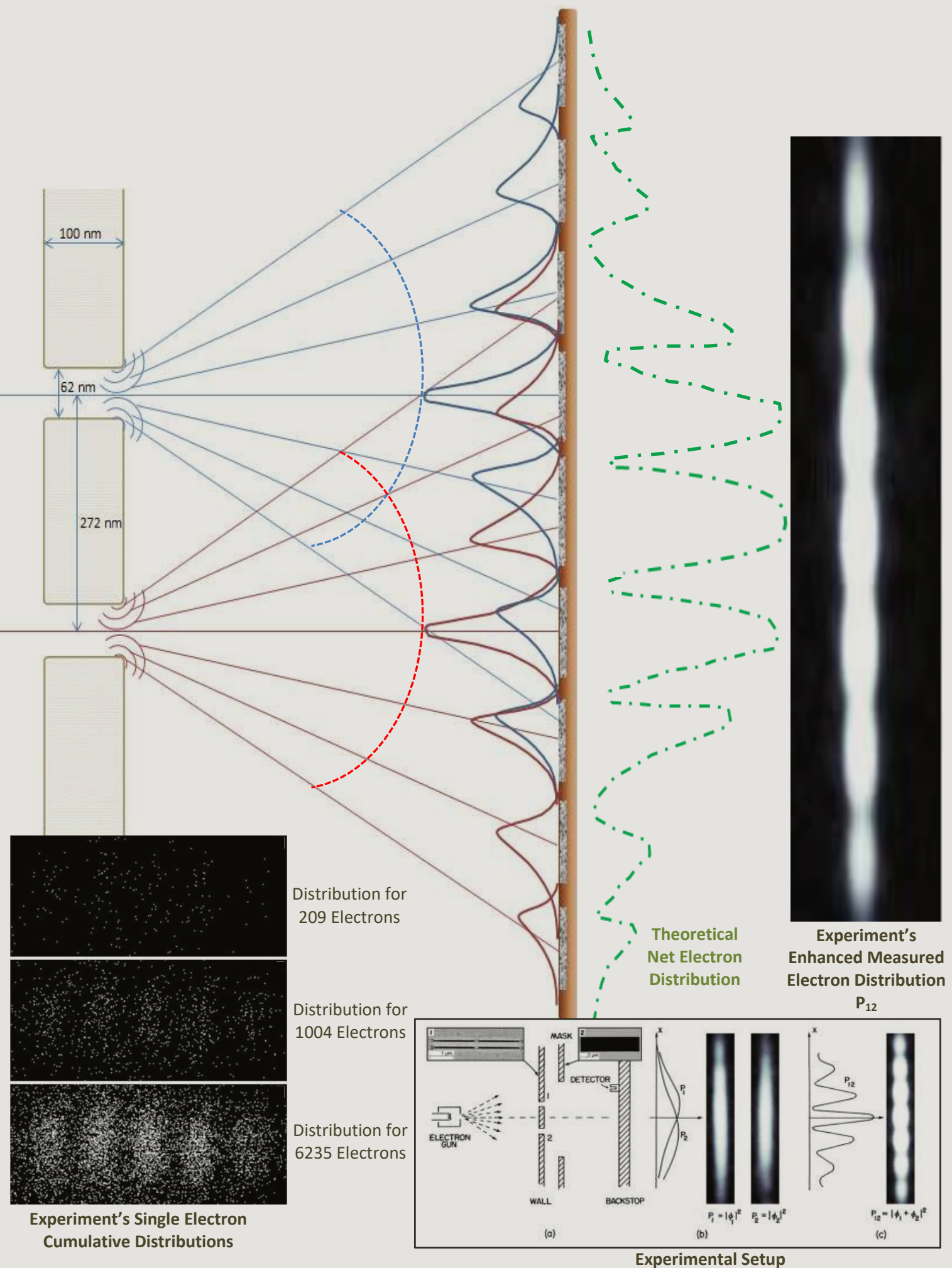


Figure 50: 2-Slit Electron Electromagnetic Deflection and Distribution Pattern

Appendix B: Electricity

Unfortunately the Nuclear Atomic model does not entertain the possibility of positrons within matter. Consequently conventional Science has difficulties in explaining electric current, particularly when it comes to semiconductor circuitry and chemistry, and is forced to introduce the abstract concept of a **hole**. A hole is considered to be an electric charge carrier with positive monopole charge characteristics: it loosely relates to the absence of an electron in an atom's outer orbital. Electron movement within an electric current is considered to be from negative to positive, whereas the positron-like hole movement is from positive to negative.

The energy-centric E2M approach considers that free electrons and positrons to be secondary (or derived) toroidal solenoidal forms of concentrated energy that are generated in approximately equal numbers from bitrons. The only physical difference between electrons and positrons is their chirality, and it is most difficult, if not impossible, to distinguish between them within matter. When ejected from matter and travelling in free space they may be distinguished by their deflection by an electromagnetic field as shown in [figure 9](#). Un-holey E2M contends that an electric current is formed by axially aligned electrons and positrons synchronously moving past each other in opposite directions (electrons leading with their N- poles and positrons with their N+ poles as shown in figure 51).

It is the screw-thread like thrust from the swirling electromagnetic energy fields (b) of the partially aligned free electrons and positrons within the conducting medium (e.g. copper wire) that causes them to shuffle past each other in opposite directions at quite low speeds (less than one metre per hour). An electric **current** (amperes) is thus considered to be a measure of the net electric charge flow rate due to the movement of free electrons and positrons albeit in opposite directions.

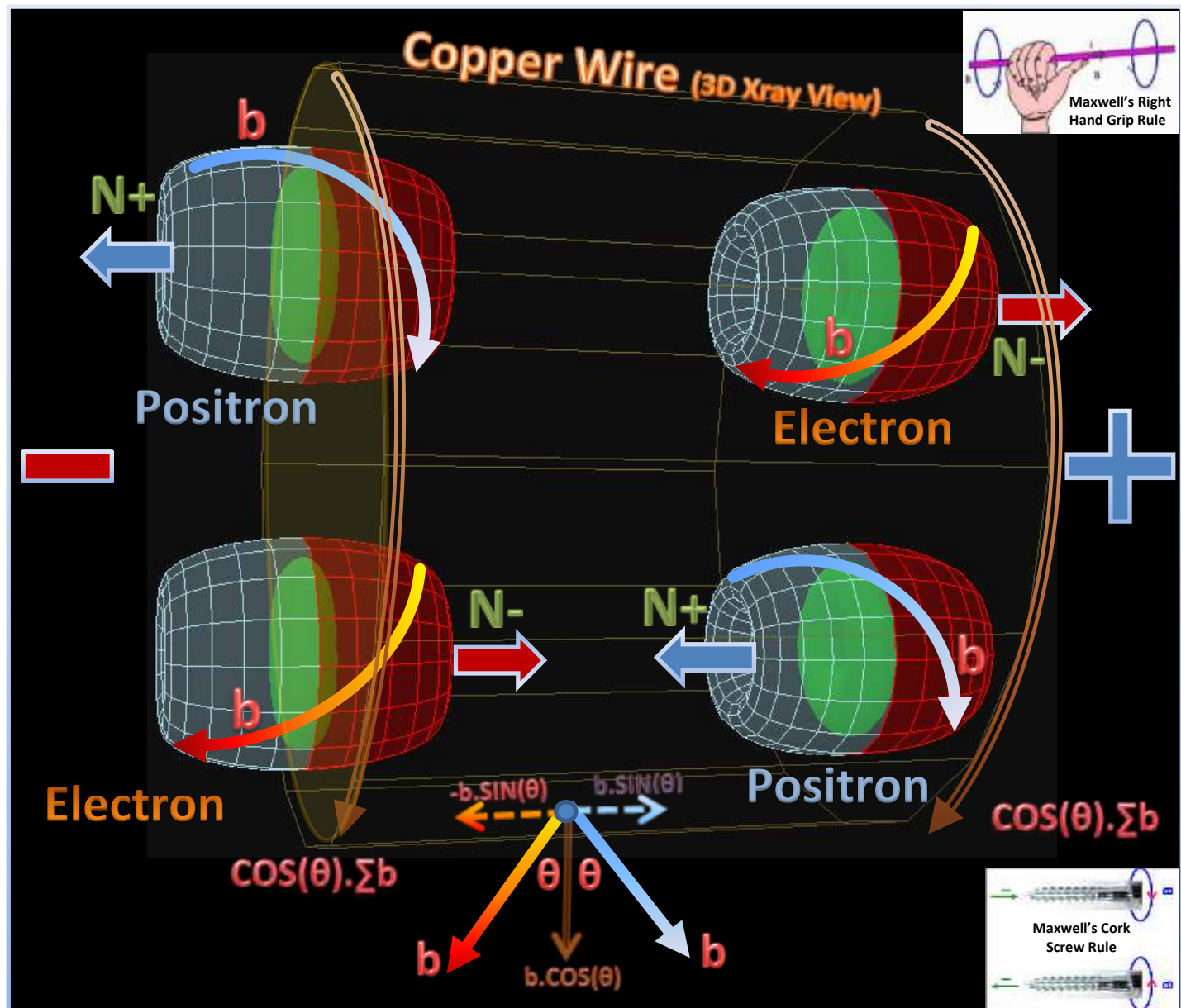


Figure 51: Electric Current: Electron and Positron Movement

The E2m view is that electricity is the synchronous movement of free electrons and positrons in opposite directions that is consequential to their alignment and concentration imbalances with electrons moving away from areas of electron concentration. Thus the negative side of an electric circuit acts as an **electron source** and a **positron sink**, and vice versa for the positive side, resulting in a reciprocating **source-to-sink** model for electricity flow.

The alignment of free electrons and positrons results in a circular magnetic field in the order of $\cos(\theta)\sum b$ around the wire in a direction conforming with Maxwell's Right-Hand Grip (or Cork Screw) Rule, as shown in figure 51 inserts. The along-wire magnetic field components ($b \sin(\theta)$) from the aligned electrons and positrons are in opposite directions so as to cancel each other out. Thus the electric potential difference is the only electromagnetic energy field internal to a wire conductor created by the electron and positron alignment.

Whenever an obstacle is encountered within an electric circuit, such as a resistor or a capacitor, the two-way movement of the electrons and positrons is restricted, causing a drop causing a drop in electric current. For a resistance forming the load for an electric circuit, Ohm's Law indicates that for a resistor of R ohms (Ω) and an electric potential difference of V volts the resulting electric current is V/R amperes when the circuit is open.

Dielectrics and Electrical Capacitors

The **dielectric material** used in an electric capacitor is an electric insulator that allows only limited levels of free electrons and positrons to enter and to be contained: when the charge source is switched off, the imbalance of electrons and positrons contained within the capacitor causes and electric current in the reverse direction.

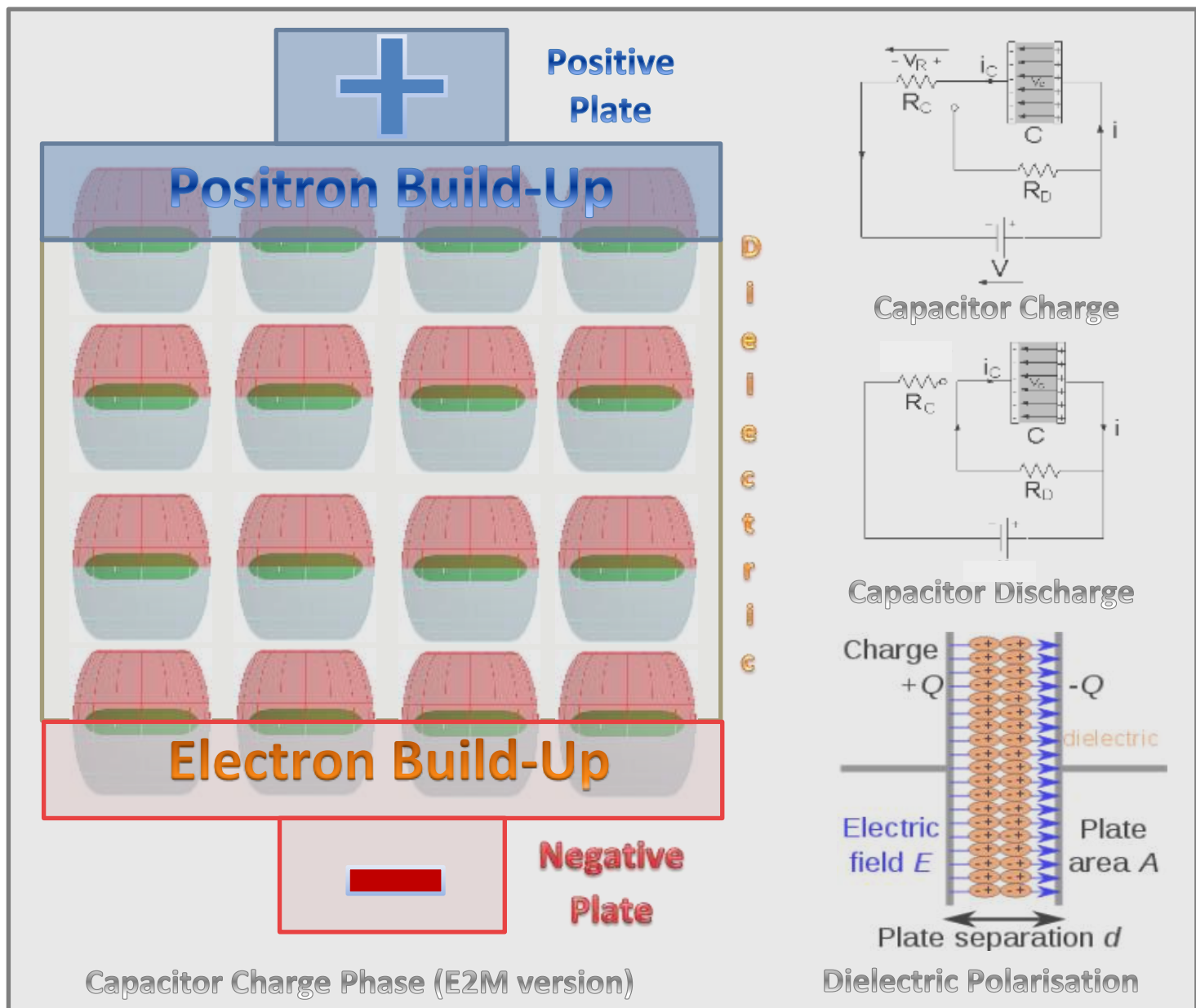


Figure 52: Electric Capacitor Charge and Discharge Phases

During the **charge phase** (top-right insert of figure 52), electrons accumulate within the dielectric resistor on the negative side within the active circuit as they cannot pass through the capacitor. Positrons moving in the opposite direction likewise accumulate within the dielectric medium on the positive side of the circuit. The build-up of accumulated electrons and positrons continues until no more can be accommodated within the dielectric, and the capacitor is then full with no current entering that section of the circuit.

For the **discharge phase**, the aligned positrons and electrons within the dielectric medium become the energy source. The concentration of electrons on the negative side of the capacitor becomes the electron provider and those on the positive side the positron provider: the result is a discharge current flowing in the reverse direction of the charging current.

Interestingly, [the Wikipedia definition for a dielectric](#) is ‘an electrical insulator that can be polarised by an applied electric field’ and their diagram for ‘dielectric polarisation’ (duplicated bottom right in figure 50) uses electric dipoles, and is remarkably similar to the E2M model. This represents an unintentional endorsement of the E2M explanation.

Chemical DC Electricity Generation and Recharge

The **Galvanic Cell** example figure 53a creates Direct Current (DC) electricity by chemical reaction (i.e. is a chemical battery). At the anode, cadmium atoms release electrons and absorb positrons as cadmium atoms in the anode are converted into cadmium cations in solution, so acting an electron source and positron sink. At the cathode, copper cations in solution release positrons and adsorb electrons to deposit copper metal at the cathode, so acting a positron source and electron sink. The parallel chemical reactions at anode and cathode plates creates an imbalance between electrons and positrons and a corresponding emf across the wire connecting them, resulting in an electric current consisting of the synchronous shuffling of electrons from anode to cathode and positrons in the opposite direction.

The **Electrolytic Cell** example of figure 53b, effectively reverses the process of the Galvanic Cell. When a DC current (shown as 0.74volts from an AC-to-DC converter) is applied, it becomes an electron supplier on the cathode side and a positron supplier on the anode side of the circuit. As the axially aligned electrons are shuffled to the cathode, they are adsorbed by cadmium cations to deposit cadmium metal onto the cathode, which acts as an electron sink. The cathode also acts as a positron supplier as positrons are also released by the same chemical reaction. At the anode, positrons from the power supply are absorbed by the copper metal and electrons are released as copper cations are released into the solution: thus the anode acts as a positron sink and an electron source.

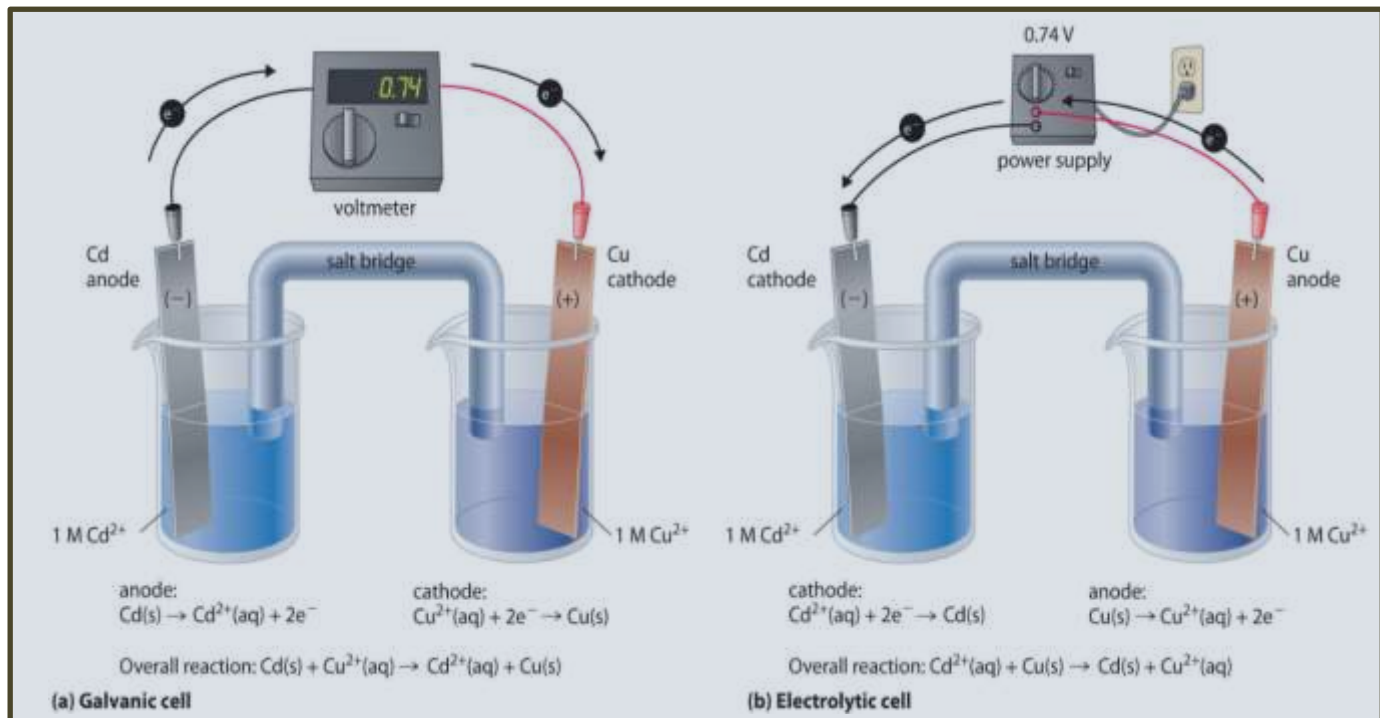


Figure 53: Galvanic and Electrolytic Cells

Such chemical cells demonstrate how concentrations of electrons and positrons, whether derived from chemical reactions or artificial power sources, create sources and sinks for free electrons and positrons, with the emf so generated aligning them and causing them to shuffle past each other in opposite directions as an electric current.

Van de Graaff Generators

A Van de Graaff generator is an electrostatic generator that uses a moving rubber belt to transfer charge to a hollow spherical metal structure and accumulate the charge to generate a very high electric potential up to several million volts.

For the positive charge generator (figure 54a), the upper roller (2) is acrylic glass or similar that loses electrons (electron source), which attach to the rubber conveyor belt and are moved down on the belt towards the lower metal roller. The acrylic roller is left with a positive charge due to the high positron-to-electron ratio (i.e. a positron source).

Many of the surplus electrons arriving at the lower metallic roller are extracted by the lower comb (7), creating an electron source that extends to the smaller metal sphere (8). Consistent with the E2M explanation of electric current flow, the electrons moving towards the small sphere cause reciprocal movement of positrons in the opposite direction, which in turn attach to the outer surface of the conveyer belt.

The upward-moving section (4) of the belt thus has a positron surplus which is harvested by the upper comb (2), building increased levels of positrons at the outer surface of the larger sphere (1) analogous to the electron build-up on the small sphere. Positron movement towards the large sphere is accompanied by the movement of electrons onto the moving conveyor belt via the comb (2).

Looking at a cross-section of the metal forming the larger hollow metal sphere (figure 54b), the arriving positrons spread up and around the sphere causing some electrons to migrate towards the inner surface of the hollow sphere and exit via the upper comb. At the large sphere's outer surface there is a considerable build-up of positron positive charge, but the inner surface maintains approximately equal numbers of electrons and positrons, keeping the inner surface electrically neutral.

The charge build-up on the spheres continues until equilibrium is reached with current no longer being generated across the combs.

The large electric potential difference between the positively and negatively charged spheres ionises air and water molecules between the two, creating low-level plasma. The plasma

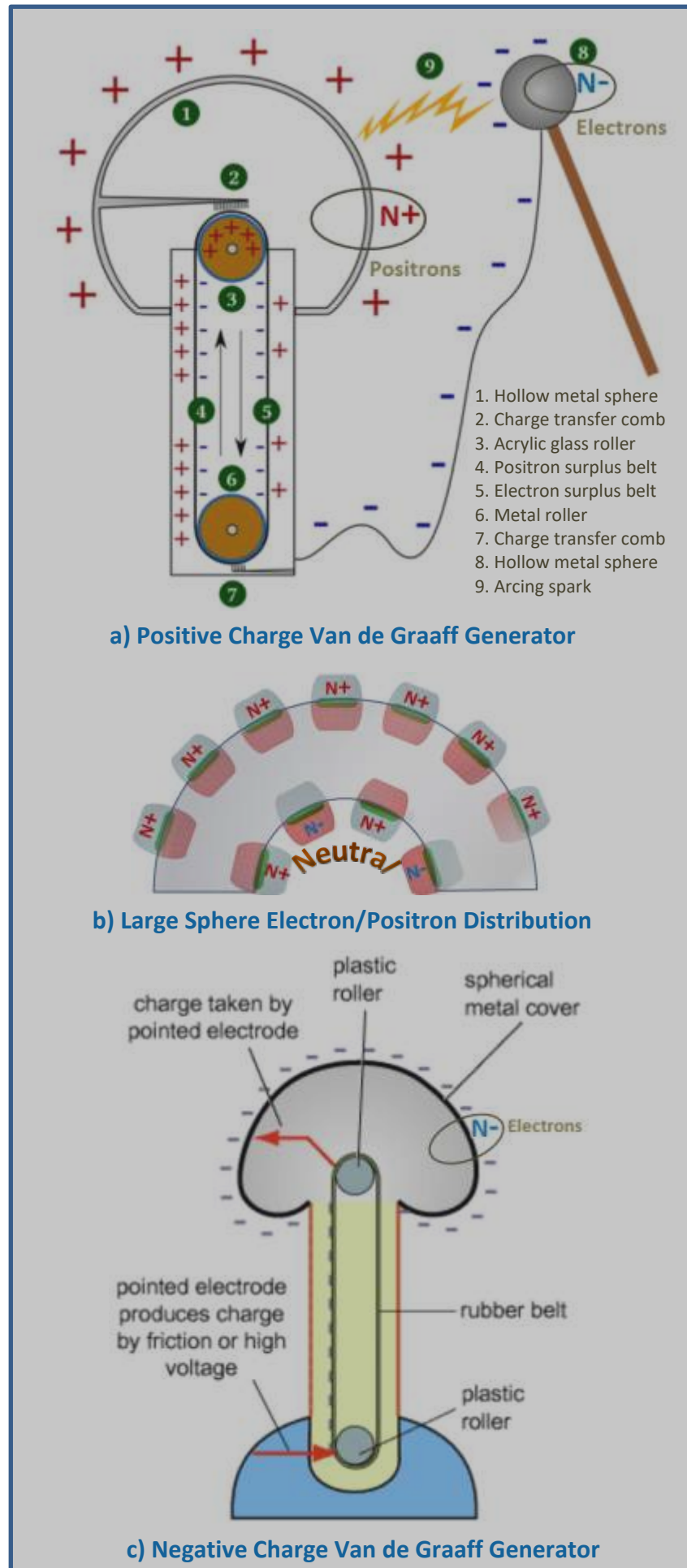


Figure 54: Van de Graaff Generators

formation process quickly escalates into a large-scale charge transfer as an **electric arc** (9), as positrons and electrons are directly exchanged between the two spheres.

A negative charge version of the Van de Graaff generator (figure 54c) uses two plastic or acrylic glass rollers and does not harvest electrons from the lower roller: positron build-up occurs within each roller and on the inner surface of the belt, with a high concentration of electrons on the outer surface of the up-belt. Quite often a high voltage is applied via the lower comb to supply the system with extra electrons thus increasing the charge build-up at the surface of the sphere.

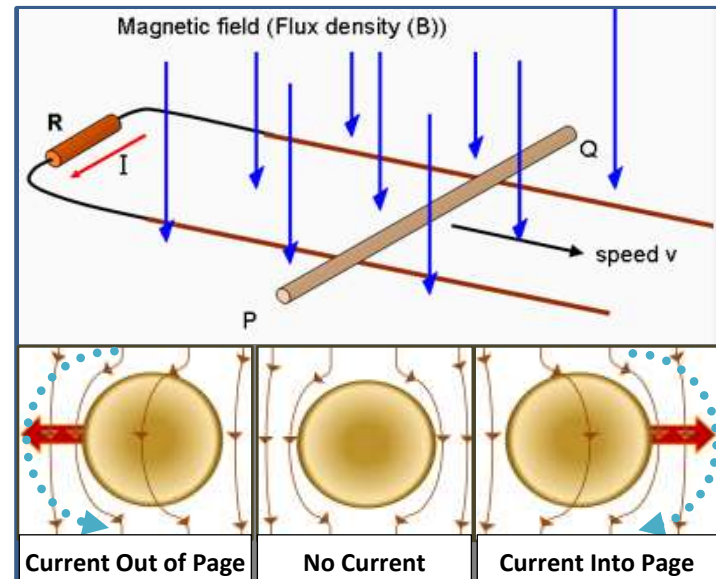


Figure 55: Magnetic Field Induced Current

Faraday's Law of electromagnetic induction states that whenever a conductor is forcefully moved in an electromagnetic field, an electromagnetic force is induced which causes a current to flow. And the E2M opinion is that the current flow represents the synchronous movement of aligned free electrons and positrons within the conductor. For this discussion only the electron movement is referred to, but synchronous reverse movement of positrons occurs.

In figure 55, the movement (at speed v) of conductor rod (PQ) through an external magnetic field (B) generates an anti-clockwise electric current (I) in the circuit.

The middle diagram (of the lower 3 in figure 55) shows the flux deflecting around the rod when it is stationary within a magnetic field; the electrons and positrons are in effect shielded from the external magnetic field and thus no current results.

When the rod moves to the right (right-most diagram), the magnetic flux is forced to pass through the rod, causing the free electrons and positrons to align, generating an electric current in the rod and thus the circuit. The alignment causes the electrons to shuffle in a direction into the page, creating a

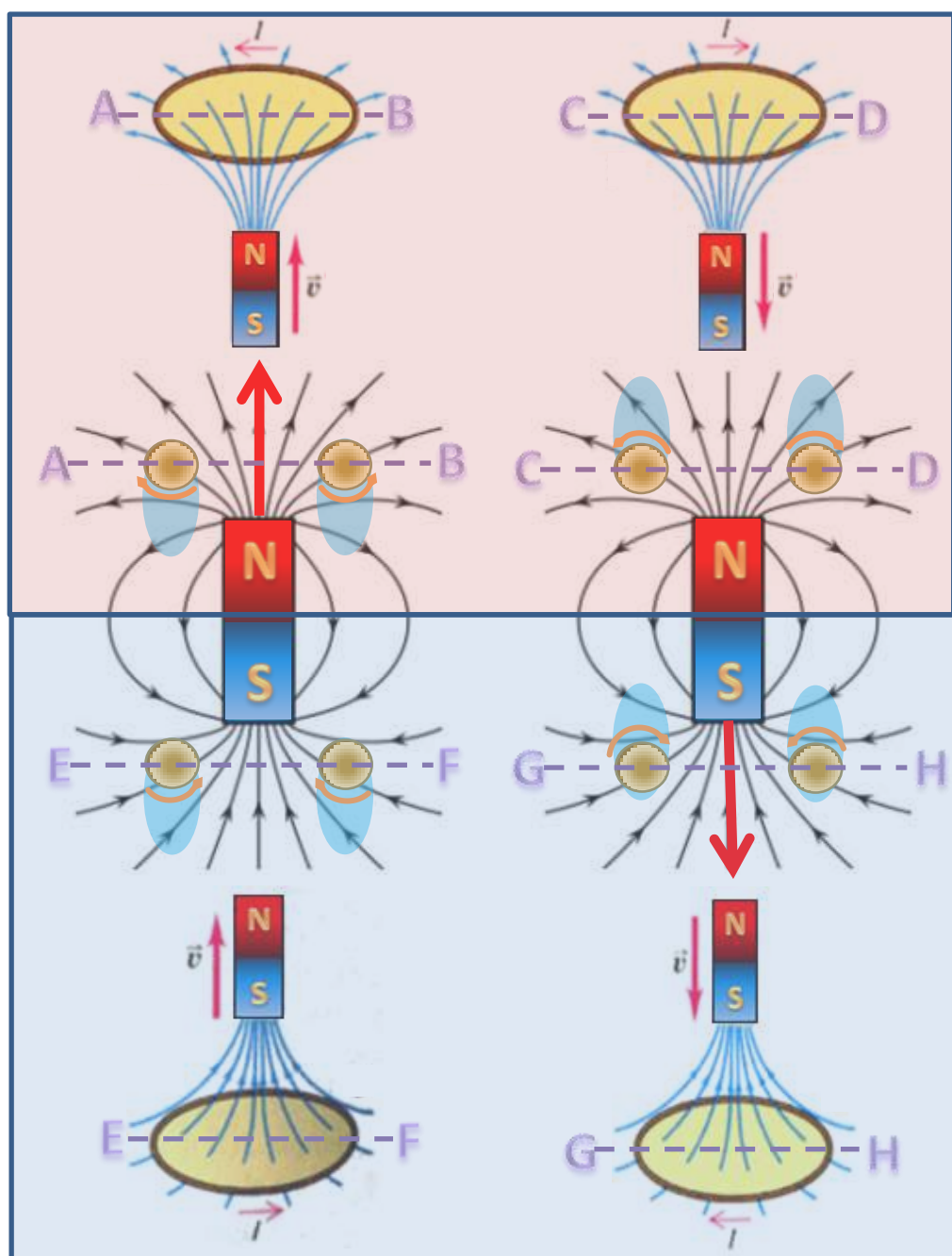


Figure 56: Magnet-Motion Induced Current within a Loop

current direction that corresponds to Maxwell's Right-hand rule plus a clockwise circular magnetic field (shown as a blue dashed arc).

When the rod moves to the left (left-most diagram), the free electrons and positrons align in the opposite direction, reversing the electric current and circular magnetic field directions.

When the direction of the external magnetic field is reversed, the direction of the induced current and circular magnetic field is also reversed for each rod movement direction.

The E2M model provides a simple, consistent causative explanation for induced current, its direction and the associated circular magnetic field. Current Science texts and associated articles provide descriptive explanation rather than a causative explanation of these phenomena. They provide is a series of inter-related rules and conventions but little real explanation, which adds mystery and confusion (just ask any high school student) around electromagnetic induction and electricity.

The electromagnetic induction of a loop circuit caused by moving a magnet towards and away from it in different N-S polar orientations is shown in figure 56.

The key to understanding the direction of the loop current and the associated circular magnetic field is to look at the cross-sectional view of the loops (AB, CD, EF and GH).

The blue oval annotation attached to each loop cross-section indicates the direction from which the magnetic flux approaches: the flux passes through the loop, aligning the free electrons and positrons therein and generating a circular magnetic as shown by the orange arc arrows.

The direction of the induced loop current can be confirmed for each of the 4 scenarios by using Maxwell's right-hand grip rule. There is no mystery here – just simple Physics.

It should be noted that the induced circular magnetic field that forms around a wire conductor is reminiscent of what E2M refers to as an electric field pattern as shown in figure 57: thus electricity in a wire conductor can be considered to not have a magnetic component. However, the electric field convergence inside a loop current generates a magnetic field pattern that is similar to that of a dipole magnet or that of an electron or positron. This effect highlights electric and magnetic field duality and the subtlety of the transition from one to the other and back again.

The main difference regarding electricity between the conventional view and that of E2M is that E2M considers an electric current to involve the synchronous two-way shuffle movement of electric dipoles (electrons and positrons), whereas the conventional Science view is that monopole electrons move from an area with high electron concentration (negative terminal) to a low-electron area (positive terminal area where the positive charge of monopole protons within atomic nuclei prevails). The failure of conventional Science to recognise positron participation in electric current formation has led to the unnecessary invention of positive electric charge carriers called '**electron holes**' to explain electric current transfer in **semiconductors**.

For the E2M approach, within an electric current approaching electrons and positrons have the same magnetic polarity which prevents them from colliding. Furthermore, it is highly likely that because of strong end-to-end electromagnetic attraction (N- attracting S+) of electrons moving in the same direction will cause them to hook-up into train-like connected strands moving in unison, pull-and-push shunting each other forward. Strands of positrons moving in the opposite direction would similarly connect, with the counter-rotational motion of the strand-like groups worming screw-like past each other, and around (and possibly through) atoms in their way.

For **alternating current** (AC), created by switching current direction at a specific frequency, the E2M view considers that the aligned free electron and positron tori are simply flipped 180° to reverse the electric current for each cycle. In other respects E2M and the conventional view are fully compatible, and as the techniques for creating AC electricity from induced currents (e.g. by rotating a U-shaped loop through a magnetic field) are well documented, as are the ways of creating and managing DC electricity: consequently they will not be addressed in this thesis paper.

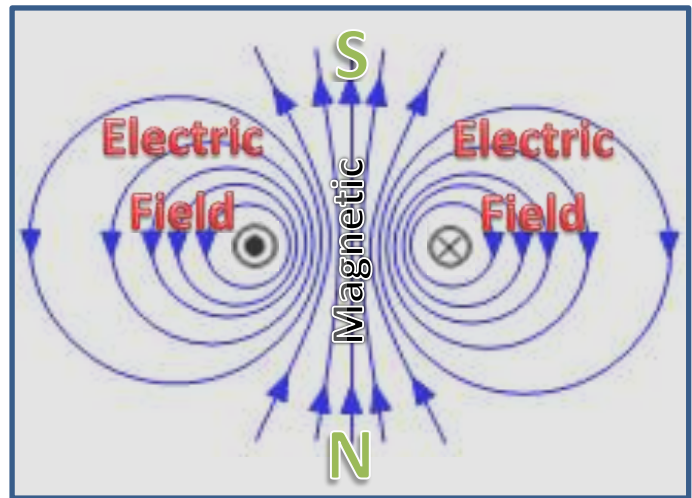


Figure 57: Electromagnetic fields around a Loop

Appendix C: The Pull of Gravity

Not all electromagnetic energy leaving CESs, electrons, positrons and photons via a North Pole returns to the corresponding South Pole: very small quantities of the normally connected swirling electromagnetic energy is leaked and ‘lost’. Although much of the ‘lost’ energy is absorbed by other adjacent electromagnetic fields, a small amount still manages to escape and accumulate as a very weak pool of ‘stagnant’ energy around the object from which it escaped. E2M contends that low-level leakage energy accumulates **atmosphere-like** around all normal matter: thus it has been called an **Enersphere**.

For nucleons within an object’s atomic structure, electromagnetic energy returning via the converging funnel-like South Pole CESs provides a positive pull on the enersphere immediately surrounding the parent object and sucks in a minuscule amount of leakage energy. E2M contends that the suction-like pull of the out-facing South Pole CESs results in a minute inwardly-directed force, the nett sum of which totalled over the billions of nucleons (1 billion = 10^9 , and one litre of water contains approximately 2×10^{27} or 2 octillion nucleons) within an object equates to the pull of **Gravity**.

The more nucleons that an object contains, then the larger its enersphere would be and the more out-facing South Pole CESs it would have that would contribute to its gravitational pull. Thus it is the total number of nucleons within an object that dictates its **mass** (implicit in $E=mc^2$), and, in relation to Earth, it is the size of an object’s enersphere and its location within Earth’s enveloping enersphere that dictates its **weight**.

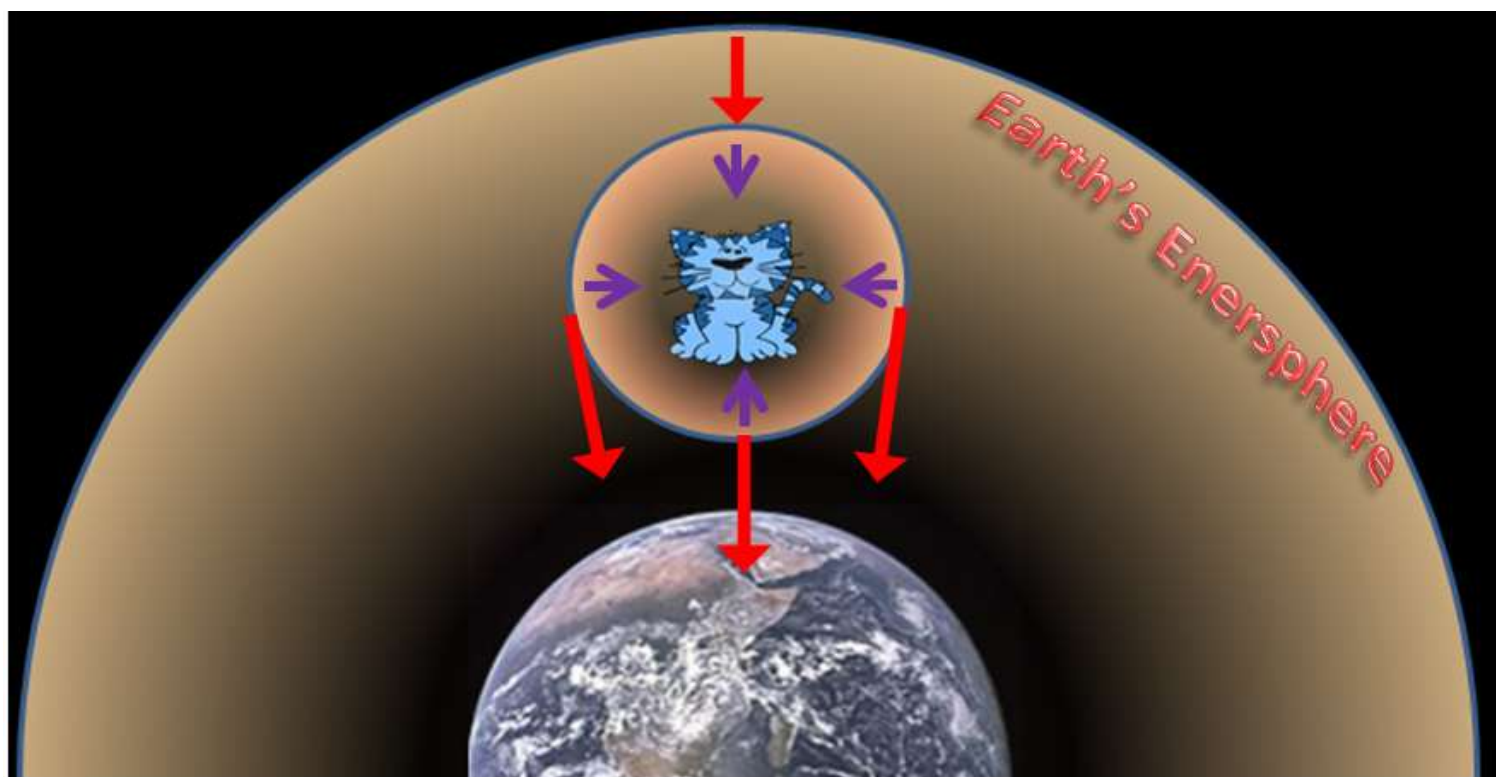


Figure 58: Model for Earth's Gravity

Figure 58 represents a cat sitting with its enersphere fully within the Earth’s enersphere. The purple arrows show the direction of the forces pulling the cat’s enersphere towards the cat, and the red arrows the considerably greater forces pulling the cat’s enersphere towards the surface of the Earth. The cat is heading earthwards, free falling under the influence of Gravity.

The depiction of figure 58 is idealised because the shown bubble boundary surface does not exist - when one object’s enersphere overlaps another’s they simply merge into one, with the energy levels of each enersphere adjusting appropriately to the other. The suction-like pull of the out-facing South Pole CESs within each object (here the cat and Earth) would continue to pull energy from the resource-in-common, their merged enerspheres. The forces acting in the zone of the cat, however, would be similar to those shown, as would be their nett effect.

At the macro level, enerspheres of large bodies extend well into space (e.g. the Moon, Earth, the Sun, the stars and galaxies) intersecting and acting together to create Gravity pull between systems. The huge, far reaching enerspheres

of large objects in space suggests that their enerspheres could possibly be in expansion mode, albeit slowly. It is difficult to imagine any region of space without enersphere energy, even if it is only from the vapour trails of photons.

Enerspheres are a remarkable bi-product of the way energy combines to make atoms and of atoms to make matter. E2M contends that the pull of Gravity is due to the retrieval of enersphere energy rather than being a mysterious external force or a result from the warping of **space-time**. It is a model that applies equally well both at the micro scale (e.g. Gravity forces applying to objects on Earth) and macro cosmological scale.

As large scale cosmological systems approach each other, their enerspheres merge causing an increase in enersphere density and thus the magnetic pull of each towards the other. For merging systems such as **neutron stars** or **black holes**, a spin embrace results (see figure right) which climaxes with a rapid compression of their combined enerspheres and consequential massive explosion of greatly compressed energy that generates **Gravity waves**.

Whereas Einstein provided a mathematical framework for Gravity waves in terms of space-time, E2M provides a physical model in terms of matter and enersphere energy compression and the explosive release of the combined compressed energy.



Historical Note. René Descartes, famous for his philosophical assertion *cogito ergo sum* ("I think, therefore I am"), in 1644 proposed that **aether**, the medium then considered to separate objects and matter (cf. space), is filled with vortices whose **inward pressure** is '*nothing else than gravity*'.



Consider **Descartes's vortices** to be CESs within nucleons and consider the **aether** to be the enersphere energy surrounding matter, then, **philosophically, Descartes' 374 year old explanation for gravity was not far removed from that of E2M**.

(It should also be noted that, at this stage, E2M does subscribe to the notion that aether is the substance or medium in space that supports the propagation of EMR in a wave form.)

